Interaction of Sexual Behavior and Hormone Gene Expression in the Labyrinthici Fish Blue Gourami (*Trichogaster trichopterus*) during Reproduction

Gad Degani

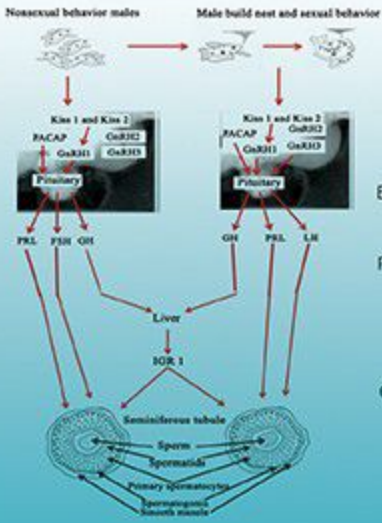

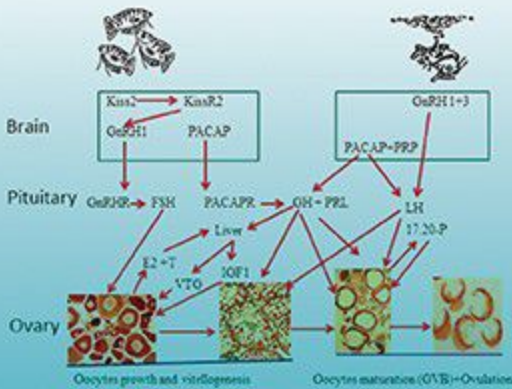

Scientific Research Publishing

Interaction of Sexual Behavior and Hormone Gene Expression in the Labyrinthici Fish Blue Gourami (*Trichogaster trichopterus*) during Reproduction

Gad Degani

Scientific Research Publishing

Interaction of Sexual Behavior and Hormone Gene Expression in the Labyrinthici Fish Blue Gourami (*Trichogaster trichopterus*) during Reproduction

Published by
Scientific Research Publishing, Inc.
ISBN: 978-1-64997-226-2
http://www.scirp.org

Abstract

Chapter 1. Labyrinth Fish

The blue gourami (*Trichogaster trichopterus*) belong to the Anabantidae family, which are ray-finned fish in the order Anabantiformes; they are commonly called labyrinth fish. The 16 known genera contain about 80 species, distributed throughout most of southern Asia, India, and central Africa. In the Labyrinthici, an air-filled breathing cavity known as the labyrinth is located above the gills under the operculum, on top of the head behind the eyes. The labyrinth is a circular spot of very wrinkled tissue, which offers more surface area for oxygen intake. This cavity supplements the breathing function, since it is well suited to gaseous interchange. The systematic characteristics of Anabantiformes are not in agreement and many synonyms are used.

Chapter 2. Molecular Variations in Gene Markers in Blue Gourami as a Model for Labyrinth Fish

Markers of genetic variation among species are important for both applied and basic research. The genes encoding the following hormones are described: kisspeptin (Kiss) 1 and 2, gonadotropin-releasing hormone (GnRH) 1, 2 and 3, growth hormone (GH), somatolactin, prolactin (PRL), follicle-stimulating hormone (FSH) and luteinizing hormone (LH), as well as mitochondrial genes encoding cytochrome b

and 12S. Based on the findings reviewed in this study, it is suggested that the 16 genetic markers in blue gourami representing markers of the suborder Anabantoidei differ from those in other bony fishes. Among the genes involved in controlling growth and reproduction, the most suitable genetic markers for distinguishing among species of the Anabantoidei are in the hypothalamic-pituitary-somatotropic (HPS) axis: pituitary adenylate cyclase-activating polypeptide (PACAP) and GH, and the 12S rRNA gene. The purpose of this chapter is to examine the sequences of the genes from studies related to growth and reproduction, as molecular markers for the suborder Anabantoidei.

Chapter 3. Reproduction in the Blue Gourami Male

This chapter describes hormone control in male blue gourami along the gonadotropic brain-pituitary-gonad (BPG) axis and the HPS axis. Gene transcription is affected by environmental, biological, and behavioral factors. Mature males were examined at two different stages—non-reproductive in high-density habitats, and reproductive in low-density habitats. Based on gene transcription, GnRH1 is involved in controlling spermatogenesis (spermatogonia to spermatids) via the BPG axis in non-reproductive and reproductive stages by controlling FSH, 11-ketotestosterone (11KT) and 17β-estradiol (E2). However, GnRH3 has a larger effect during the reproductive stage via the BPG axis (spermatids to sperm) on LH, 11KT, and 17α-hydroxyprogesterone (17P). At the same time, the HPS axis is involved in spermatogenesis

via PACAP and its related peptide PRP (formerly known as GHRH-like peptide) in the brain, and GH in the pituitary affects synthesis of insulin-like growth factor 1 (IGF1) in the liver.

Chapter 4. Reproduction in the Blue Gourami Female

This chapter describes the hormones involved in controlling the reproductive system of a model female blue gourami fish. In the whole-brain transcriptome of blue gourami, transcription of 17 genes changes during vitellogenesis in the brain. The hormones involved in reproduction in blue gourami and described in this chapter include: Kiss2 and its receptors 1 and 2 (KissR1 and 2), GnRH1, 2 and 3, GnRH receptor, PACAP and PRP, somatolactin, FSH, LH, GH, PRL, E_2, testosterone, vitellogenesis and 17α,20β-dihydroxy-4-pregnen-3-one (17,20P). A proposed qualitative model is presented of brain control of oogenesis in blue gourami. This chapter summarizes the various complex factors involved in the interactions between external and internal elements acting on the brain during fish reproduction in the order Anabantiformes. It is suggested that the involvement of hormone receptors, pheromones, and genome changes be further studied.

Chapter 5. Biotic and Abiotic Factors Affecting the Reproduction of Blue Gourami

Effects of temperature, light, and container size on blue gourami breeding were studied. Environmental variables affecting construction of the bubble nest, the number of larvae that hatch from the eggs, and

the optimal temperature were measured under laboratory conditions. Nest-building was significantly reduced (to 25%) when three males were held in one aquarium (experimental group) compared to 50% in the control (one male per aquarium). It was suggested that when two males were held in a cage in the same aquarium, they were only affected by the pheromones of one male, reducing the number of nests built. The aggressive male behavior that enhances their ability to defend their territories was studied in detail. The study supported the hypothesis that territoriality also prevents the effect of other males' pheromones on sexual behavior and nest-building. During reproduction, only the dominant male, which had a territory, built nests. Effect of temperature on the relative mRNA levels of GnRH3, PACAP, PRP, and IGF1 in brains of blue gourami males maintained in groups (non-reproductive conditions) were studied.

The mRNA levels of brain hormones (GnRH1 and GnRH3) and pituitary hormones (βLH, βFSH, GH and PRL) of males under reproductive conditions in various concentrations of underground water were studied. GnRH1 mRNA levels were significantly higher in 50% and 100% underground water compared to 0%; PRL mRNA levels were significantly higher in 100% underground water compared to 0%; and GnRH3 mRNA levels were significantly higher in 50% underground water compared to 0%. On the other hand, no significant differences were found for βLH, βFSH or GH mRNA levels for the different percentages of underground water.

Acknowledgements

I would like to thank the Ph.D. students working in my laboratory who contributed directly or indirectly to this paper: Dr. Gal Levy, Dr. Karen Jackson, Dr. Svetlana Yom Din, Dr. Tzchori Itai, Dr. David Kushnirove, Dr. Avshalom Hurvitz, Dr. Oren Pearlson, and Dr. Tali Goldberg; and the M.Sc. students Meital Ezagouri, Lior Sahder, and Dali David; my colleagues at MIGAL and Tel-Hai Academic College, Prof. Dani Bercovich, Dr. Doron Goldberg, and Dr. Ari Meerson; and my colleagues for their past and current collaboration on the study of fish endocrinology, Prof. Berta Levavi-Sivan, Prof. Yoav Gothilf, and Prof. Yonathan Zohar.

Contents

Chapter 1

Labyrinth Fish

1.1. Distribution

The blue gourami (*Trichogaster trichopterus*; syn, *Trichopodus trichopterus*) belongs to the Anabantidae family of ray-finned fish, in the order Anabantiformes, commonly referred to as labyrinth fish (Van Der Laan et al., 2014) (**Figure 1**, **Figure 2**). The 16 known genera contain about 80 species, distributed throughout most of southern Asia, India, and central Africa (Degani, 2001; Forselius, 1975; Vierke, 1988) (**Figures 3-5**, **Figure 7**).

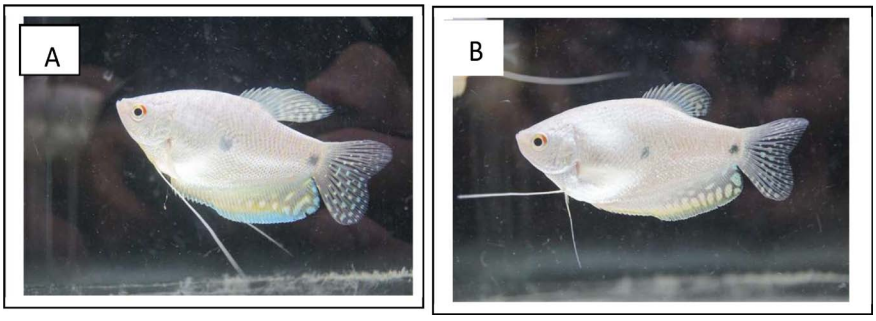

Figure 1. Male (A) and female (B) blue gourami.

Labyrinth fish have an air-filled breathing cavity, known as labyrinth, located above the gills under the operculum, on top of the head behind the eyes (Degani, 2001). The labyrinth is a circular area of

highly wrinkled tissue, which offers more surface area for oxygen intake. This cavity, which is well suited to gaseous exchange, supplements the breathing function (Degani, 2001) (**Figure 2**). The systematic characteristics of Anabantiformes have not been agreed upon and many synonyms are used.

According to Vierke (1988), taxonomists classify the labyrinth fish into four families: Anabantidae (genera: *Sandelia*, *Ctenopoma*, *Anabans*), Belontiidae (genera: *Trichopsis*, *Trichogaster*, *Sphaerichthys*, *Pseudosphromenus*, *Parosphromenus*, *Malpulutta*, *Hlostoma Ctenops*, *Collisa*, *Betta*, *Belontia*), Osphromenidae (genus *Osphronemus*), and Helostomatidae (genus *Helostoma*). These fish can survive in water with very low oxygen content.

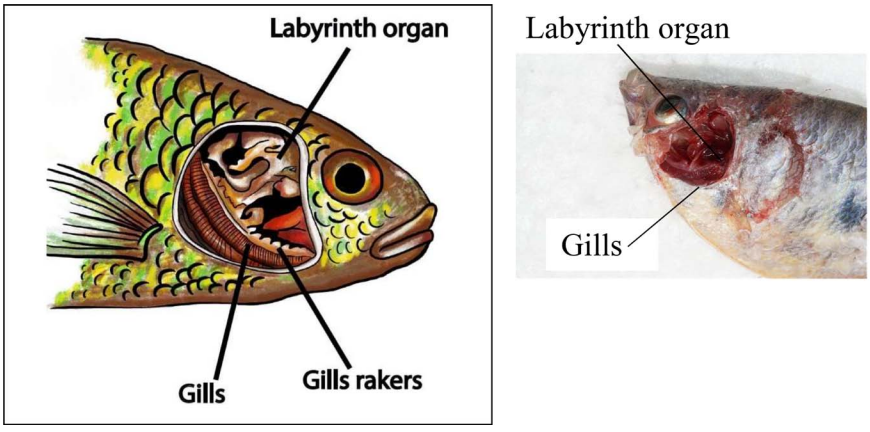

Figure 2. The suborder Labyrinthici is characterized by the presence of a chamber on the gills that retains air for breathing in low-oxygen environments (a *Helostoma* fish is shown).

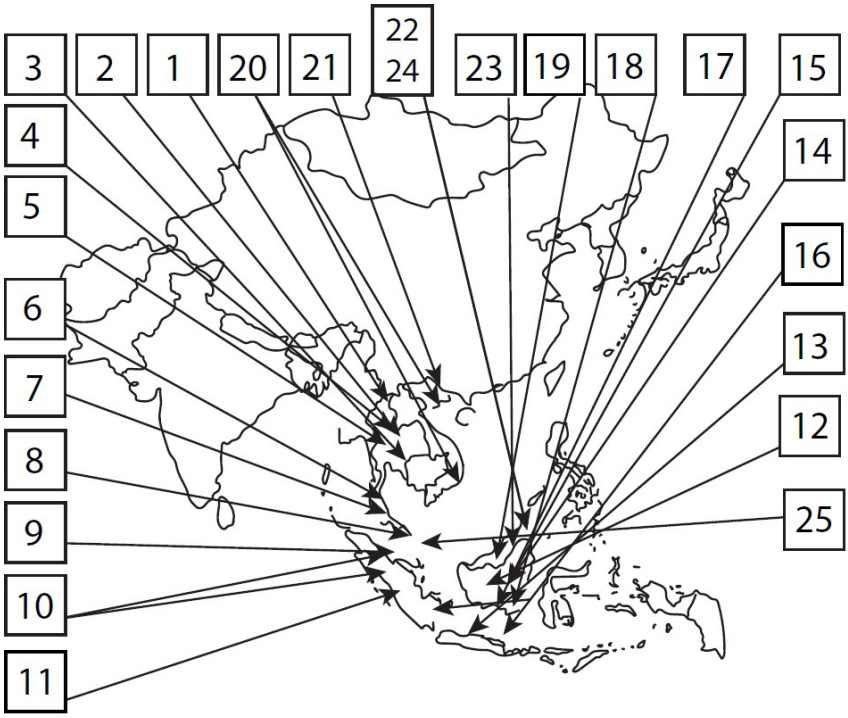

Batta omnellis	6	Parasphromenus deissneri	25
Batta splend'ens	5	Trichogaster leeri	9
Trichogaster trichoptenus	4	Trichogaster trichoptenus	10
Trichoposis punilus	3	Trichoposis punilus	11
Trichogaster microlepis	2	Trichogaster microlepis	12
Batta smaragdna	1	Batta smaragdna	13
Macropdus chinesis	24	Macropdus chinesis	14
macropdus operculars	20	macropdus operculars	15
Trichogaster pectoralis	21	Trichogaster pectoralis	16
Batta unimculata	22	Batta macrostoma	17
Batta macrostoma	23	Parosphromenus paludicola	18
Parosphromenus paludicola	7	Batta pugnax	19
Batta pugnax	8		

Figure 3. Distribution of labyrinth fish in Southeast Asia (Degani, 2001; Vierke, 1988).

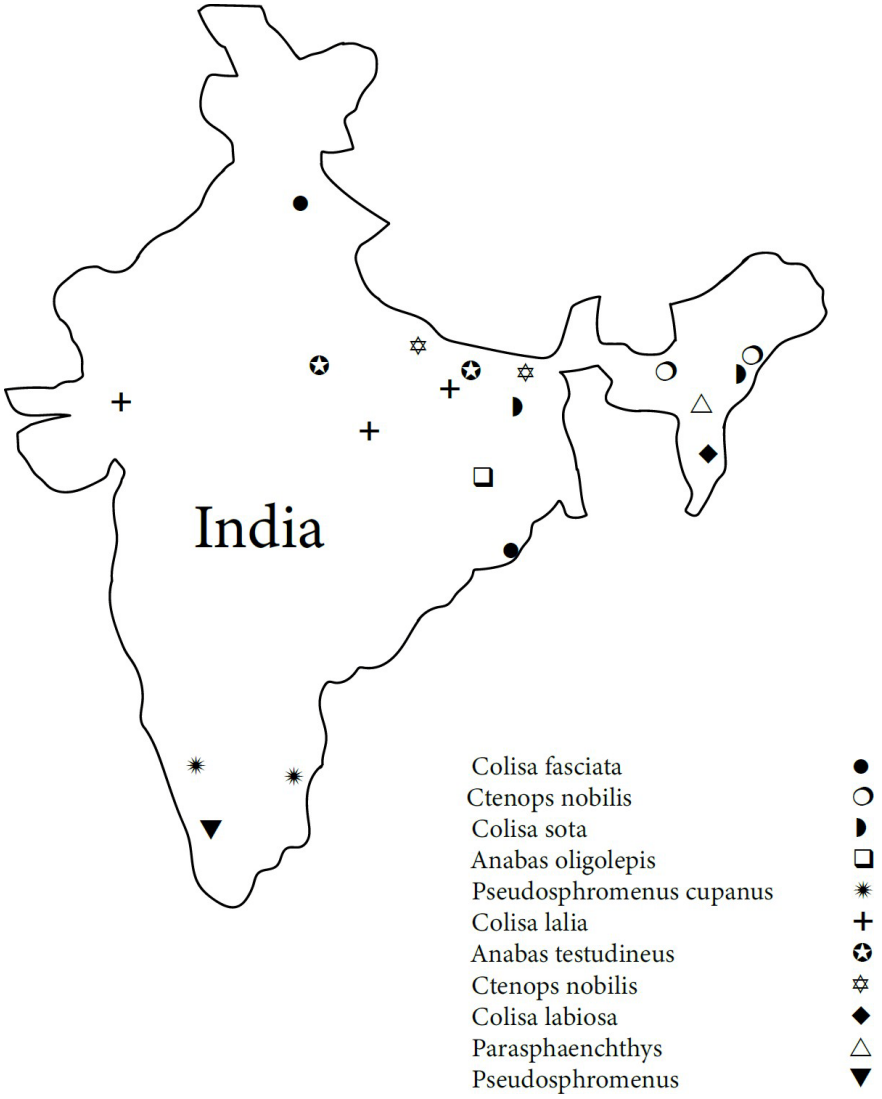

Figure 4. Distribution of labyrinth fish in India (Degani, 2001; Vierke, 1988).

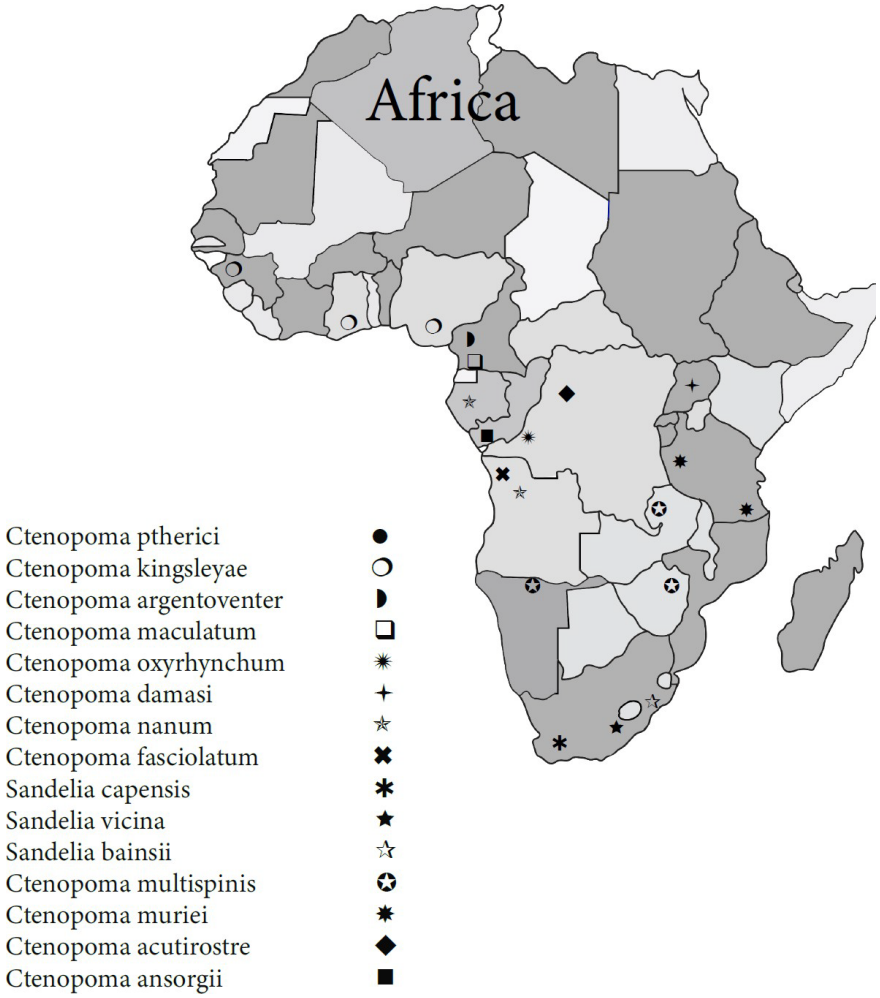

Figure 5. Distribution of labyrinth fish in Africa (Degani, 2001; Vierke, 1988).

Labyrinth fish habitats (**Figure 6**) include: among vegetation and reeds, water canals, ponds, streams that are rich in vegetation, and rice fields. Their habitats are characterized by seasonal changes in water volume, mainly due to rain (Degani, 2001).

Figure 6. Breeding habitat of labyrinth fish.

Chapter 2

Molecular Variations in Gene Markers in Blue Gourami as a Model for Labyrinth Fish

2.1. Introduction

Genetic variability among organisms occurs across the genome (whole DNA) due to difference in genes controlling the amino acid structures of proteins. These variations in DNA or mRNA can serve as molecular markers to distinguish between organisms, including fish, at all systemic levels (Chauhan and Rajiv, 2010; Degani, 2013; Degani and Veit, 1990; Degani et al., 2006, 2019a, 2019b; Maqsood and Ahmad, 2017; Okumus and Ciftci, 2003). In comparison to studies of genetic markers in some fish species of great economic value, little research has been done on the labyrinth fish.

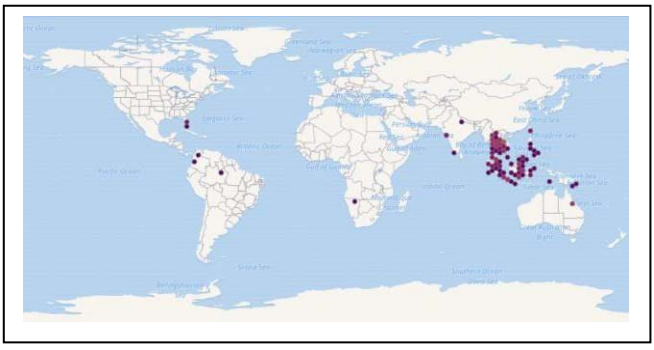

Figure 7. Known global distribution of blue gourami (*Trichogaster trichop-*

terus). Indicated locations are in Australia, Papua New Guinea, Indonesia, Malaysia, the Philippines, Taiwan, Vietnam, Cambodia, Laos, Thailand, Myanmar, India, Namibia, Colombia, Brazil, and the United States. Note: locations in southern Florida were not used to select source points in the climate match, as their introduction there is considered to have failed (Degani, 2001; Vierke, 1988; Froese, and Pauly, 2019).

2.2. Sequencing Analysis of Cytochrome Genes to Analyze Variations in the Blue Gourami among the Anabantoidei

2.2.1. Introduction

The decline of ornamental fish populations in their native habitats, mainly in tropical areas (due to overfishing for the tropical fish market), has led to their introduction into aquaculture and to the development of this relatively new industry. The Anabantoidei suborder has thus become important to the ornamental fish industry (Degani, 2001). However, information on molecular variations in species belonging to the Anabantoidei in the order Perciformes (perch-like) is very limited (Degani, 2013; Degani and Veit, 1990; Ruber et al., 2006). Twenty-two isozyme systems in the muscle and liver of 10 species of the Anabantidae family were investigated by starch gel electrophoresis (Degani and Veit, 1990). Two species of this family—*Trichogaster trichopterus* and *Trichogaster leerii*—are similar morphologically and in geographical distribution. Another species, *Colisa lalia*, does not exhibit an overlapping geographical distribution, but shows a high similarity to *Betta betta*, which is distributed in the small area covered by the *Trichogaster* genus. However, the gene loci

of *Colisa* species show a higher degree of similarity to those of the *Trichogaster* species than to those of the *Betta* species (Degani and Veit, 1990). The population structures of *Trichogaster pectoralis* collected from five locations in Thailand (Samut Prakan, Phitsanulok, Suphan Buri, Ubon Ratchathani and Pattani) were studied by isozyme analysis (Pongthana, 2001).

2.2.2. Mitochondrial DNA Sequence Analysis of Blue Gourami Compared to Other Anabantoidei Fish

Several sets of degenerate oligonucleotides were used to clone DNA fragments encoding portions of the cytochrome *b* and 12S genes (Degani, 2013). Using these genes, the genetic variations among species of this suborder were examined by mitochondrial gene-sequencing analysis. The results demonstrated the similarity between gene sequences of the various Belontiidae species, leading us to hypothesize that these genes could serve as molecular markers for the systematic study of Belontiidae reproduction.

Looking at the cytochrome *b* gene (**Figure 8** and **Figure 9**), the most similar strains were *Trichogaster trichopterus* (gold) and *Trichogaster trichopterus* (blue) (100%). *Trichogaster leerii* was less similar to them (86.0%), and even lower similarity was found between *T. trichopterus* and *Trichogaster labiosus* (85.6%). *T. labiosus* was found to be more similar to sequences of the *Colisa* genus (88.0%) than to those of the *Trichogaster* genus. The least similarity was observed between *Betta betta* and the genera *Colisa* (50.2%) and *Trichogaster* (60.1%). The

similarity value for *Macropodus opercularis* was between that of *Betta* and *Colisa*.

The 12S gene sequences of the species *T. trichopterus* (gold), *T. trichopterus* (blue), *T. leerii*, *C. lalia* and *B. betta* are shown in **Figure 10**,

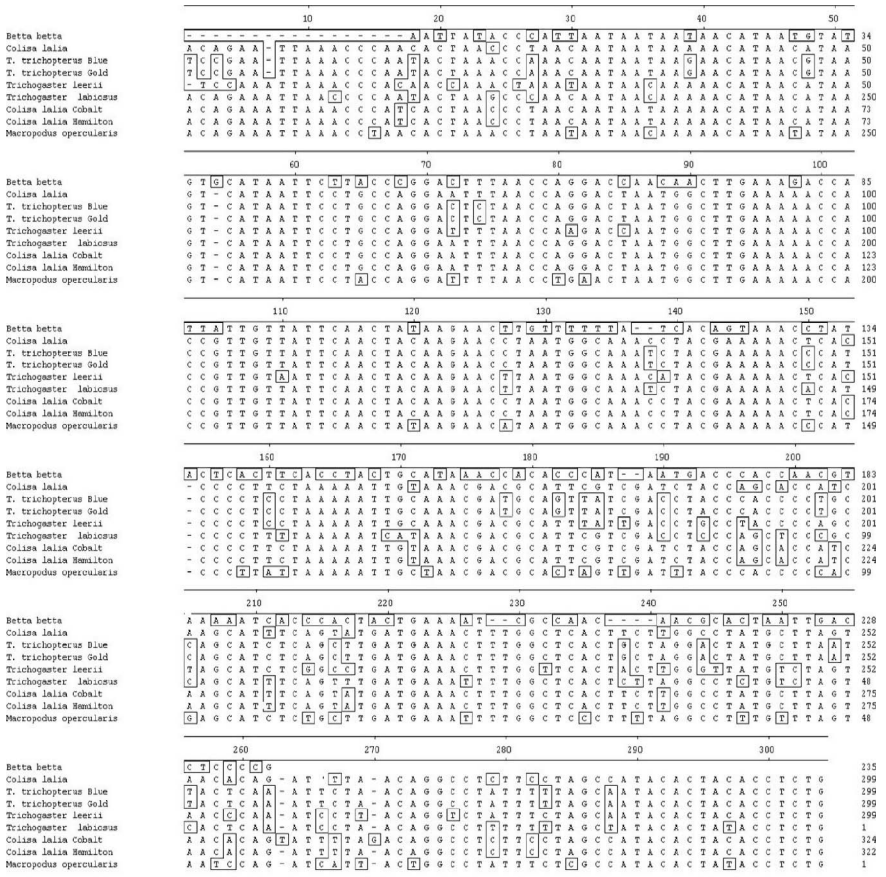

Figure 8. Comparison of cytochrome *b* nucleotide sequences in *Trichogaster trichopterus* (blue and gold gourami), *Trichogaster leerii* (pearl gourami), *Colisa lalia* (dwarf gourami), *Trichogaster labiosus* (*Colisa labiosa*), *Betta betta* (Regan) (fighting fish) and *Macropodus opercularis* (Degani, 2013).

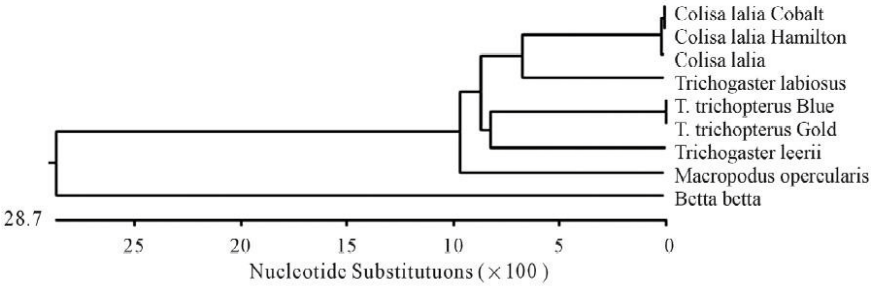

(a)

Percent Identity

1	2	3	4	5	6	7	8	9		
	60.2	58.9	58.9	60.2	60.2	60.2	37.1	35.8	1	Betta betta
		86.6	86.6	83.9	99.7	99.7	41.0	39.7	2	Colisa lalia
			100.0	86.0	86.3	86.3	39.0	38.6	3	T. trichopterus Blue
				86.0	86.33	86.3	39.0	38.3	4	T. trichopterus Gold
					83.9	83.9	40.0	38.0	5	Trichogaster leerii
						100.0	41.0	40.0	6	Colisa lalia Cobalt
							41.2	40.3	7	Colisa lalia Hamilton
								84.5	8	Macropodus opercularis
									9	Trichogaster labiosus

(b)

Figure 9. Composite phylogeny tree. (a) Tree constructed from the analysis of cytochrome *b* sequences of: *Trichogaster trichopterus* (blue gourami and gold gourami), *Trichogaster leerii* (pearl gourami), *Colisa lalia* (dwarf gourami), *Trichogaster labiosus* (*Colisa labiosa*), *Betta betta* (Regan) (fighting fish) and *Macropodus opercularis.* The phylogenetic tree was constructed by Clustal W method using the MegAlign program (DNASTAR). Branch lengths represent evolutionary distances. (b) Table of identities according to analysis (Degani, 2013).

and the nucleotide similarity phylogenetic tree is presented in **Figure 11** (Degani, 2013). The 12S gene phylogenetic tree results were very similar to those of the cytochrome *b* gene. The sequence similarity between the species belonging to the *Trichogaster* genus was high (91.4% - 100%), and there was less similarity between this genus

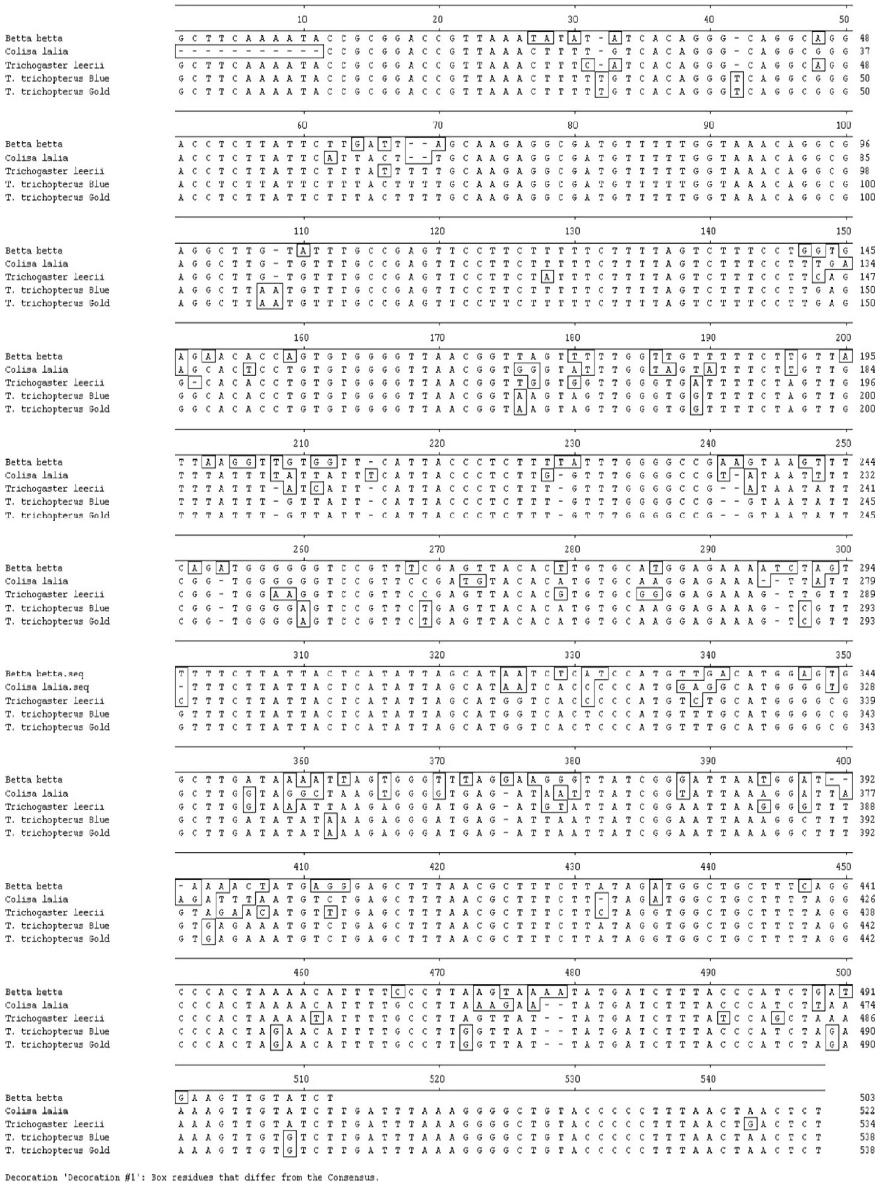

Figure 10. Comparison of the 12S gene nucleotide sequences in *Trichogaster trichopterus* (blue gourami and gold gourami), *Trichogaster leerii* (pearl gourami), *Colisa lalia* (dwarf gourami) and *Betta betta* (Regan) (fighting fish) (Degani, 2013).

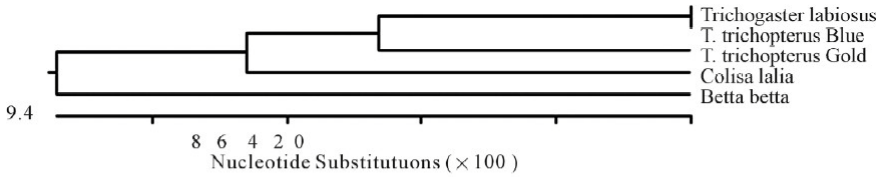

(a)

Percent Identity

1	2	3	4	5		
	84.0	82.6	82.6	82.8	1	Betta betta
		88.4	88.4	87.5	2	Colisa lalia
			100.0	91.4	3	T. trichopterus Blue
				91.4	4	T. trichopterus Gold
					5	Trichogaster leerii

(b)

Figure 11. Composite phylogeny tree (a) constructed from analysis of 12S sequences of *Trichogaster trichopterus* (blue gourami and gold gourami), *Trichogaster leerii* (pearl gourami), *Colisa lalia* (dwarf gourami) and *Betta betta* (Regan) (fighting fish). The phylogenetic tree was constructed by Clustal W method using the MegAlign program (DNASTAR). Branch lengths represent evolutionary distances. (b) Table of identities according to analysis (Degani, 2013).

and *C*. *lalia* (88.4%). In addition, less similarity was evident between *T. trichopterus* and *C. lalia* than between *T*. *trichopterus* and *B*. *betta* (82.6% and 84.0%, respectively) (Degani, 2013).

The Anabantoidei fish cytochrome *b* and 12S gene sequences were compared to those of other fish and are presented as a phylogenetic tree of nucleotide similarity (**Figure 12**, **Figure 13**). In this comparison, some fish which do not belong to the Anabantoidei seemed to have a high similarity to the Anabantoidei fish.

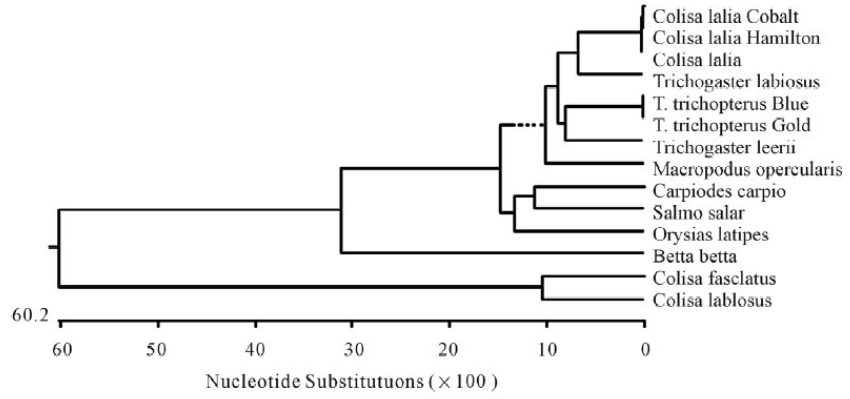

(a)

Percent Identity

1	2	3	4	5	6	7	8	9	10	11	12	13	14		
	59.2	60.1	60.1	60.9	60.1	59.2	59.2	58.4	59.2	42.3	38.5	59.1	56.7	1	Betta betta
		85.9	85.9	83.9	88.0	99.7	99.7	83.9	78.6	43.5	42.8	79.2	82.9	2	Colisa lalia
			100.0	86.0	85.6	85.6	85.6	81.6	77.9	46.2	42.1	74.8	76.9	3	T. trichopterus Blue
				86.0	85.6	85.6	85.6	81.6	77.9	46.2	42.1	74.8	76.9	4	T. trichopterus Gold
					82.3	83.9	83.9	81.6	78.9	43.5	44.1	77.5	78.6	5	Trichogaster leerii
						87.7	87.7	83.3	77.7	43.3	41.0	78.9	80.0	6	Trichogaster labiosus
							100.0	83.7	78.7	43.2	42.5	78.6	82.7	7	Colisa lalia Cobalt
								83.7	78.7	43.3	42.7	78.6	80.7	8	Colisa lalia Hamilton
									77.7	45.0	45.0	76.3	79.3	9	Macropodus opercularis
										43.9	41.9	76.9	80.7	10	Carpiodes carpio
											82.3	42.5	44.5	11	Colisa fasclatus
												42.5	43.9	12	Colisa lablosus
													78.6	13	Orysias latipes
														14	Salmo salar

(b)

Figure 12. Unrooted phylogenetic tree (a) of the cytochrome *b* fragment based on nucleotide sequences of various fish species. The length of each pair of branches represents the distance between sequence pairs, while the units at the bottom of the tree indicate the number of substitution events. The phylogenetic tree was constructed by Clustal W method using the MegAlign program (DNASTAR). (b) Table of identities according to analysis (Degani, 2013).

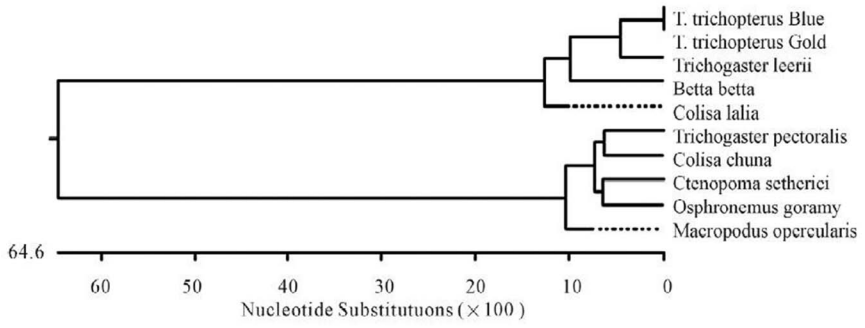

(a)

Percent Identity

1	2	3	4	5	6	7	8	9	10		
■	39.8	88.6	40.9	87.0	89.3	88.8	39.8	40.5	40.5	1	Trichogaster pectoralis
	■	39.9	84.0	40.3	41.3	39.4	82.8	82.6	82.6	2	Betta betta
		■	40.8	85.3	86.8	87.2	40.2	41.4	41.4	3	Colisa chuna
			■	41.9	42.3	40.9	87.8	88.4	88.4	4	Colisa lalia
				■	85.7	88.2	41.1	41.1	41.1	5	Ctenopoma setherici
					■	87.7	41.8	41.9	41.9	6	Macropodus opercularis
						■	40.2	40.5	40.5	7	Osphronemus goramy
							■	91.4	91.4	8	Trichogaster leerii
								■	100.0	9	T. trichopterus Blue
									■	10	T. trichopterus Gold

(b)

Figure 13. Unrooted phylogenetic tree (a) of the 12S fragment based on nucleotide sequences. The length of each pair of branches represents the distance between sequence pairs, while the units at the bottom of the tree indicate the number of substitution events. The phylogenetic tree was constructed by Clustal W method using the MegAlign program (DNASTAR). (b) Table of identities according to analysis (Degani, 2013).

2.2.3. DNA Sequence Analysis of Genes Encoding Hormones of the Hypothalamus-Pituitary Gland (HPG) Axis as Molecular Markers for Genetic Similarity between Species of Blue Gourami and Other Anabantoidei Fish

In teleosts, as in other vertebrates, kisspeptin (Kiss) has recently garnered considerable attention as a potential key player in indirect

neuroendocrine control of reproduction (Oakley et al., 2009). Kiss is a member of the RFamide peptide family. Originally identified as a metastasis suppressor in mammals, the Kiss1 gene produces several Kiss peptides in mammals. Kiss-54 and its endogenous variants, Kiss-14, Kiss-13 and Kiss-10, are generated by proteolytic cleavage of the Kiss precursor derived from the Kiss1 gene.

The Kiss peptides share a common core sequence of 10 amino acids (aa) (Kiss-10) at their C terminus, which allows them to bind to their cognate G-protein-coupled receptor (GPR54) or Kiss1 receptor (Kiss1R) (Servili et al., 2011). Thus, Kiss1 controls the HPG axis, acts on the caudal hypothalamus, and seems to affect receptors of gonadotropin-releasing hormone (GnRH) (Servili et al., 2011; Shahjahan et al., 2010). It controls the release of pituitary gonadotropins (GtHs), follicle-stimulating hormone (FSH) and luteinizing hormone (LH), which in turn control gametogenesis (Yaron and Levavi-Sivan, 2011) through steroids (Degani, 1990; Degani and Boker, 1992a, 1992b). Studies on Kiss peptides in teleosts have shown some variation in their involvement in reproduction; more detailed studies are required due to the relatively large systematic class and high variations of hormones involved in reproduction. The brain of zebrafish (*Danio rerio*), one of the most intensively studied model fish, has two Kiss genes, *Kiss1* and *Kiss2*, and two Kiss receptors (GPR54), Kiss1R and Kiss2R (Lee et al., 2009; Servili et al., 2011), similar to other fish, such as lamprey (*Petromyzon marinus*) (Lee et al., 2009), medaka (*Oryzias*

latipes) (Kitahashi et al., 2009), goldfish (*Carassius auratus*) (Huang et al., 2009) and sea bass (*Morone saxatilis*) (Espigares et al., 2017).

Degani et al. (2017) studied the DNA sequence of the brain Kiss2 and two Kiss receptors (GPR54), Kiss1R and Kiss2R, in blue gourami. The deduced partial sequences of Kiss2 in blue gourami were compared with homologous sequences from a number of other fish species (**Figure 14**).

There was a low degree of similarity at both the nucleotide and amino acid levels between the blue gourami Kiss2 sequences and those of the other fish (**Figure 14**). A higher degree of cDNA similarity was found between blue gourami *Kiss2R* and that of the other fish species than for *Kiss2* (**Figure 15**).

The deduced sequences of Kiss1R in the blue gourami were compared with homologous sequences from a number of other fish species. There was a low degree of similarity at both the nucleotide and amino acid sequence levels between the blue gourami and the other fish species (**Figure 16**).

To determine whether *Kiss1*, *Kiss2*, *Kiss1R* and *Kiss2R* genes are expressed in the brains of females, total RNA was reverse-transcribed using quantitative (q) PCR amplification and compared to the *β*-actin gene. Amplification curves represented cDNA detected in samples treated for ALDOA siRNA (**Figure 16**).

GnRH plays a central role in the control of vertebrate reproduction

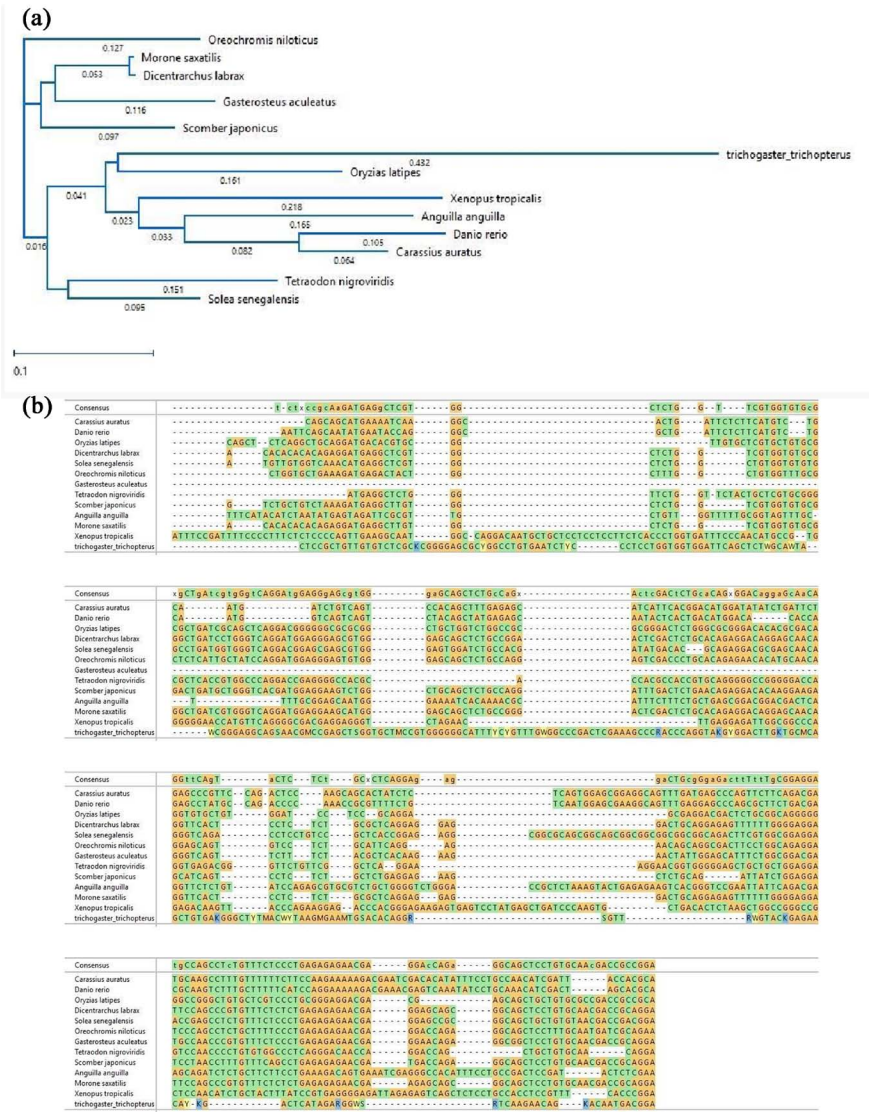

Figure 14. (a) Phylogenetic tree showing the relationship between *Kiss2* cDNA sequences in fish. The tree was generated using DNA Star MegAlign PRO MAFFT. The blue gourami sequence was obtained from Degani et al. (2017). All other sequences were obtained from NCBI GenBank according to the accession numbers described in detail in Degani et al. (2017). (b) Nucleotides and deduced amino acid sequences.

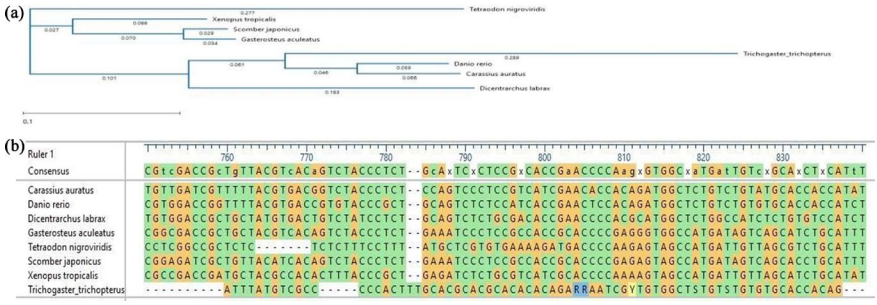

Figure 15. (a) Phylogenetic tree showing the relationship between vertebrate Kiss2R amino acid sequences. The tree was generated by maximum Clustal W using DNAStar WI Megalign software. (b) Sequence alignment was conducted using DNA Star MegAlign Pro Clustal Omega. *Trichogaster trichopterus* sequence was obtained from Degani et al. (2017). All other sequences were obtained from NCBI GenBank.

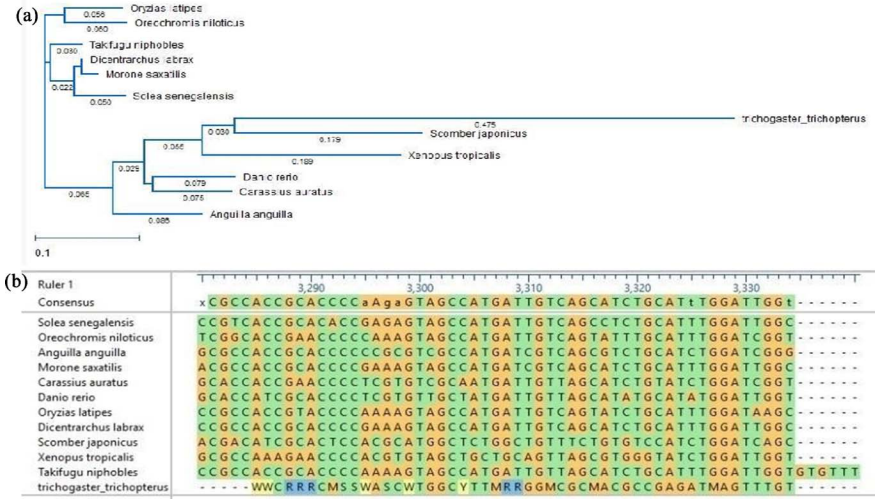

Figure 16. (a) Phylogenetic tree showing the relationship between vertebrate *Kiss1r* cDNA sequences. The tree was generated using DNA Star MegAlign PRO MAFFT. (b) Sequence alignment. *Trichogaster trichopterus* sequence was obtained from Degani et al. (2017). All other sequences were obtained from the NCBI GenBank according to the accession numbers provided in Degani et al. (2017). The units of branch length represent nucleotide substitutions per site.

by affecting various hormones, e.g., GtHs and the growth hormone (GH) family, which in turn regulate gametogenesis and steroidogenesis (Levy and Degani, 2012; Sower et al., 2009). cDNA cloning of three GnRH forms (GnRH1, GnRH2 and GnRH3) from blue gourami was described (Levy and Degani, 2012, 2013; Levy et al., 2009). The blue gourami *GnRH1* cDNA is 393 bp long, and it has an open reading frame of 273 bp encoding a 90-aa precursor peptide. The 5' and 3' untranslated regions (UTRs) are 59 and 61 bp in length, respectively. A putative poly(A) signal, AATAAA, was recognized 22 bp upstream of the poly(A) tail. The GnRH1 precursor is comprised of a 22-aa signal peptide, the GnRH decapeptide, a 3-aa processing site (GKR) and a 58-aa GnRH-associated peptide (GAP). The blue gourami *GnRH2* cDNA is 525 bp long, and it has an open reading frame of 258 bp encoding an 85-aa precursor peptide. The 5' and 3' UTRs are 103 and 164 bp in length, respectively. A putative poly(A) signal, ATTAAAA, was recognized 17 bp upstream of the poly(A) tail. The GnRH2 precursor is comprised of a 23-aa signal peptide, the GnRH decapeptide, a 3-aa processing site (GKR) and a 49-aa GAP (**Figure 17**).

The schematic structure of the GnRH3 cDNA sequence is presented in **Figure 18(A)** (Levy et al., 2009). The full-length cDNA sequence of GnRH3, which was compiled from the data obtained from 5' and 3' RACE, and its deduced amino acid sequence are shown in **Figure 18(B)** (EMBL acc. no. EU107388). The blue gourami *GnRH3* cDNA is

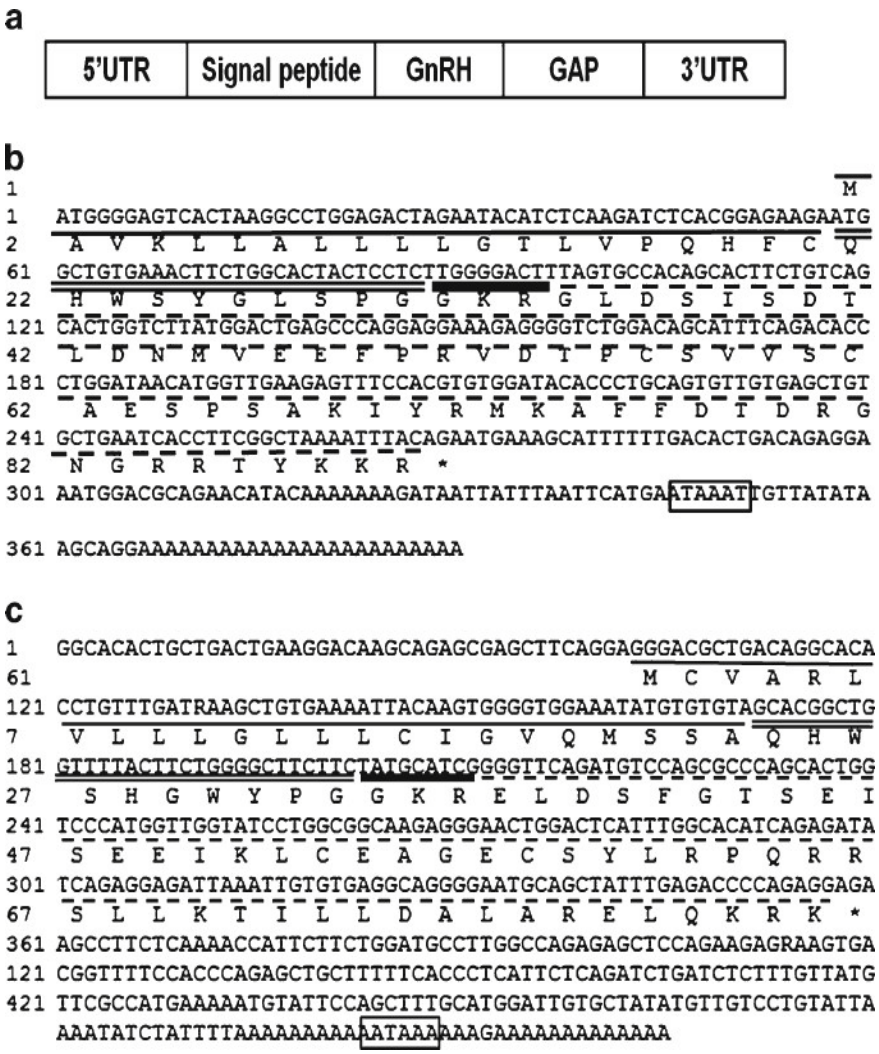

Figure 17. Schematic structures and sequences of GnRH. (a) Schematic structure of the prepro-GnRH of blue gourami. (b) cDNA sequence of GnRH1. (c) cDNA sequence of GnRH2. GnRH1 and GnRH2 cDNA signal peptides are underlined with a solid black line. GnRH sequence is double-underlined and the cleavage site is marked by a bold black line. The GAP sequence underlined with a dashed black line and the 3' poly(A) signal AATAAA-associated protein is boxed. UTR, untranslated region (Levy and Degani, 2011; Levy et al., 2009).

A

B

```
  1                                          M  E  A  R  S  R  A  M  V  Q  A
  1 CATGCTAACAGGTCCAGTACAAAGCTCCAATGGAGGCGCGAAGCAGAGCGATGGTGCAGG

 21   V  L  L  A  L  V  V  Q  V  S  L  S  Q  H  W  S  Y  G  W  L
 61 CGGTGCTGCTGGCGCTGGTGGTCCAGGTCAGCCTGTCCCAGCACTGGTCCTACGGATGGT

 41   P  G  G  K  R  S  V  G  E  L  E  A  T  I  R  M  M  G  T  G
121 TACCGGGTGGAAAGAGAAGCGTGGGAGAGTTGGAGGCGACCATCAGGATGATGGGCACAG

 61   G  V  M  S  L  P  D  E  P  S  A  Q  T  H  E  R  L  R  P  Y
181 GAGGAGTGATGTCTCTTCCTGACGAGCCAAGTGCCCAAACCCATGAGAGGCTTAGACCAT

 81   N  V  I  N  E  D  S  G  P  F  D  R  K  K  R  F  S  P  N  *
241 ACAATGTTATTAACGAGGATTCCGGTCCTTTTGACCGAAAGAAAAGGTTTTCTCCTAACT

301 GAGGAGCTGATGGAACAAATGGAAACGCAGGCTATGTTAACAAGTCGTCACATGTATGAT

361 TACGCTATTATCAGTCATGCGTCTGTGACGTTTTAATCTGTGGCTCATTAGAATAAAGTT

421 TTTGAAACCAAAAAAAAAAAAAAAAAAAAAAAAAAA
```

Figure 18. Schematic structures and sequences of GnRH3. (A) Schematic structure of the prepro GnRH3 of blue gourami. (B) cDNA sequence of GnRH3. Signal peptide is underlined with a solid black line. The GnRH3 sequence is double-underlined and the cleavage site position is underlined with a bold black line. The GAP sequence is underlined with a dashed black line and the 3' poly(A) signal ATAAA is boxed. UTR, untranslated region (Levy et al., 2009).

456 bp long, and it has an open reading frame of 275 bp, encoding a 90-aa precursor peptide. The 5' and 3' UTRs are 29 bp and 154 bp in length, respectively (Levy et al., 2009). A putative poly(A) signal, AATAAA, was recognized 18 bp upstream of the poly(A) tail. The GnRH3 precursor is comprised of a 23-aa signal peptide, the GnRH decapeptide, a 3-aa processing site (GKR) and a 54-aa GAP. The cal-

culated molecular mass of the GnRH3 polypeptide chain is 10,027 Da, with an isoelectric point of 9.39. As shown in **Table 1** (Levy et al., 2009), the degree of identity between the blue gourami GnRH1 pre-prohormone amino acid sequence and that of other fish was 80% - 82.2% (Levy et al., 2009).

Table 1. Nucleotide and amino acid similarity (%) between cDNA sequence of GnRH1 of blue gourami and other teleosts.

Order	Species	Accession No.	% Amino acid identity	% Nucleotide identity
Perciformes (Scombridae)	*Thunmus thynmus*	EU239500	70.3	74.3
Perciformes (Serranidae)	*Epinephelus bruneus*	FJ380047	64.8	72.3
Perciformes (Cichlidae)	*Oreochromis niloticus*	AB101665	67	68.2
Perciformes (Moronidae)	*Morone chrysops*	DQ000672	61.5	62.6
Pleuronectiformes	*Paralichthys olivaceus*	DQ074693	50.5	51.4
	Verasper variegatus	HM131600	62.6	70.5
Atherinomorpha	*Odontesthes bonariensis*[a]	AY 744689	33	22.6
	Fundulus heteroclitus	AB302265	65.9	60.8
	Coregomus clupeaformis[b]		47.3	54.2
Mugilomorpha	*Mugil cephalus*	AY373450	62.6	59

There was a higher degree of similarity at both the nucleotide and amino acid levels between the blue gourami sequence and the respective sequences of *Dicentrarchus labrax* and *Pagrus major* (belonging to the order Perciformes). In other perciforms (*Cynoscion*

nebulosus, Rachycentron canadum, Sciaenops ocellatus and *Mugil cephalus*), a higher degree of amino acid sequence similarity was found compared to the more variable nucleotide sequence (Levy et al., 2009).

2.2.4. DNA Sequence Analysis of Genes Encoding FSH and LH as Molecular Markers for Genetic Similarity between Species of Blue Gourami and Other Anabantoidei Fish

The *FSH* and *LH* cDNAs from the pituitary gland of blue gourami encoding the α and *β* subunits of the GtH hormones FSH and LH (Jackson et al., 1999) were cloned. The two cDNAs were sequenced and analyzed. The deduced amino acid sequences of FSH-*β* and LH-*β* cDNAs are presented in **Figure 19** and **Figure 20**.

Blue gourami FSH-*β* was most similar to its striped bass counterpart, with the two polypeptides sharing 73% of their residues. The lowest similarity was found between blue gourami FSH-*β* and that of goldfish, with only 44% identical residues. The relationships among the various of FSH-*β* subunits are presented in **Figure 21(A)** (Jackson et al., 1999). Similarly, the amino acid sequence of the blue gourami LH-*β* was compared with those of other fish (**Figure 21(B)**) (Jackson et al., 1999). The dendrogram shows highest similarity with striped bass LH-*β*, with 84% identical residues. The lowest similarity was found with the Baikal omul LH-*β* (only 65% identical residues).

A.

```
   1  GTCTGTACAGATGTTTAGAGAGTAACAGGCAAAACCTGCAGCAGAGGTTCAACGAGACAA   60

  61  CAGAGATTTACAGGCGTCTGTGCTGCACCCAAAGGATGCAGCTGGTTGTCATGGCAGCAG  120
                                          MetGlnLeuValValMetAlaAlaV

 121  TGTTGGCAGTGGCGGGGGTGGGACAGGGTTGCCGCTTCGGCTGTCATCTAACCAACATCA  180
      alLeuAlaValAlaGlyValGlyGlnGlyCysArgPheGlyCysHisLeuThrAsnIleS

 181  GCTTCCCCGTAGACAGCTGTGGCATCACCGAGTTCATCTACACCACCATATGCGCAGGAC  240
      erPheProValAspSerCysGlyIleThrGluPheIleTyrThrThrIleCysAlaGlyH

 241  ATTGCTACCACGAGGATCCAGTCTACATCGGCCACGATGACTGGGCTGAACAGAAAATCT  300
      isCysTyrHisGluAspProValTyrIleGlyHisAspAspTrpAlaGluGlnLysIleC

 301  GTAACGGGGACTGGACCTACGAAGTAAAACACCTACAAGGATGTCCGGTGGCTGTCACGT  360
      ysAsnGlyAspTrpThrTyrGluValLysHisLeuGlnGlyCysProValAlaValThrT

 361  ACCCTGTTGCCAGAAACTGCGAGTGTACTGCTTGTAATGCAGGAAACACATACTGTGGTC  420
      yrProValAlaArgAsnCysGluCysThrAlaCysAsnAlaGlyAsnThrTyrCysGlyH

 421  ACTTTCATGGATACATACCCAGCTGTCTGTGATTTCAAAGGCACTCATCATTCATCCCAC  480
      isPheHisGlyTyrIleProSerCysLeu

 481  GTTTACTTTGCATCTTTCTCTGATGGTACTAAAATAAACAGATATGTCTTAAAAAAAAAA  540

 541  AAAAAAAAAAAAAAAAAAAAAAAAAAAAAA  570
```

B.

```
   1  CTGGCTAACCTGCCGCTGACACTAAAGAGGATGATGACTGTAGAAATAAGCAAAGTGTTT   60
                                          MetThrValGluIleSerLysValPhe

  61  GTCCTAATGATGTTAAACCTCTTTCTGGGAGCTTCATCTTCCATTTGGTCTGTGGCTCCA  120
      ValLeuMetMetLeuAsnLeuPheLeuGlyAlaSerSerSerIleTrpSerValAlaPro

 121  GCAGCAGCCTTCCAGCTGCCACCGTGTCAGCTCATCAACCAGACTGTCTCTCTGGAGAAG  180
      AlaAlaAlaPheGlnLeuProProCysGlnLeuIleAsnGlnThrValSerLeuGluLys

 181  GAAGGCTGCCCCAGGTGTCACGCAGTGGAAACGACAATCTGCAGTGGCCACTGCCTCACC  240
      GluGlyCysProArgCysHisAlaValGluThrThrIleCysSerGlyHisCysLeuThr

 241  AAGGACCCAATCATCAAGATACCGTTCAGCAATGTGTACCAGCACGTGTGCACATACCGG  300
      LysAspProIleIleLysIleProPheSerAsnValTyrGlnHisValCysThrTyrArg

 301  GATTTGTTCTATAAGACATTTGAGTTTCCTGACTGTCCTCCTGGTGTGGACCCAGTCGTC  360
      AspLeuPheTyrLysThrPheGluPheProAspCysProProGlyValAspProValVal

 361  ACCTACCCTGTGGCTCTGAGCTGCCACTGCAGCCGTTGTGTGATGGACACATCCGATTGC  420
      ThrTyrProValAlaLeuSerCysHisCysSerArgCysValMetAspThrSerAspCys

 421  ACCTTCGAGAGTCTTCAGCCAGACTTCTGCATGAATGACATACCTTTCTACTACTAGTCT  480
      ThrPheGluSerLeuGlnProAspPheCysMetAsnAspIleProPheTyrTyr

 481  GATGAAATAGCTGCACAGCAAACCAAAAGCAAAAGTAAAATAAATGAATTGTGACAAAAA  540

 541  AAAAAAAAAAAA  552
```

Figure 19. Nucleotide sequences of blue gourami FSH-β (A) and LH-β (B). The amino acid sequence of each hormone appears in its three-letter code. GenBank accession numbers: AF157630 and AF157631, respectively (Jackson et al., 1999).

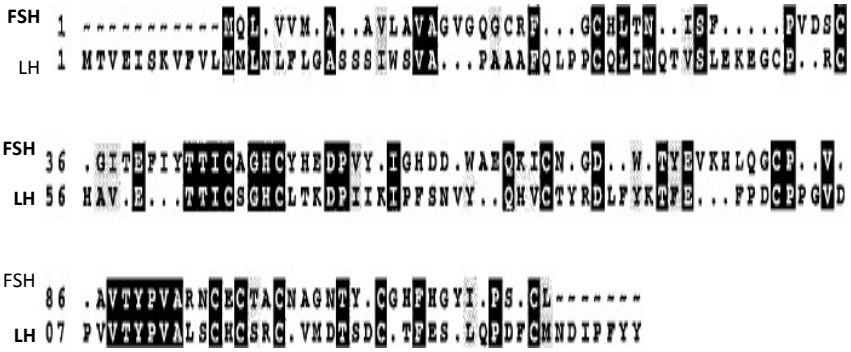

Figure 20. Comparison of the amino acid sequences of FSH-β and LH-β. Identical amino acids are boxed in black, and residues with similar physicochemical properties are boxed in gray (Jackson et al., 1999).

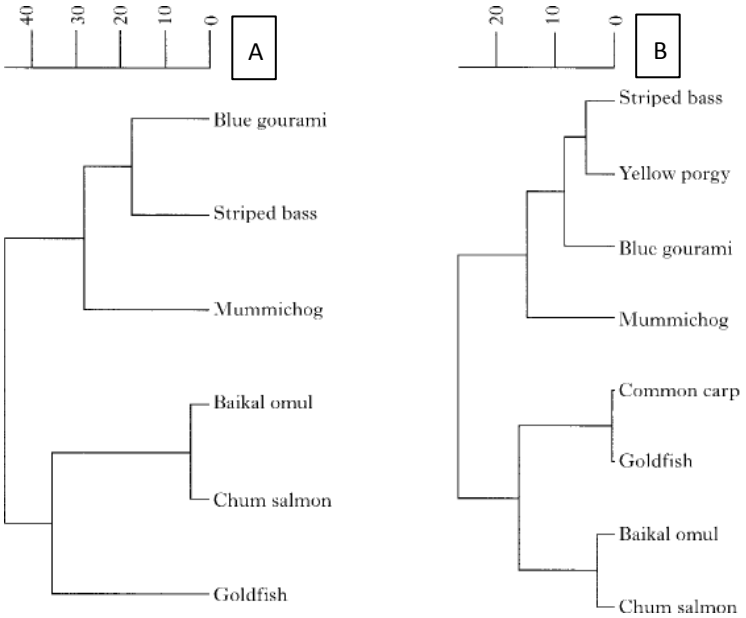

Figure 21. Dendrograms providing a graphical representation of the relations among various fish FSH-β (A) and LH-β (B). The dendrograms were created by UPGMA from similarity matrices produced from the corresponding sequence alignments. The scale bar is a measure of the estimated number of amino acid substitutions per 100 residues, found by comparing the sequences in a pairwise fashion (Jackson et al., 1999; Yom Din et al., 2008).

2.2.5. DNA Sequence Analysis of Genes Encoding Components of the Hypothalamic-Pituitary-Somatotropic (HPS) Axis as Molecular Markers for Genetic Similarity between Species of Blue Gourami and Other Anabantoidei Fish

Pituitary adenylyl cyclase-activating polypeptide (PACAP) and PACAP-related protein (PRP) are members of the secretin/glucagon/vasoactive intestinal polypeptide (VIP) family. PACAP was first isolated from the ovine hypothalamus (Levy et al., 2010), and its sequence has also been established in representative species of non-mammalian vertebrates. In fish, PRP (formerly known as GHRH or GHRH-like peptide) was first isolated from the hypothalamus of common carp (Vaughan et al., 1992). In teleosts, the complete sequence of the *PRP* and *PACAP* cDNA has been cloned from several species (Levy et al., 2010). In all vertebrates, PACAP preprohormone consists of a signal peptide, a cryptic peptide, a PRP segment and a PACAP segment. Two processing sites, Lys-Arg and Gly-Arg-Arg, exist between the PRP and PACAP fragments and in the PACAP sequence, resulting in three peptides: PRP, PACAP27 and PACAP38. In several teleosts, two transcripts of PRP-PACAP exist as a result of exon skipping. This stems from alternative splicing resulting from the partial excision of exon 4 which encodes part of PRP (residues 1 - 32), leaving the PACAP-encoding region in the correct reading frame (Small and Nonneman, 2001).

PACAP can bind specifically to three G-protein-coupled receptor

(GPCR) variants (PACAP-Rs) termed: PAC1-R, VPAC1-R, and VPAC2-R (Levy et al., 2010). Differential distribution of PACAP-R has been identified in the brain, pituitary, heart, spleen, liver, gut, gills, kidney, skin, blood and gonads (Levy et al., 2010). PRP-R also belongs to the GPCR family, but has only been identified in non-mammalian species, e.g., the goldfish pituitary (Castro et al., 2009).

These findings suggest the exertion of evolutionary pressure to strongly preserve the bioactive sequence of PACAP, and clearly indicate that the peptide must exert important physiological functions. PACAP and PRP are involved in growth promotion and GH control. In teleosts, PACAP is involved in various physiological processes, such as brain development, ventilation and cardiac baroreflex control, digestive physiology, immune response, food intake and growth promotion (Lancien et al., 2011).

The structures of the *PRP-PACAP* cDNA are presented in **Figure 22(A)** (Levy et al., 2010), and the full-length cDNA sequence of the *PRP-PACAP* precursor, compiled from data obtained from 5’ and 3’ RACE, and its deduced amino acid sequence, are shown in **Figure 22(B)** (Levy et al., 2010).

Sequence analysis of overlapping 5’ and 3’ RACE products, isolated from the brain of gourami, revealed *PRP-PACAP* cDNA that is 985 bp long, with an open reading frame of 525 bp, encoding a 174-aa precursor peptide. The 5' and 3' UTRs are 275 bp and 184 bp in length, respectively, and the putative poly(A) signal is located 41 bp up

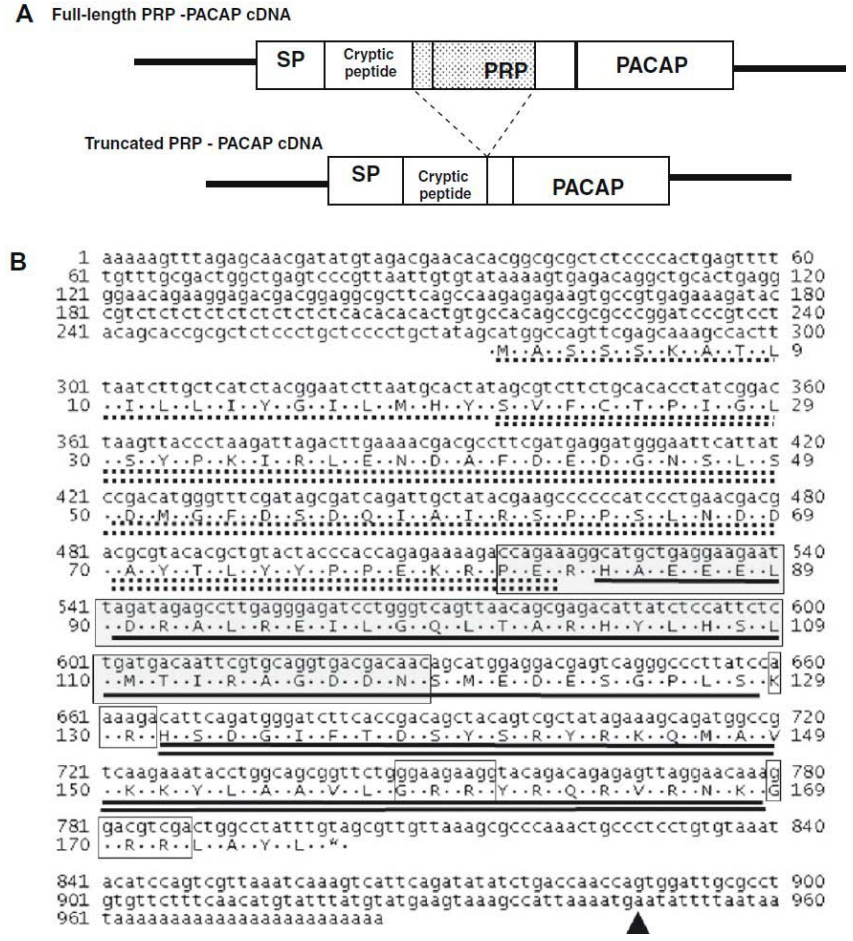

Figure 22. Schematic structures and sequences of PRP-PACAP. (A) Schematic structures of the prepro PRP-PACAP cDNA of the blue gourami. (B) cDNA sequence of PRP-PACAP. The signal peptide is underlined with a dashed black line, the cryptic peptide is underlined with dashed double lines, the PRP sequence is underlined with a single black line, the cleavage site positions are boxed, and the PACAP sequence is underlined with double black lines. The gray box designates the region that is deleted in the PRP-PACAP short form. The triangle denotes the poly (A) signal ATTAAA. UTR, untranslated region.

stream of the poly(A) tail. The blue gourami PRP-PACAP precursor is comprised of a 20-aa long signal peptide, a 62-aa long cryptic peptide and a 45-aa long PRP segment, a 2-aa processing site (KR) and a 38-aa long PACAP segment. The PACAP sequence was found to be similar to the PACAP38 form, containing the GRR sequence at a position which could yield the PACAP27 peptide. The deduced nucleotide and amino acid sequences of this gene in the blue gourami were compared with homologous sequences from a number of other fish species (**Figure 23**) (Levy et al., 2010). The peptide-cleavage sites, located at nucleotide positions 660, 747 and 780 and producing the

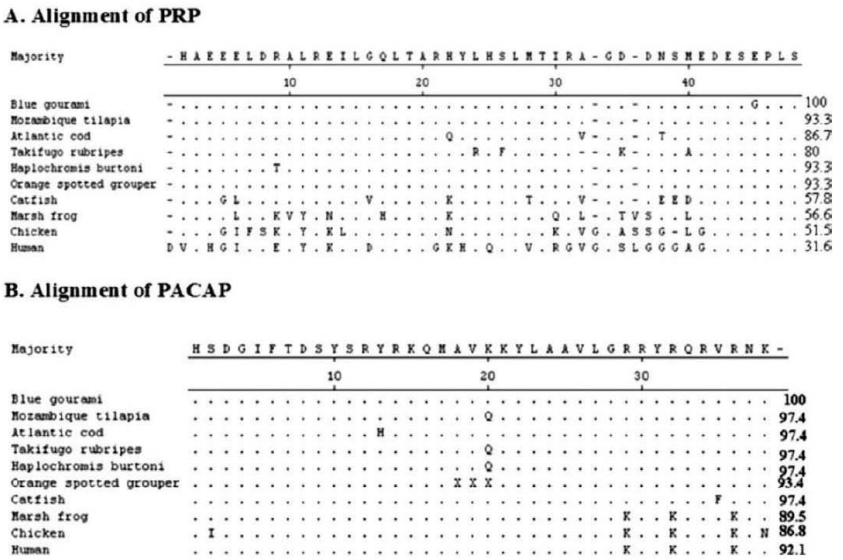

Figure 23. Amino acid sequence comparison of PRP (A) and PACAP (B) peptides. Sequence alignment was conducted using DNAStar WI Megalign ClustalW in the analysis of PRP and PACAP mature peptide sequences. PRP and PACAP of blue gourami were aligned with corresponding sequences of other vertebrates.

PRP, PACAP27 and PACAP38 isoforms, were fully conserved. Identical amino acids are represented by dots, whereas differing residues are shown in the single letter code for amino acids. PACAP is highly conserved, in contrast to PRP (Levy et al., 2010). In addition, the gourami had a shorter (by 114 bp) PRP-PACAP form, corresponding to the excision of 3 aa of the cryptic peptide and the first 35 aa of PRP (**Figure 23**) (Levy et al., 2010). Sequence alignment of the PRP amino acid sequence revealed that only the first 32 aa at the N terminus are highly conserved in closely related fish. There was 80.0% - 93.3% sequence similarity between the blue gourami PRP sequence and that of other teleosts, whereas there was only 31.6% - 56.6% sequence similarity with other tetrapods and fish (**Figure 23(A)**). On the other hand, the amino acid sequence of PACAP is highly conserved in mammals through fish.

2.2.6. DNA Sequence Analysis of the Genes Encoding GH and Prolactin (PRL) Family Hormones as Molecular Markers for Genetic Similarity between Species of Blue Gourami and Other Anabantoidei Fish

In the HPS axis, we analyzed genes that control growth and are involved in cell division in blue gourami but not in other species of Anabantoidei fish (Degani et al., 2006; Goldberg et al., 2004; Levy and Degani, 2012; Levy et al., 2010, 2011). cDNA encoding the complete GH of blue gourami was cloned by RACE-PCR using several sets of degenerate oligonucleotides. The full-length cDNA sequence was de-

termined from an 863-bp long clone that included a 43-bp poly(A) tail. The blue gourami GH showed an open reading frame starting at nucleotide 46 and ending at nucleotide 660 (Goldberg et al., 2004). The open reading frame encoded a pre-protein of 204 aa. The deduced amino acid sequence showed a putative signal peptide of 18 aa and a mature hormone of 186 aa (Goldberg et al., 2004) (**Figure 24**).

A dendrogram which graphically shows the relations among various fish GHs is shown in **Figure 25**.

The complete cDNA of blue gourami *PRL* was cloned by RACE-PCR (Degani et al., 2010). The 5' and 3' ends of the *PRL* cDNA were cloned separately, but with a short overlap that allowed them to be joined properly into a single nucleotide sequence, spanning the entire coding region. The full-length cDNA of blue gourami *PRL* was compiled from the data obtained by the 5'- and 3'-RACE, and the nucleotide and deduced amino acid sequences (acc. no. AY765377) (Degani et al., 2010). The cDNA was 1301 bp long and had an open reading frame of 687 bp, beginning with the first ATG codon at nucleotide 56 and ending with the stop codon at nucleotide 691. A putative poly(A) signal, AATAAAA, was recognized 24 bp upstream of the poly(A) tail. The position of the signal peptide cleavage site was predicted to be at 89 bp, yielding a signal peptide of 31 aa and a mature peptide of 181 aa. One putative N-linked glycosylation site was found 18 bp from the N terminus of the putative mature peptide. The deduced amino acid sequence of the blue gourami PRL was compared with homologous

```
  1  TGTATCAGAAGTGAACCTGAACCTGTATCTGATTTCACAACCGCTATGGACAAAGTCCTG   60
                                                 M  D  K  V  L

 61  TTTCTGCTCTTCGTCCTTTCTTTGGGCGTCTCTTCTCAGCCAATCACAGACAGCCAGCGT  120
     F  L  L  F  V  L  S  L  G  V  S  S  Q  P  I  T  D  S  Q  R

121  CTCTTTTCCATCGCTGTTAGCAGAGTCCAACACCTGCACCTGCTCGCCCAGAGACTCTTC  180
     L  F  S  I  A  V  S  R  V  Q  H  L  H  L  L  A  Q  R  L  F

181  ACTGACTTTGAGAGTTCTTTGCAGATTGAAGAGCAGCGTCAGCTCAACAAAATCTTCCTC  240
     T  D  F  E  S  S  L  Q  I  E  E  Q  R  Q  L  N  K  I  F  L

241  CAGGACTTTTGTAATTCTGATTACATCATCAGTCCCATAGACAAGCACGAGACACAGCGC  300
     Q  D  F  C  N  S  D  Y  I  I  S  P  I  D  K  H  E  T  Q  R

301  AGCTCTGTGCTGAAGCTCTTATCAATCTCTTATCGGCTGATTGAGTCCTGGGAGTTCCCC  360
     S  S  V  L  K  L  L  S  I  S  Y  R  L  I  E  S  W  E  F  P

361  AGCCGCTCTCTATATGGAGGTTCTGCTCAGAGATACCAGATTTCTCCCAAACTGTCAGAG  420
     S  R  S  L  Y  G  G  S  A  Q  R  Y  Q  I  S  P  K  L  S  E

421  CTGATGAGAGGCATTCAGCTGCTGATCAAGGCCAATCAGGACGGAGCAGAGATGTTCTCT  480
     L  M  R  G  I  Q  L  L  I  K  A  N  Q  D  G  A  E  M  F  S

481  GATGGCGTGGTTCCGCAGCTTGCTCCATATGGAAACTACTACCAGAGTCTGGGAGAGGAC  540
     D  G  V  V  P  Q  L  A  P  Y  G  N  Y  Y  Q  S  L  G  E  D

541  GAGTCGCTCAGGCGCAGCTACGAACTTCTGGCCTGCTTCAAGAAGGACATGCACAAGGTG  600
     E  S  L  R  R  S  Y  E  L  L  A  C  F  K  K  D  M  H  K  V

601  GAGACATACCTGACTGTGGCTAAATGCAGACTTTCTCCAGAAGCTAACTGCACTCTGTAG  660
     E  T  Y  L  T  V  A  K  C  R  L  S  P  E  A  N  C  T  L  *

661  cccctcgacctaaataataacataatcatctgtgttctgtagtcctgttctttaatgtgt  720
721  tgactagcattagcattagtttctttcttgcattgtctttgttccagttccagcacaatg  780
781  tgatttcagactgccagcatatgaaataaaatttgtttgattcagaaaaaaaaaaaaaaa  840
841  aaaaaaaaaaaaaaaaaaaaaa  863
```

Figure 24. Nucleotide sequence of the blue gourami GH cDNA together with the hormone's putative amino acid sequence (in three-letter code). In a comparison with similar fish hormones found in the GenBank database, the blue gourami GH was found to be most similar to *Sparus aurata* GH (86% identical residues) and least similar to *Anguilla japonica* GH (43% identical residues). The sequence similarity was in accordance with prevailing systematics (Goldberg et al., 2004).

subunits from a number of other fish species (**Table 2**). The highest degree of homology was found between the blue gourami and the Perciformes *Perca flavescens*, *Dicentrarchus labrax*, and *Sparus aurata*, fol-

lowed by the Salmoniformes, Siluriformes, and Cypriniformes. The lowest level of homology was observed with the Anguilliformes (**Table 2**).

Somatolactin, a pituitary hormone belonging to the PRL superfamily, is involved in background adaptation, osmoregulation, reproduction

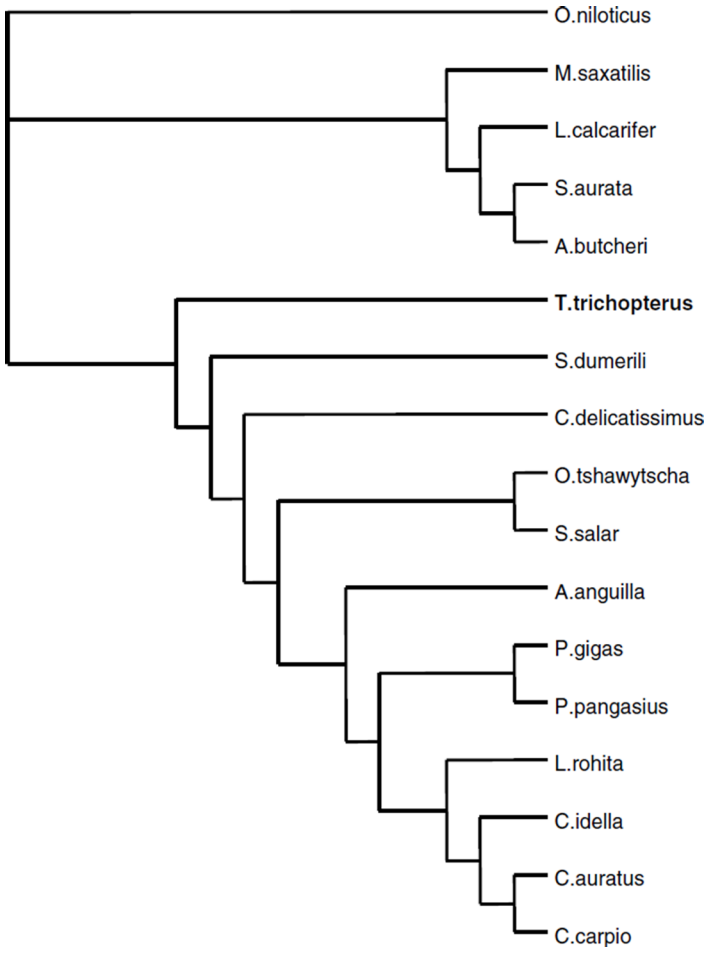

Figure 25. A dendrogram which graphically shows the relations among various fish GHs. The dendrogram was created by neighbor joining for cluster analysis (Goldberg et al., 2004).

Table 2. Degree of homology between blue gourami (bg) PRL and PRL of other classes.

Species	Class/order	Accession no. bgPRL (%)	
Perca flavescens	Perciformes	AY332491	79
Dientrarchus labrax		X78723	79
Spaurus aurata		AF060541	77
Paralichthys olivaceus		AF047616	75
Onchorhynchus mykiss	Salmoniformes	M24738	66
Coregonus autummalis		Z23114	66
S. salar		X84787	66
Heteropneustes fossilis	Siluriformes	AF372653	62
l. punctatus		AF267990	62
Hypoththalmichtys molitrix	Cypriniformes	X61052	62
Danio rerio		AY135149	61
Cyprinus carpio		X12541	61
A. japonica	Anguiliformes	AY158009	59
A. anguila		X69149	59

and fatty acid metabolism. The cDNA of blue gourami somatolactin was cloned, sequenced and analyzed (Degani, 2015a). The partial blue gourami somatolactin sequence was compared to those of other fish species (**Figure 26**).

The highest degree of homology with blue gourami somatolactin was found in the Perciformes *Perca flavescens* and *Cyclopterus lumpus*. The lowest level of homology was observed with *Anguilla anguilla*.

2.2.7. Discussion

We reviewed the genes involved in various growth and reproduction

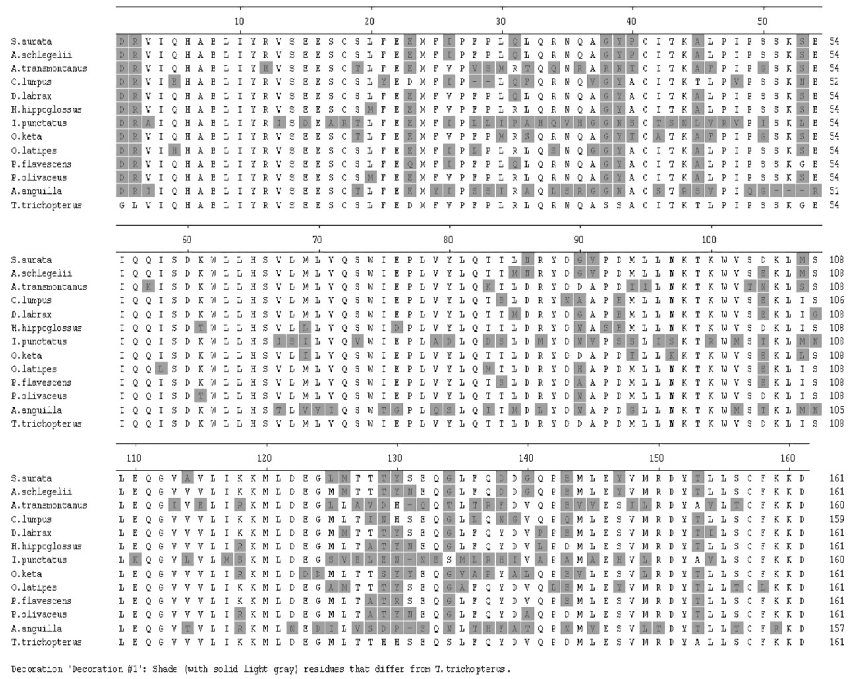

Figure 26. Comparison of blue gourami somatolactin cDNA sequence to those of other fish species. The amino acid sequences of somatolactin were compared by Clustal W method. The phylogenetic tree showing their relationships is presented in **Figure 27**.

processes, along with mitochondrial DNA, which might serve as molecular markers to distinguish between labyrinth fish, suborder Anabantoidei, and other fish. This knowledge is of great importance in understanding the differences between the Labyrinth fish group and others (Okumus and Ciftci, 2003) (**Table 3**). The various molecular markers studied in blue gourami were mitochondrial or nuclear DNA, but not microsatellites or single-nucleotide polymorphisms (**Table 3**). Most of the genetic markers in blue gourami were associated with functions of growth (PACAP, GH and PRL) and reproduction

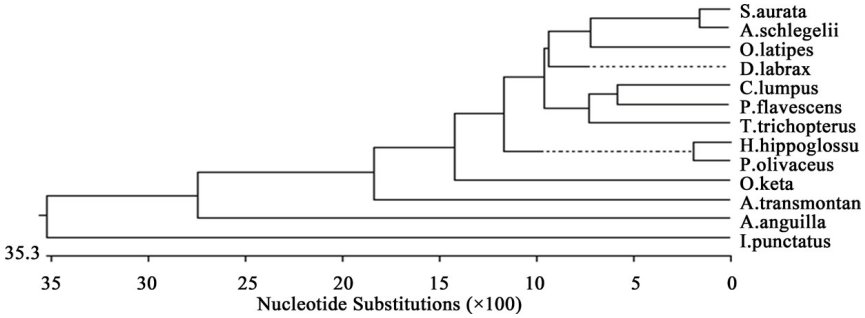

Figure 27. Phylogenetic tree showing the relationship between somatolactin amino acid sequences from various fish species. The tree was generated by maximum Clustal W using DNA Star WI Megalign software. All sequences were obtained from NCBI GenBank according to the accession numbers provided in Degani (2015a).

Table 3. Degree of nucleotide sequence homology (%) of blue gourami (*Trichogaster trichopterus*) genes with their counterparts in different species (Degani, 2013; Degani et al., 2010; Goldberg et al., 2004; Levy et al., 2009, 2010; Yom Din et al., 2008):Perciformes, Pleuronectiformes, Atherinomorpha, suborder Anabantoidei, Cichliformes, Tetraodontiformes, Gadiformes, Carangiformes, Salmoniformes, Siluriformes, Anguilliformes, Acipenseriformes.

Cytochrome *b*	Mitochondrial 12S gene	GH	PRL	PACAP	GnRH1	GnRH2	GnRH3
Trichop-terus (gold) 100%	Tricho-gaster trichop-terus (gold) 100%	Lates calcarifer 48%	Perca flaves-cens 79%	Oreo-chromis mos-sam-bicus 97.4%	Thun-nus thy-nnus 74.3%	Epin-ephelus bruneus 78.5%	Di-cen-trar-chus labrax 77.4%
Colisa lalia 86.6%	Tricho-gaster leerii 91.4%	Seriola dumerili 84%	Dicen-trar-chus labrax 79%	Gadus morhua 97.4%	Epin-ephelus bruneus 72.3%	Ve-ra-sper va-rie-gatus 74.9%	Pagrus major 70.2%
Tricho-gaster leerii 86.0%	Colisa lalia 44.8%	Sparus aurata 83%	Sparus aurata 77%	Taki-fugu ru-bri-pes 97.4%	Verasper va-rie-gatus 70.5%	Para-lich-thys olive-ceus 73.4%	Cyno-scionne-bu-losus 58.1%

Tri-cho-gaster labiosus 85.6%	Betta betta 82.6%	Acan-tho-pagrus butcheri 82%	Para-lich-thys olivaceus 77%	Hap-lo-chromis burtoni 97.4%	Oreo-chromis niloticus 68.2%	Thun-nus thyn-nus 72.8%	Rachy-centron ca-na-dum 57.7%
Ma-cro-podus oper-cu-laris 81.6%	Colisa chuna 41.4%	Oreoch-ro-mis nilo-ticus 97%	Onc-ho-rhynchus mykiss 66%	Epin-ephelus coioides 97.4%	Morone saxatilis 62.6%	Morone saxatilis 72.2%	Mi-cro-pogonias un-du-lates 57.5%
Cyprinus carpio 77.9%	Tri-cho-gaster pec-tor-alis 40.5%	Morone saxatilis 97%	Coregonus autumnalis 66%		Fundu-lus hete-ro-clitus 60.8%	Odontes-thesbo-na-riensis 65.2%	Scia-enops ocel-latus 57.5%
Betta betta 58.9%	Cterno-pona se-therici 41.1%	Caranx deli-cates-simus 74%	Salmo salar 66%		Mugil ce-pha-lus 59%	Mugil ce-pha-lus 65%	
Salmo salar 76.9%	Ma-cro-podus oper-cu-laris 41.1%	On-co-rhynchu stshawyt-scha 69%	Hete-ro-pneustes fossilis 62%		Core-gonus clu-pea-formis 54.2%	Fun-dulus hete-ro-clitus 61.8%	
Tri-cho-gaster fascia-tus 86.4%	Osph-ro-nemus goramy 40.5%	Salmon salar 68%	Ictalurus punctatus 62%		Odon-tes thesbo-na-ri-ensis 22.6%	Core-gonus clu-pea-formis 59.6%	
		Pangsius pangasius 64%	Hy-po-phthalm ich-thys molitrix 62%				
		Pan-ga-sinodon gigas 64%	Danio rerio 61%				
		Cyprinus carpio64%	Cyprinus carpio61%				
		Carassius auratus 63%	Anguilla japonica 59%				

		Cte-no-pharyn-godon idella 62%	**Anguilla anguilla 59%**				
		Labeo ro-hita 60%					
		Anguilla anguilla 59%					
		Acipenser guel-den-staedtii 97%					

(GnRH1, GnRH2, GnRH3, LH and FSH) (Degani, 2020a). Only two mitochondrial genes (cytochrome *b* and 12S) were studied. Some other genes, e.g., isozyme markers, have been studied in Labyrinth fish (Degani and Veit, 1990). We were able to compare molecular markers encoding hormones to a marker that is in the mitochondrial DNA (**Table 3**). The similarity between labyrinth fish species with respect to cytochrome *b* was between 86% and 46%, and for 12S, between 91% and 40%. Comparing the sequences of genes encoding hormones in blue gourami to those in different fish species indicated a lower similarity than for the cytochrome *b* and12S genes, between 97% and 22% (**Table 3**). These comparisons should be examined with caution because the fish species belonged to different orders. Our comparison of blue gourami DNA sequences to their counterparts in other fish was in agreement with many such comparisons appearing in the literature (Chauhan and Rajiv, 2010; Davey et al., 2011; Degani, 2013; Degani and Veit, 1990; Degani et al., 2019a, 2019b, 2006; Hu-

bert et al., 2012; Maqsood and Ahmad, 2017; Okumus and Ciftci, 2003).

Hormone-encoding sequences in blue gourami had high similarity to other species in the order Perciformes (Degani, 2001). The gene sequences for GH and PRL, both belonging to the same group of hormones, were relatively similar (Degani et al., 2010, 2017b; Yom Din et al., 2008). Research in aquaculture is mainly concerned with the production of edible fish for human consumption, and less so with the ornamental fish industry (Chauhan and Rajiv, 2010; Maqsood and Ahmad, 2017). Nevertheless, the principle of different markers is the same for the whole group of fish. We can therefore sum up by saying that genes which may serve as genetic markers in blue gourami may represent the bony fish. Among the genes involved in the control of growth and reproduction, the most suitable as genetic markers were in the HPS axis (PACAP and GH).

2.2.8. Sequence Analysis of Genes Encoding Mitochondrial Cytochrome c Oxidase Subunit 1 (COI) as Markers for Blue Gourami and Other Anabantoidei Fish

The nucleotide sequence of the COI gene of blue gourami is 628 bp in length. The COI gene sequence is widely used as a barcoding system to identify the kinship of fish species (Syaifudin et al., 2019). A comparison of this sequence in blue gourami to other fish species is presented in phylogenetic trees (**Figure 28** and **Figure 29**).

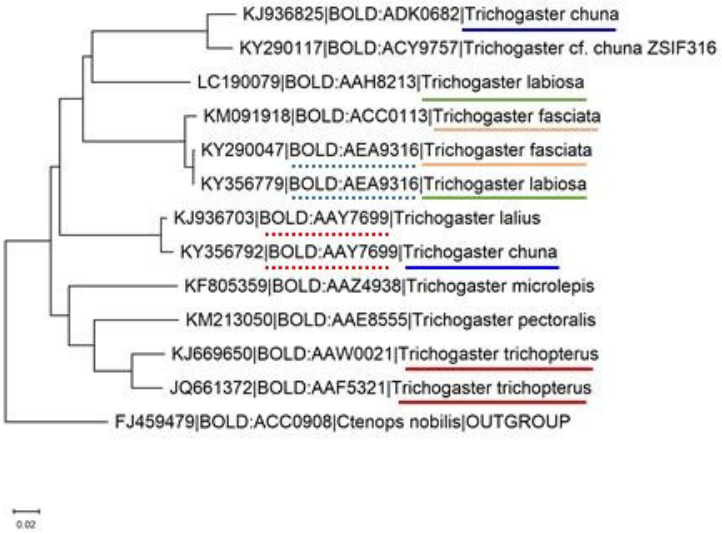

Figure 28. Rooted phylogenetic tree of the COI-5p gene records of the genus *Trichogaster*. Twelve nucleotide sequences from eight species were retrieved from BoldSystem (Ratnasingham and Hebert, 2007), such that every species is represented by sequences from unique bins. The tree was constructed using the neighbor-joining method and the Kimura 2 Distance Model, with pairwise deletion and MUSCLE alignment in MEGA-X software (Kumar et al., 2018). A sequence from the genus *Ctenops* was used as the outgroup. Branches are marked with the species' Genbank_accession numbers. Sequences belonging to species that appear more than once in the tree are underlined in the same color. Bins that appear more than once are underlined with a dotted line.

Figure 29. Rooted phylogenetic tree of the COI-5p gene records for the order Anabantiformes. Nineteen nucleotide sequences from different species were retrieved from BoldSystem (Ratnasingham and Hebert, 2007), such that every genus is represented by one sequence. The tree was constructed using the neighbor-joining method with the Kimura 2 Distance Model, with pairwise deletion and MUSCLE alignment in MEGA-X software. The sequence of *Mastacembelus brachyrhinus* in the order Synbranchiformes was used as the outgroup. Branches are marked with their GenBank accession numbers. Sequences belonging to the same taxonomic family are underlined in the same color.

Chapter 3

Reproduction in the Blue Gourami Male

3.1. The Male

Blue gourami fish can be sexed by observing their dorsal fin: more pointed in the males, and shorter and more rounded in the females (**Figure 1**). The mature female body containing eggs can be easily identified. In their natural habitat, reproduction occurs year-round, but more profusely during heavy rains, when more areas are available for the male's territory. Descriptions of the blue gourami's sexual behavior (Degani, 1989, 2001, 2020b) are based on studies under artificial conditions.

In the male, the onset of the reproductive period is marked by the development of nuptial coloration, the initiation of nest-building behavior, and increasing aggressiveness. During non-reproductive periods, both sexes are generally uniformly pale and do not show aggression or any kind of territorial behavior (**Figure 30** and **Figure 31**). Like many other anabantids, blue gourami deposit their eggs in a floating bubble nest (**Figure 31**), which is made of bubbles formed by air enveloped in oral mucus. The bubbles are released at the surface, and tend to stick together. The form and composition of the nests vary among species.

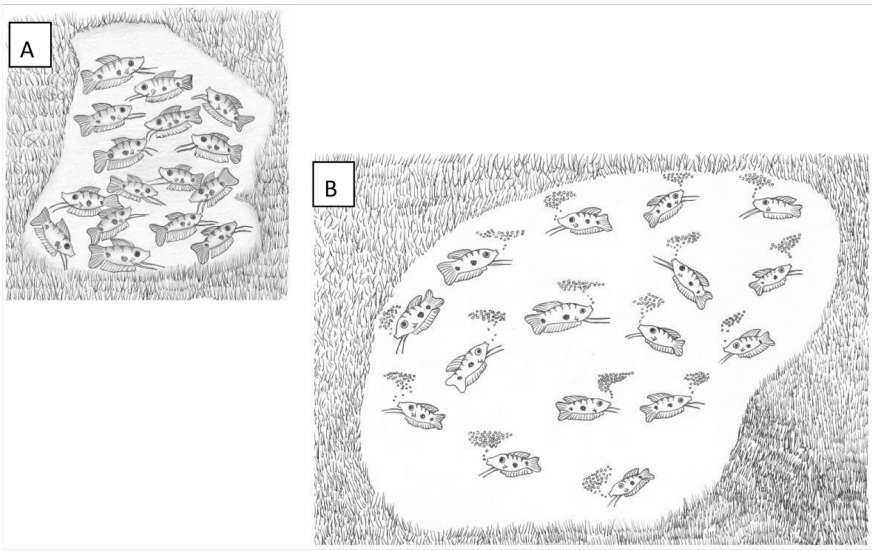

Figure 30. Two habitats, with high and low densities of males. (A) At high density, the male does not build a nest. (B) At low density, the male builds a nest and exhibits sexual behavior (Degani, 1989, 2001, 2020b; Degani and Ziv, 2016).

Labyrinth fish undergo two different periods during their life cycle: (i) before labyrinth organ development, from eggs to juveniles, when oxygen is retained over the entire surface by diffusion; (ii) after labyrinth development, when the organ becomes important for breathing (Degani, 2001). The complex sexual and nest-building behaviors of fish belonging to the Anabantoidei species have been described. In natural habitats, when there is a low density of mature males, they become territorial, build a bubble nest and protect it from other males (**Figure 31**). The adaptation for the development of eggs and fry in water with low oxygen concentrations involves laying eggs in this bubble nest.

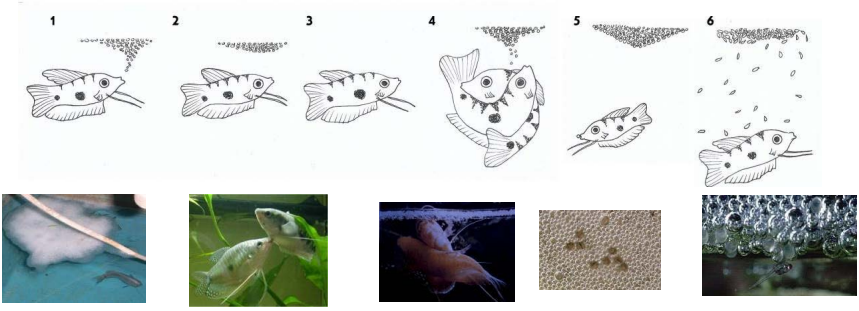

Figure 31. Sexual behavior of male blue gourami during the reproductive cycle. (1) The male builds a nest. (2 and 3) Male courts female under the nest. (4) Fertilization takes place and the fertilized eggs float up and stick to the bubble nest. (5) The male guards the eggs in the nest. (6) The male further protects the fry immediately after hatch while they swim in the nest area (Degani, 2020a, 2020b).

After courting and fertilization, the female swims under the bubble nest and spawns eggs into it. The male guards the nest with the eggs. If an egg falls out, the male returns it to the nest. It also protects the fish in the first period, immediately after hatch.

The sexual and nest-building behaviors of blue gourami males have been described in detail in their natural habitat (Degani, 2001) and under experimental conditions (Degani, 1993a, 2020a, 2020b; Degani and Ziv, 2016).

The blue gourami in particular exhibits a very complex social and spawning behavior, and because of this, it has become a common subject for ethological studies. Miller (1964) detailed the social and spawning behavior of the blue gourami. The literature contains other studies on the same subject (Cheal and Davis, 1974; Degani, 1989). The aggressive behavior that enhances the male blue gourami's abil-

ity to defend its territory in signal contests has also been studied in detail (Degani and Ziv, 2016). In blue gourami, as in many other vertebrate species that exhibit resource-defense polygyny, males establish their territories well in advance of the arrival of females and are therefore able to defend them over a relatively long period of time (Degani and Ziv, 2016). A very distinct characteristic of nest-building by *T. trichopterus* is the active incorporation of vegetation into the nest. Female nest-building is absent or very rare (Miller and Robison, 1974), and Cheal and Davis (1974) found that in many cases, the presence of a nest is not a prerequisite for spawning. The spawning procedure can be divided into courtship and pre-spawning behavior, spawning (gonadal release and fertilization), and post-spawning behavior, when the male takes care of the young larvae.

Visual, mechanical and chemical cues are involved during the entire process. Courtship is characterized by aggressive behavior of the male toward the female: he approaches her and either chases or bites her (Degani and Ziv, 2016). Some males are very aggressive, while others ignore the female and simply take care of the nest (Miller, 1964). If the female is not ready to spawn, she hides far from the nest, usually at the opposite end of the tank. When the female shows signs of readiness, the male begins the so-called lateral spread display, which is characterized by the erection of dorsal and anal fins and spreading of the caudal fin. The body also curves and at maximum intensity, it acquires an S shape.

Courtship and spawning behavior are quite difficult to distinguish, but butting or biting by the female seems to have an important signaling function in limiting male aggression. The male takes a position anterior to the female, who is inclined at 30˚ to the horizontal with the head higher than the tail. He then moves back and forth, stroking the female with his dorsal fin. In the last stage of spawning behavior, he swims forward or bends his body in the middle, remains perpendicular to the center of the female's body, and finally flexes into a U-shape, into the middle of which the female enters (**Figure 31**). The male squeezes the body of the female very tightly and both fish roll over. The roll ceases with the female belly up and the male over her. First, the male emits a cloud of sperm and a few seconds later, the female releases a clutch of eggs, which are immediately fertilized on their way to the surface. The female is then released and both fish sink to the bottom of the tank. The last stage is repeated several times at each spawning.

The male blue gourami's nest-building behavior is affected by other males, and these interactions have been studied under experimental conditions by Degani and Ziv (2016) (**Figure 32**). Males found in the area control the territory and sexual behavior, and are influenced by the behavior of other males. Results showed that the sexual behavior (nest-building) of male blue gourami is affected by both the behavior and pheromones of other males. It was suggested that males must defend their territories to prevent these two factors

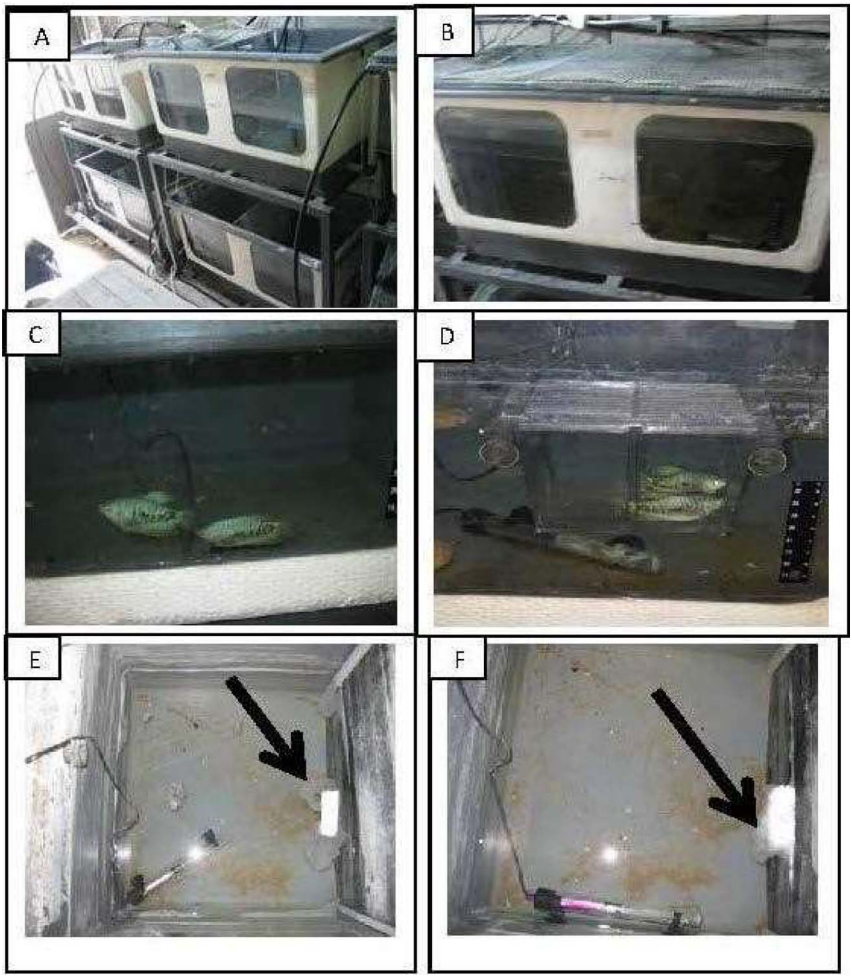

Figure 32. The experimental aquarium systems. (A) and (B) illustrate the aquarium systems. (C) Two males in experiment 1. (D) Two males in the cage in experiment 3. (E) and (F) illustrate male nest-building in the aquariums (Degani and Ziv, 2016).

from interfering in nest-building (Degani and Ziv, 2016).

Testis samples (**Figure 33**) were fixed in Bouin and processed for light microscopy (Degani, 2020b). Paraffin sections of 6 μm were

Figure 33. Testis of male blue gourami (Degani, 2001).

stained with hematoxylin and eosin. The histology of the testes in juvenile non-reproductive and reproductive blue gourami males, presented in **Figure 34**, was classified into the following categories: testes containing a small number of spermatogonia (**Figure 34(A)** and **Figure 34(B)**), and mature testes exhibiting active spermatogenesis with spermatocytes and spermatids (**Figure 34(C)** and **Figure 34(D)**) (Degani, 2020b).

3.2. Hormonal Control of Reproduction in Blue Gourami Males

In the blue gourami, as in all vertebrates, reproduction and growth are closely linked, with both being controlled by complex hormonal interactions at the brain-pituitary-gonad (BPG) level (**Figure 35**).

Mature males were examined in two different stages: non-reproductive

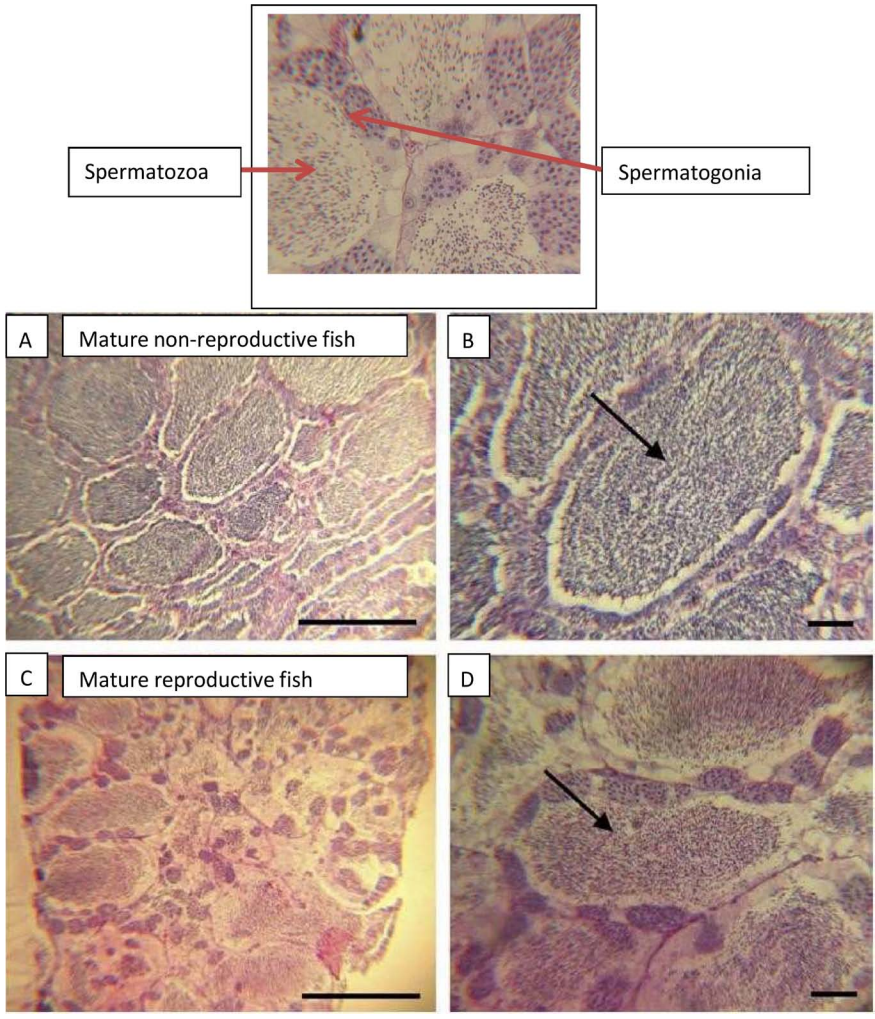

Figure 34. Histological section showing different stages of testis development in blue gourami. (A) Testis of mature non-reproductive fish, bar = 170 µm. (B) Testis of mature non-reproductive fish (note the concentration of spermatozoa in the middle of the lobule; see arrow), bar = 35 µm. (C) Testis of mature reproductive fish during sexual behavior, bar = 170 µm. (D) Testis of mature reproductive fish during sexual behavior (note the decrease in the quantity of spermatozoa in the center of the lobule of reproductive fish compared to non-reproductive fish; see arrow), bar = 35 µm (Degani, 2020b).

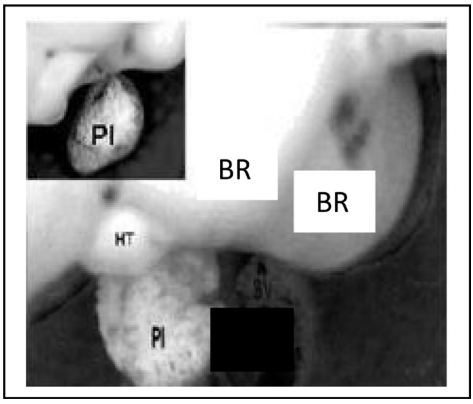

Figure 35. Gonadotropic brain-pituitary-gonad (BPG) axis and hypothalamic-pituitary-somatotropic (HPS) axis. BR, brain; PI, pituitary gland; HT, hypothalamus (Gad Degani, unpublished data).

in high-density habitats and reproductive in low-density habitats. Based on gene transcription, GnRH1 is involved in controlling spermatogenesis (spermatogonia to spermatids) via the BPG axis in non-reproductive and reproductive stages by controlling FSH (Degani, 2020b; Levy and Degani, 2013) (**Figure 36**), 11-ketotestosterone (11KT) and 17β-estradiol (E_2). However, GnRH3 has a larger effect during the reproductive stage via the BPG axis (spermatids to sperm) on LH, 11KT, and 17α-hydroxyprogesterone (17P). At the same time, the HPS axis is involved in spermatogenesis via PACAP and PRP in the brain, and GH in the pituitary affects synthesis of insulin-like growth factor 1 (IGF1) in the liver.

The level of GnRH3 transcription increases significantly from the juvenile stage to the mature male stage, and to the stage of mature male with sexual behavior (nest-building) (**Figure 37**).

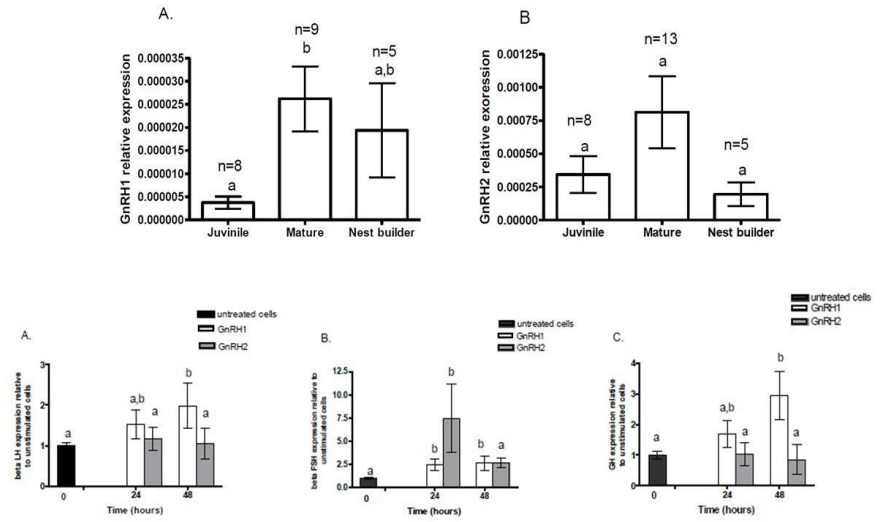

Figure 36. In males, GnRH1 gene expression increases in mature non-reproductive males, and increases *β*GtH and GH gene expression. GnRH2 gene expression does not change during the reproductive cycle, but *β*GtH gene expression increases. The relative amount of GnRH3 mRNA was normalized to that of 18S rRNA using the CT cycle method, where 2_DCT reflects the relative amount of the specific gene precursor's transcription (Degani, 2020b; Levy and Degani, 2013).

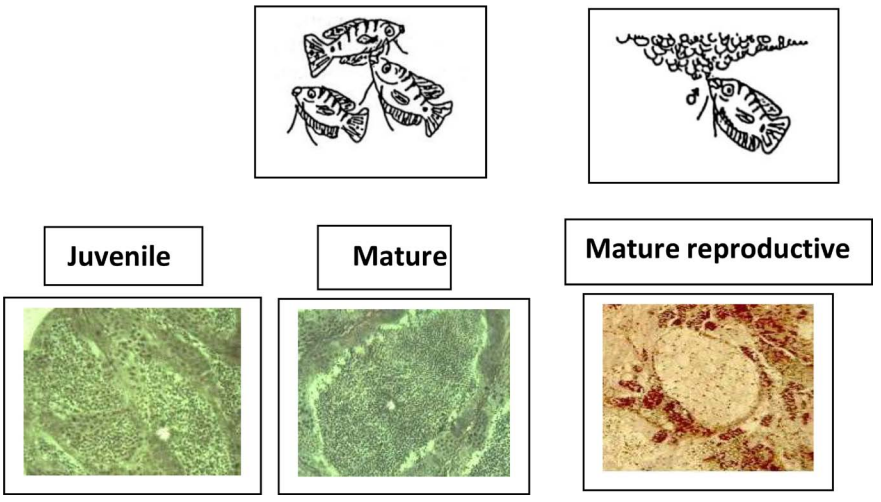

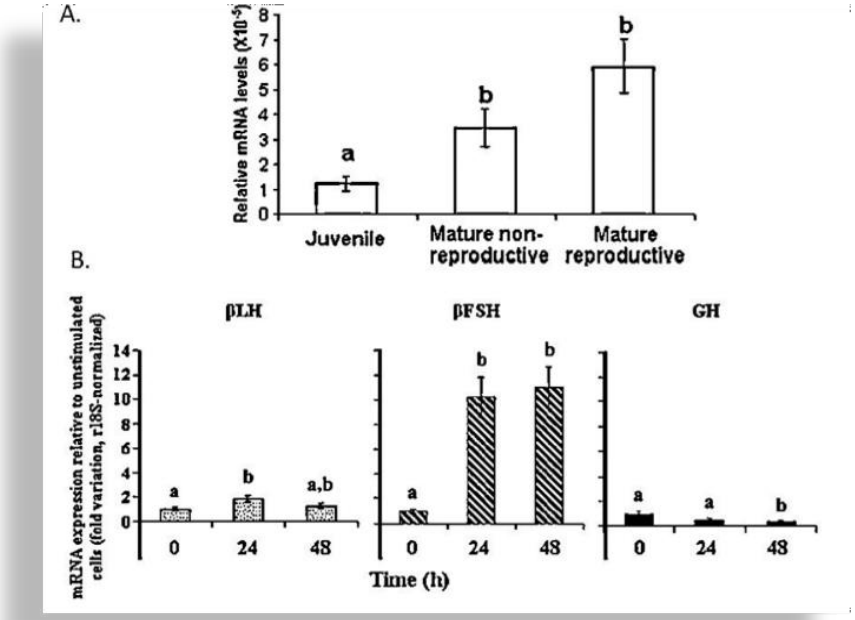

Figure 37. The level of GnRH3 transcription increases significantly from the juvenile stage to that of the mature male and to the stage of the mature male with sexual behavior (nest-building). Different letters indicate significant difference at $P < 0.05$ by ANOVA and t-test.

3.2.1. Effect of PACAP38, GnRH Analog (GnRHa) on *β*FSH and GH mRNA Levels in a Culture of Dispersed Pituitary Cells of Blue Gourami Males

PACAP38 or GnRHa stimulated *β*FSH gene expression after 48 h. However, PACAP38 inhibited GnRHa-induced *β*FSH gene expression after 24 h (**Figure 38(A)**). GnRHa increased GH gene expression, and PACAP decreased GH gene expression following 24 h of treatment. However, cotreatment of cells with GnRHa and PACAP38 inhibited either GnRHa's or PACAP38's effect on GH expression after 24 h

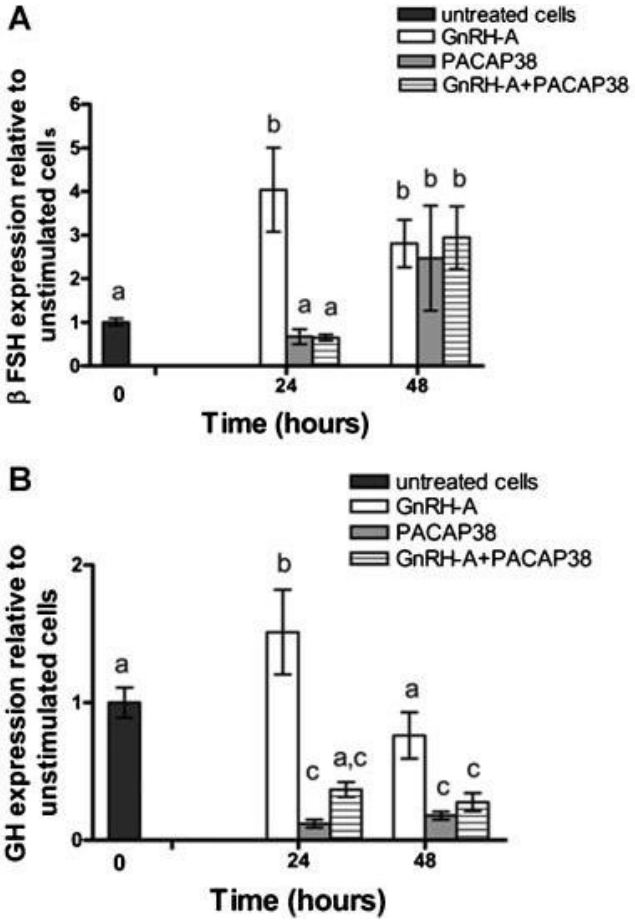

Figure 38. Effect of PACAP38 and GnRH analog (GnRHa) on *β*FSH (A) and GH (B) mRNA levels in a culture of dispersed pituitary cells from gourami males. Gourami pituitary cell culture from mature non-reproductive males was co-treated with 100 nM GnRHa and 10 nM PACAP38 for 24 and 48 h. Total RNA was extracted, reverse-transcribed to cDNA and used as a template for real-time qPCR. *β*FSH and GH mRNA levels were normalized to that of 18S rRNA using the CT cycle method, where 2_DCT reflects the relative amount of a specific gene precursor's transcript. Each histogram presents means ± SEM, reflecting fold change relative to the mRNA level of the untreated cells, set to 1. Different letters denote a significant difference (Degani, 2020b; Levy and Degani, 2013) in mRNA levels of control and combined stimulation (ANOVA and LSD post-hoc test; $P < 0.05$).

(**Figure 38(B)**) (Levy and Degani, 2013).

Levy and Degani (2013) suggested a model (**Figure 39**) of the correlation between brain hormones in blue gourami and male reproductive functions. Based on this model, low gene expression of PRP, PACAP, and GnRH in juveniles (Levy et al., 2010, 2011) was

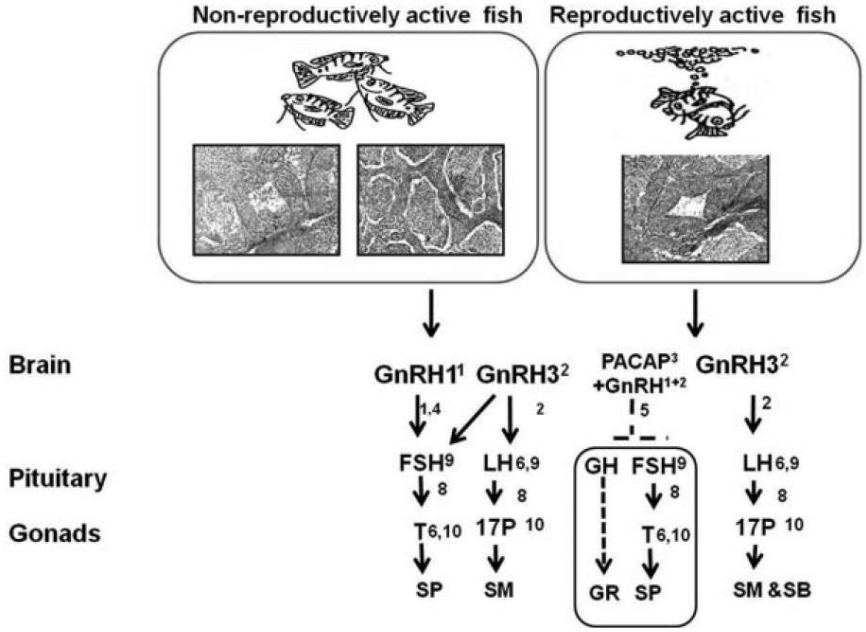

Figure 39. Suggested qualitative model showing the mechanism of PACAP, PRP and GnRH1, 2 and 3 gene transcription during spermatogenesis in the mature blue gourami male. The broken lines indicate the combined inhibitory effect of PACAP and GnRH on GH and FSH gene transcription. The black dashed line indicates possible involvement of GH in spermatogenesis. SB, sexual behavior; SP, spermatogonium proliferation; SM, spermiation; GR, growth rate; T, testosterone; GtH, gonadotropin; P, progesterone. 1—Levy and Degani (2012, 2013); 2—Levy et al. (2009); 3—Levy et al. (2010); 4—Levy and Degani (2011); 5—Levy and Degani (2012, 2013); 6—Degani (2015b), 7—Mananos et al. (1997); 8—Degani (2015b, 2020a, 2020b); 9—Degani (2015b, 2020a, 2020b); 10—(Degani, 2015b, 2020a, 2020b).

consistent with low levels of *β*LH and *β*FSH gene expression in the pituitary (Degani et al., 2003), pituitary levels of *β*LH, and progesterone and testosterone levels (Degani, 1993a; Mananos et al., 1997), resulting in a low rate of spermatogenesis, low body weight values, and no sexual behavior. The changes in brain peptide genes' expression during ontogeny, as described in that study, might affect pituitary hormone gene expression, as previously demonstrated, by the following mechanisms: (i) GnRH1 and GnRH3 stimulate *β*LH and *β*FSH gene expression to induce steroid synthesis in the testis; spermatogenesis is then initiated (Degani, 1990, 1993a; Levy and Degani, 2013); (ii) a dual effect on GH gene expression: stimulatory effect of GnRH1 and PRP, and inhibitory effect of GnRH3. This hypophysiotropic effect can be exerted directly on somatotrophs through specific binding sites, as demonstrated in carp and goldfish. In mature, reproductively active males, the elevation in GnRH3 and PACAP gene expression might regulate the final stages of spermatogenesis and sexual behavior by the following mechanisms: (i) GnRH3 stimulates *β*LH gene expression and promotes spermatogenesis through the *β*LH, 17P, and 17α,20*β*-dihydroxy-4-pregnen-3-one (17,20P) pathways (Degani, 1993a, 2020b; Levy et al., 2009), supported by in vivo plasma levels of LH and FSH (Degani, 1993a, 2020b; Mananos et al., 1997); (ii) sexual behavior in blue gourami males can be promoted through sensory reception by PACAP and GnRH3 neurons, which can be involved in visual, olfactory and social inputs as shown for different fish species and in blue gourami (Levy and Degani, 2013; Levy et

al., 2009). Specifically, GnRH3 is related to nest-building behavior through the integration of sensory inputs. Thus, visual and olfactory inputs through retina PACAP and GnRH3 neurons are suggested to interact with the GnRH and PACAP hypothalamic-pituitary neuronal systems to upregulate *β*LH gene expression and steroidogenesis in the testes as part of the regulatory mechanisms of sexual behavior and nest-building (Degani, 1993a, 1993b, 2020b); (iii) biphasic (time-dependent) effect of co-incubation with PACAP and GnRH on *β*FSH and GH gene expression: the blocking effect on *β*FSH and GH gene expression after 24 h of exposure was eliminated after 48 h of treatment. Attenuation of GnRH-induced *β*FSH gene expression by PACAP can be explained by paracrine mechanisms involving follistatin-activin factors (Levy and Degani, 2011, 2012, 2013; Levy et al., 2010), which decrease the rate of the early stages of spermatogenesis.

However, extended exposure might inhibit this, to promote early stages of spermatogenesis. The discrepancies between short- and long-term GnRHa and PACAP stimulation demonstrate an additional level of central regulation of spermatogenesis. The effects of GnRHa and PACAP on GH gene expression have not been demonstrated previously in vertebrates. However, from a physiological standpoint, this might explain the growth-puberty interactions in animals in which the rate of body weight increase is attenuated in the transition to reproductively active nest-building fish. It was thus demonstrated that brain peptides can act individually or in cooperation with other peptides to exert physiological responses. Individually, GnRH1 might be

involved in the regulation of spermatogenesis and PACAP might be involved in the regulation of sexual behavior. However, PACAP and GnRHa counteract each other's effects on *β*FSH and GH gene expression, thereby attenuating the increase in body weight and the decrease in early stages of spermatogenesis in mature blue gourami males. It is abundantly clear that complex crosstalk between various factors in the brain-pituitary axis is the general pathway regulating the transcription of hormones (Degani, 2015b, 2020b; Levy and Degani, 2011, 2012, 2013; Levy et al., 2010, 2011, and see **Figure 39**).

A model is suggested to describe hormone control in male blue gourami along the gonadotropic BPG axis and HPS axis (**Figure 40**) (Degani, 2020b). This model is based on the cloning and transcription of genes encoding hormones of the two axes involved in spermatogenesis during blue gourami reproduction. Gene transcription is affected by environmental, biological, and behavioral factors.

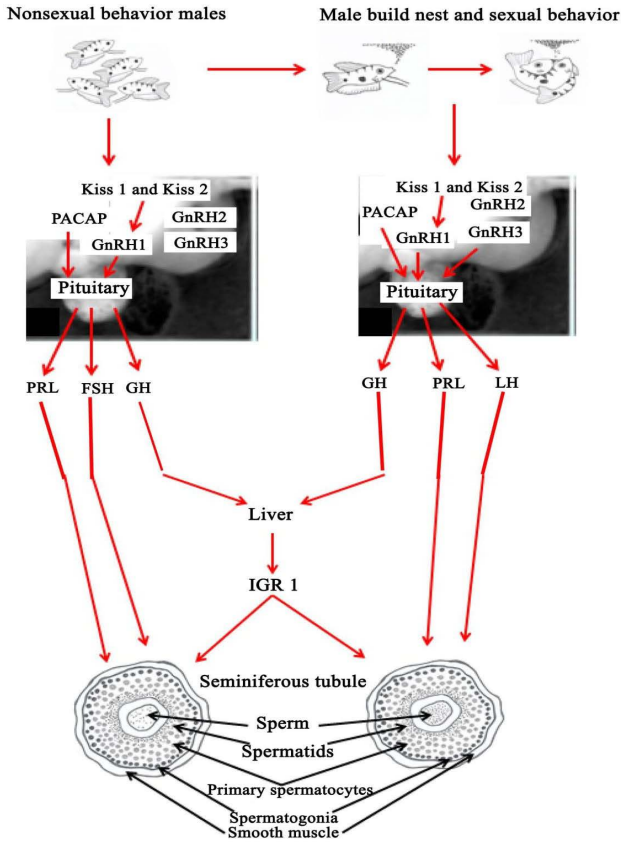

Figure 40. Gene transcription and hormone secretion along the BPG axis involved in spermatogenesis in the testis during male reproduction. These are affected by environment (David and Degani, 2011), sexual behavior (Degani, 1993a; Degani and Ziv, 2016), pheromones, kisspeptin (Kiss1 and 2) (Levy and Degani, 2011, 2012), gonadotropin-releasing hormone (GnRH1 and 3) (Levy and Degani, 2012, 2013), follicle-stimulating hormone (FSH) (Degani and Yom Din, 2011; Degani et al., 2003), luteinizing hormone (LH) (Degani et al., 2003; Mananos et al., 1997), pituitary adenylate cyclase-activating polypeptide (PACAP) (Levy et al., 2010) and its related peptide (PRP) (Levy et al., 2010), growth hormone (GH) (Degani, 2014c), and prolactin (PRL) (Degani et al., 2010). FSH and LH act on the ovary to synthesize the steroids 17β-estradiol (E_2), testosterone (T) and 17α,20β-dihydroxy-4-pregnen-3-one (17,20P) (Degani, 2017; Degani and Boker, 1992a, 1992b); and on the liver to synthesize vitellogenin (VTG) and insulin-like growth factor 1 (IGF1) (Degani, 2014c).

Chapter 4

Reproduction in the Blue Gourami Female

4.1. Oogenesis in the Blue Gourami

In blue gourami, as a model of hormone control of reproduction in Labyrinthici fish, the sexual behavior of the male (Degani, 1993a) and pheromones (Becker et al., 1992; Degani and Schreibman, 1993) affect the gonadotropic axis—the brain pituitary-gonadal (BHPG) axis (Yaron and Levavi-Sivan, 2011) and the somatotropic axis (Degani, 2020a)—the brain-pituitary-liver and body (BPLB) axis. These axes are very complex and they control the oocyte phase from vitellogenesis to maturation, ovulation, and spawning (Degani, 1993a, 2001, 2016) (**Figure 41(F)-(J)**).

Oogenesis in the female blue gourami has been described in detail (Degani, 2018; Jackson et al., 1994).

Different stages of oogenesis are presented in **Figures 42-44**. The gonadal development of juvenile females is presented in **Figure 42**, showing the histology of 38-day-old, 11-mm long juveniles. Before this age, it is very difficult to identify the gonads by light microscopy. In the 38-day-old larvae, it is possible to identify the ovary just after differentiation, with primary oocytes at the perinuclear stage, kidney,

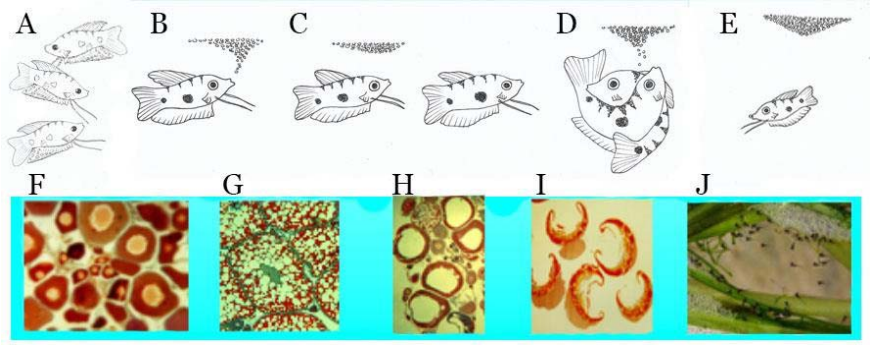

Figure 41. Relationship between sexual behavior, oogenesis and nursing in blue gourami (Degani, 2001). (A) High density—no reproduction occurs. (B) Low density—the male builds a bubble nest. (C) Sexual behavior under the nest. (D) The male wraps his body around the female and the female spawns eggs that will be deposited in the nest. (E) The bubble nest with eggs in it. (F) Oocytes pre-vitellogenesis. (G) Oocytes in vitellogenesis. (H) Mature oocytes. (I) Ovulating oocytes. (J) Fry hatch in the nest (Degani, 2020a).

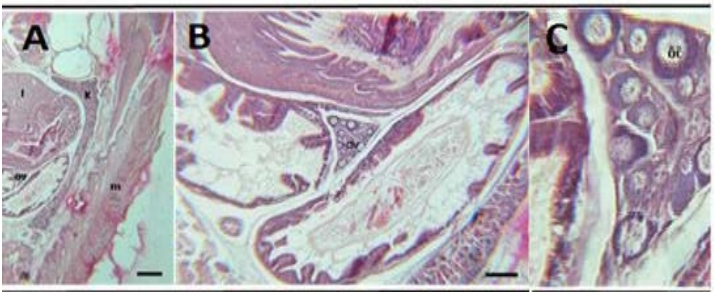

Figure 42. Histological section of a juvenile female ovary, 11 mm long, 38 days old. (A) ov, ovary; k, kidney; g, gut; l, liver; m, muscle. Bar = 190 μm. (B) Bar = 71 μm. (C) Oocyte (OC) at the perinuclear stage. Bar = 20 μm (Degani, 2018).

gut, liver and muscle (**Figure 42**).

In female larvae at the age of 55 days, and length of 22 mm, the number of oocytes at the perinuclear stage increases and their diameter is larger than 50 μm (**Figure 43**).

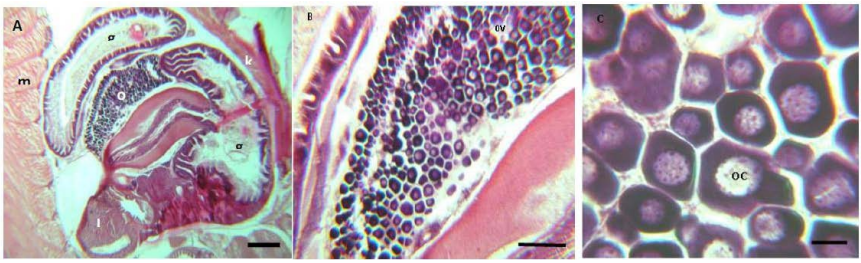

Figure 43. Histological section of a 55-day-old, 22 mm long juvenile female (A) ov, ovary; k, kidney; g, gut; l, liver; m, muscle. Bar = 320 µm. (B) Bar = 121 µm. (C) Oocyte (OC) at the perinuclear stage. Bar = 20 µm (Degani, 2018).

In the female larva at the age of 80 days and a length of 45 mm, it is possible to recognize several oocytes at the brining of granulose continuous vitellogenin (**Figure 44**).

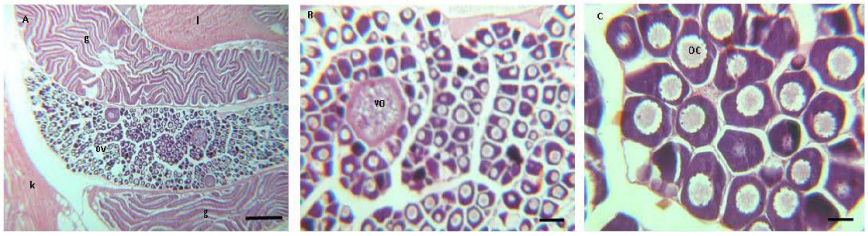

Figure 44. Histological section of an 80-day-old, 45 mm long female larva. (A) ov, ovary; k, kidney; g, gut; l, liver. Bar = 360 µm. (B) vo, vitellogenic oocyte. Bar = 45 µm. (C) Oocyte (OC) at the perinuclear stage. Bar = 20 µm (Degani, 2018).

Oogenesis in mature female blue gourami is described in detail in the following (Jackson et al., 1994).

Chromatin nucleolus stage. The oocytes measure 30 - 60 µm in diameter. The cytoplasm is strongly basophilic, with a central nucleus and 2 - 3 nucleoli per section. The nucleus-to-cytoplasm ratio

(N/C) is 0.5. The oocytes are surrounded by a single cell layer.

Perinucleolar stage. The oocyte diameter is 60 - 150 μm. N/C is 0.45. The perinucleolar stage is characterized by multiple nucleoli at the periphery of the germinal vesicle, 5 - 8 per section. From mid to late perinucleolar stage, the vitelline envelope begins to form. By the end of primary oocyte growth, the oocyte has grown from a diameter of 10 - 20 μm at the leptotene stage to a diameter of 100 - 150 μm. During the perinucleolar stage, in several oocytes, the nucleus contains an abnormal spherical structure, with an external capsule and an internal homogeneous and granular region. At its maximal size, the sphere occupies one-third of the nuclear volume.

Cortical alveolar stage. The oocyte diameter measures 150 - 370 μm in the section. N/C is 0.38. Spherical cortical alveoli appear at the circumference and are stained by periodic acid-Schiff (PAS) reagent. When the cortical alveoli begin to appear, they are dispersed in the cytoplasm, but in subsequent stages, they are displaced to the periphery of the oocyte by the yolk protein, which accrues centripetally. During the cortical alveolar stage, lipid droplets are formed in the perinuclear cytoplasm. In ovaries stained en bloc with 1% osmium tetroxide, the droplets stain intensely black. In paraffin-embedded tissue previously cleared with alcohol and xylene, the lipid droplets appear as empty vacuoles. Surrounding the oocytes there now appear two cell layers, the internal granulosa and an external theca layer. Another characteristic of this stage is the formation of nuclear

blebs. These are irregular outgrowths of the nuclear periphery containing karyoplasma and nucleoli; the nucleus thus displays a distorted appearance (**Figure 45**, 2a,b). The nuclear blebs disappear during early vitellogenesis and the nucleus assumes a rounded contour (**Figure 45**, 2c).

Vitellogenesis*.* Oocyte diameters range between 370 and 500 μm at the beginning of vitellogenesis and reach 500 - 580 μm toward the end of it. N/C is 0.19. Yolk granules are acidophilic and react positively to protein stains such as bromophenol blue. In the females of group 3 (**Figure 45**), in addition to the four developmental stages observed in those of groups 1 and 2 (**Figure 45**), the ovaries also show maturing oocytes, characterized by a large apical lipid vesicle formed from the coalescence of the small lipid droplets in the cortical alveolar stage (**Figure 45**, 3). The formed lipid vesicle occupies a large portion of the cell volume, and the nucleus that, up to this point, had been at the cell center, migrates toward the periphery, its first position during the migration being at the inner edge of the vitelline belt that surrounds the lipid vesicle (**Figure 45**, 4a). Then the nucleus traverses the vitelline belt and lies at its outer side, embedded in a region of homogeneous cytoplasm without vitelline granules (**Figure 45**, 4b).

In oocytes with a peripheral nucleus, the vitelline membrane opposite the nucleus thins, elongates, and invaginates slightly toward the nucleus (**Figure 45**, 4c and **Figure 46**, 5a,b, 6). Inside the invagination,

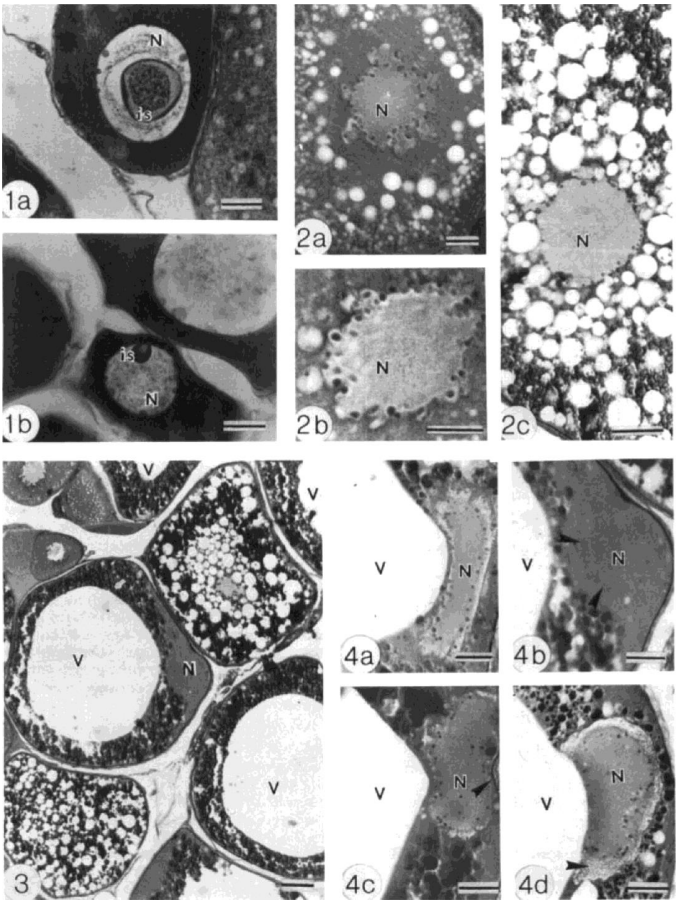

Figure 45. (1a) Perinucleolar oocyte with an intranuclear spherical structure (is). N, nucleus. (1b) Magnification of 1a. Bar = µm. (2a) Nucleus (N) of a cortical alveolar stage oocyte with irregular outgrowths of the nuclear periphery containing karyoplasm and nucleoli. Bar = 35 µm (2b) Higher magnification of 2a. Bar = 30 µm (2c) Nucleus (N) of an early vitellogenic oocyte with rounded contours. Bar = 40 µm (3) Maturing oocytes with apical lipid vesicles (V). N, nucleus. Bar = 100 µm. (4a) Migrating nucleus (N) of a maturing oocyte at the periphery of the lipid vesicle (V). (4b) Migrating nucleus surrounded by homogeneous ooplasm near the oocyte envelope. The nuclear envelope is not well defined (arrowheads). (4c) Opposite the nucleus, the oocyte envelope invaginates slightly (arrowhead). (4d) Remnants of the disintegrating nuclear envelope between the nucleus and the ooplasm (arrowhead). Bars= 50 µm (Jackson et al., 1994).

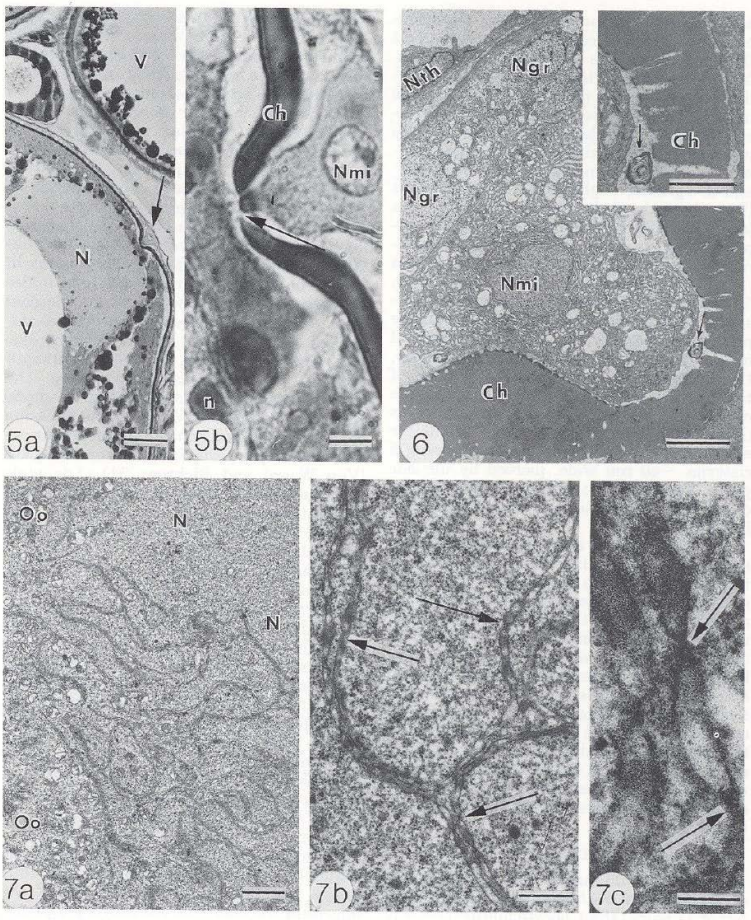

Figure 46. (5a) Micropylar cell (arrow) inside the invagination of the chorion. Bar = 50 µm. (5b) Image in 5a at higher magnification. The micropylar cell blocks the micropyle (arrow). n, nucleolus at the nuclear periphery; Ch, chorion; Nmi, nucleus of micropylar cell. Bar = 5 µm. (6) Cytoplasmic processes of the micropylar cell inside the chorion (arrow points to a lysosome). Ngr, nucleus of a granulosa cell; Nth, nucleus of a theca cell. Bar = 5 µm. Inset: micropylar cell at higher magnification. Arrow points to a lysosome. Bar = 2.5 µm. (7a) Fragments of the disintegrated nuclear envelope at the boundary between the nucleus and cytoplasm. Oo, ooplasm; N, nucleus. Bar = 2 µm. (7b) Magnification of 7a: the nuclear envelope is a double membrane enclosing an interspace pierced by nuclear pores (arrows). Bar = 0.5 µm. (7c) As in 7b, very high magnification. Bar = 0.1 µm (Jackson et al., 1994).

a large follicular cell, the micropylar cell, appears (**Figure 46**, 5a,b, 6), sending thin cytoplasmic processes that penetrate the zona radiata (**Figure 46**, 6), thus forming the micropyle (**Figure 46**, 5a,b). The micropylar cells contain many lysosomes and phagosomes, indicating intense phagosomal activity (**Figure 46**, 6). Once the nucleus approaches the vitelline membrane, the nucleolemma disintegrates and pieces of the nuclear envelope lie dispersed in the cytoplasm, surrounding the nucleus (**Figure 45**, 4d and **Figure 46**, 7a,b,c). The disintegrated nuclear envelope is a double membrane enclosing a cisterna, 40 nm wide, pierced by nuclear pores. The shape of the nucleus remains unchanged after disintegration of the karyolemma.

About 5 - 10 h after the introduction of a male and female into the same aquarium, mature oocytes are observed. In some specimens, the nuclei of several oocytes have already migrated to the oocyte periphery and the nuclear membrane has disintegrated. In other specimens, nuclear migration has barely started. In females sampled after 20 h, the micropyle is fully formed, consisting of a vestibule and continuous with it, the micropylar canal. In those pairs that have fertilized eggs, mature oocytes are absent from the ovary and only remnants of the follicular envelope prove that ovulation has occurred shortly beforehand.

4.2. Cellular Events in the Pituitary Involved in Oogenesis

The brain of Anabantoidei fish contains neurons that secrete hor-

mones involved in the complex control of growth and reproduction and their interactions, as summarized in **Figure 47**. The environment, pheromones, sexual behavior, and hormones are involved in oogenesis

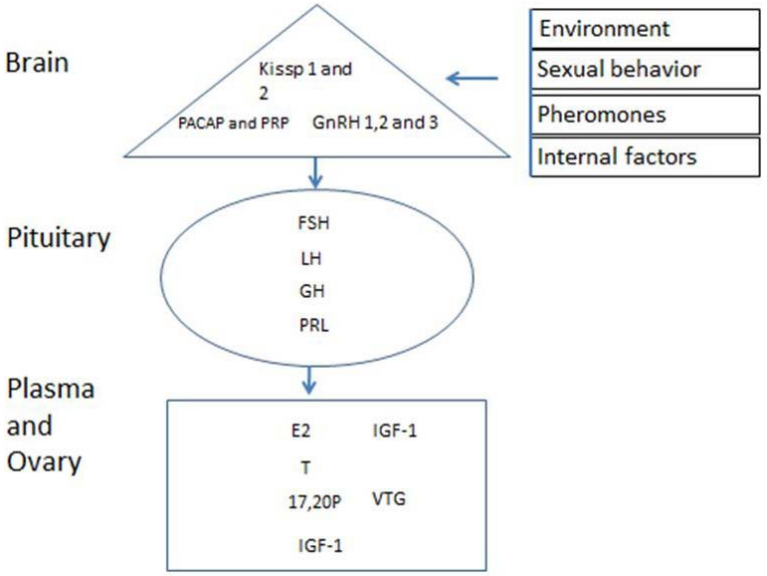

Figure 47. Hormones in the BPG and BPLB axes of female blue gourami during the reproductive phase. The environment (Degani et al., 2011; Levy et al., 2011), sexual behavior (Degani, 1993a) and pheromones (Degani and Schreibman, 1993) affect the brain. In the brain, kisspeptin (Kiss1 and 2) (Degani et al., 2017a) is suggested to affect gonadotropin-releasing hormones (GnRH1 and 3) (Levy and Degani, 2011), which in turn affect secretion of the gonadotropins follicle-stimulating hormone (FSH) and luteneizing hormone (LH) (Degani et al., 1997; Jackson et al., 1999) from the pituitary. Pituitary adenylate cyclase-activating polypeptide (PACAP) and its related protein PRP (Levy and Degani, 2011) secreted from the brain affect growth hormone (GH) (Goldberg et al., 2004) and prolactin (PRL) secretion (Degani et al., 2010) in the pituitary. FSH and LH act on the ovary to synthesize the steroids 17β-estradiol (E_2) (Degani, 2017; Degani et al., 1995), testosterone (T) (Degani, 2017; Degani et al., 1995) and 17α,20β-dihydroxy-4-pregnen-3-one (17,20P) (Degani, 2017; Degani et al., 1995), and on the liver to synthesize vitellogenin (VTG) (Jackson et al., 1994) and insulin-like growth factor 1 (IGF1) (Degani, 2014c).

and the interactions between the two axes of blue gourami, BPG and BPLB, as presented in **Figure 47** and supported by a relatively large number of studies (Degani, 2020a).

The pituitary gland is an important regulator of reproduction in blue gourami, as in other vertebrates (Jackson et al., 2005). This gland is closely associated with the brain (**Figure 48**) and can be divided into two principal structures based on embryogenesis: the adenohypophysis (AH), or anterior pituitary, and the neurohypophysis (NH), or posterior pituitary. In teleosts, the AH is further organized into rostral (rostral pars distalis—RPD) and proximal (proximal pars distalis—PPD) portions based on the topography and distribution of the cell types. In addition, an intermediate lobe (pars intermedia—PI) is found at the point of contact between the AH and NH (**Figure 49**).

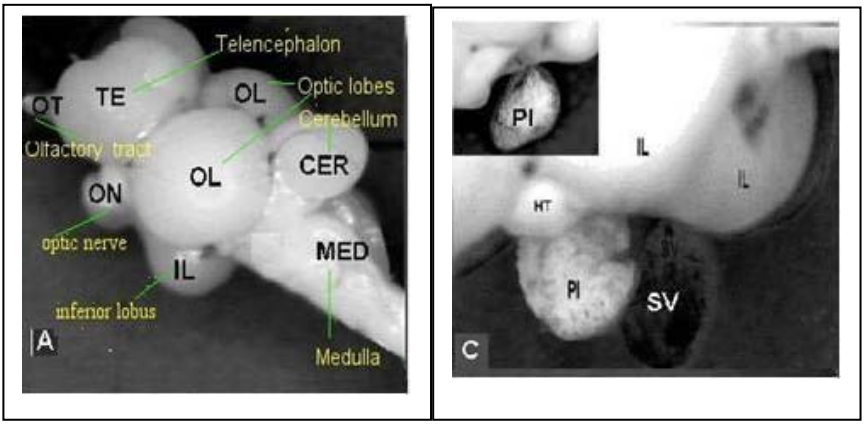

Figure 48. The brain and pituitary glands of blue gourami. PI, pituitary; HT, hypothalamus; IL, inferior lobes.

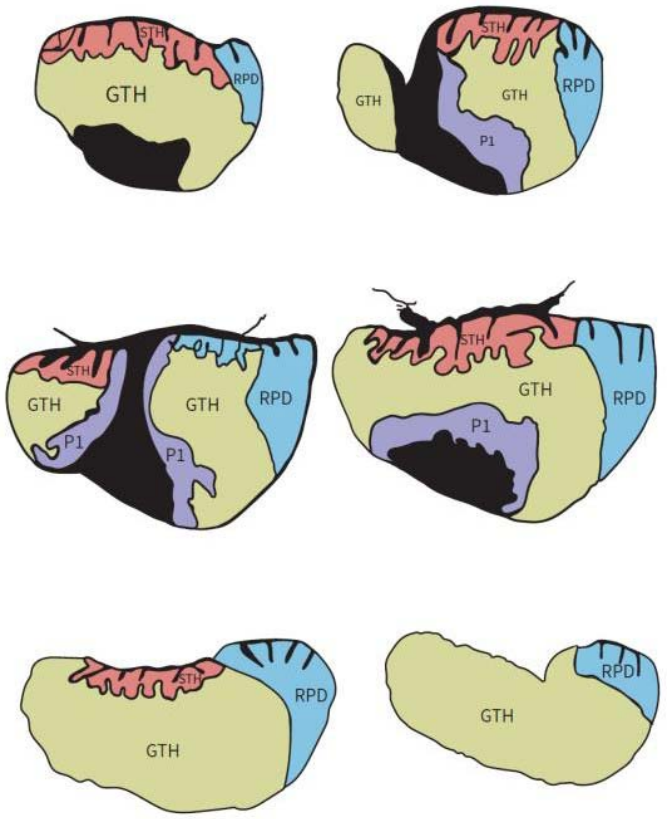

Figure 49. Pituitary of *Trichogaster trichopterus*. Schematic representation of serial sections: STH, somatotrophs (GH); GTH, gonadotropic cells; RPD, rostral pars distalis; PPD, proximal pars distalis; PI, pars intermedia (Jackson et al., 2005).

Teleost pituitaries exhibit extraordinary variability in terms of shape, cell-type distribution and location relative to the hypothalamus, but only a general cell-type arrangement in the AH (**Figure 50**). The RPD contains two cell types: corticotrophs (adrenocorticotropic hormone [ACTH]-producing cells) and PRL-producing cells. Gonadotrophs (GtH-producing cells) and somatotrophs (GH-producing cells)

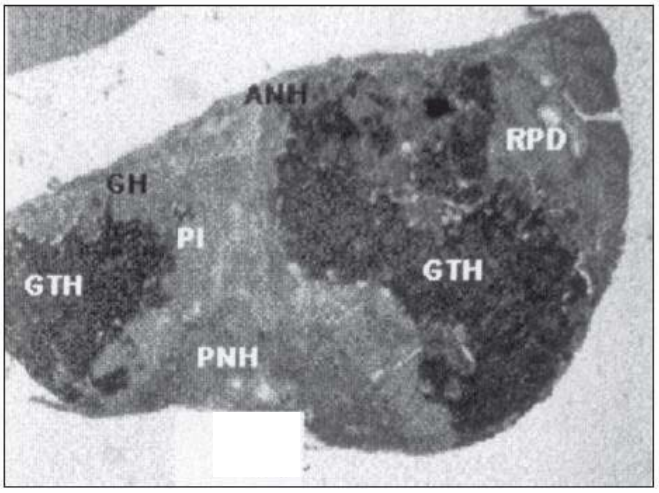

Figure 50. Sagittal section of the gourami pituitary showing the different regions. PI, pars intermedia; RPD, rostral pars distalis; PNH, distal neurohypophysis; ANH, proximal neurohypophysis; and localization of the two cell types of the proximal pars distalis (PPD): growth hormone (GH) and gonadotropic (GTH) cells. PAS-ABOG trichrome staining, X250 magnification (Jackson et al., 2005).

are characteristic of the PPD. Cells producing somatolactin- and melanocyte-stimulating hormone (MSH) cells are found in the PI. Thyroid-stimulating hormone (TSH)-secreting cells can be found in the RPD. The role of the pituitary in the reproductive process has been studied in several teleost species. Drastic physiological changes take place in the ovaries during the reproductive cycle, including morphological changes and alterations in the steroids produced (Degani and Boker, 1992a, 1992b). These changes are the result of the secretion of pituitary hormones. In early studies, morphological changes occurring in the AH cells were generally related to ovarian development, but not to the period of transition from vitellogenesis to final oocyte matura-

tion (Jackson et al., 2005). Only a few descriptions of pituitary cell events during this period are available, because the exact onset of final oocyte maturation is difficult to determine in most of the teleost species studied.

4.2.1. General Aspects of the Blue Gourami Pituitary

The blue gourami pituitary is devoid of a distinct stalk: the thin floor of the hypothalamus itself forms the NH. The AH can be divided into RPD, PPD and PI. The NH penetrates the AH in the middle of the gland, apparently dividing the PPD into two regions. The NH sends branches to the three AH regions, and branches out intensively in the PI (**Figure 49**, **Figure 50**). Sagittal sections subjected to PAS and alcian blue/orange G (PAS-ABOG) trichrome staining after oxidation with paracetic acid revealed a well-defined RPD containing two different cell types. The first and more numerous type was lightly stained by orange G. These acidophilic cells were elongate and organized into follicles. They are probably homologous to the PRL cells of other species (**Figure 51**).

The PRL cell region was easily discerned under the electron microscope, since the prolongation of stellate cells, which is characteristic of this region, was found between the membranes of the adjacent, opposed PRL cells (**Figure 52**). The structure of the gourami PRL cells (**Figure 53**) is similar to that of related cells in other previously described teleosts (Jackson et al., 2005).

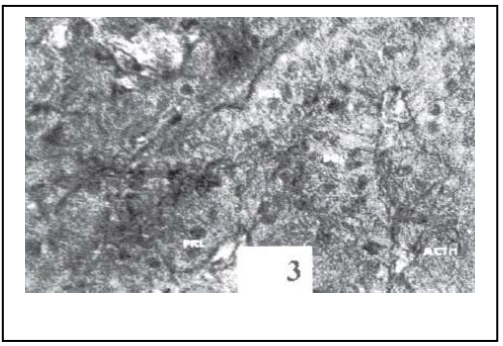

Figure 51. Detail of the rostral pars distalis (RPD) of blue gourami showing PRL- and ACTH-secreting cells. PAS-ABOG-stained trichromes. X1000 magnification.

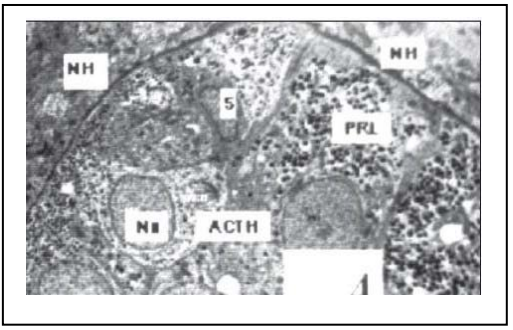

Figure 52. Rostral pars distalis (RPD) of the blue gourami pituitary. PRL- and ACTH-secreting cells, nucleus (Nu), neurohypophysis (NH), stellate cells (S).

The most pronounced characteristic was the presence of a well-developed lamellar endoplasmic reticulum (ER) found along the periphery. Electron-dense granules, usually accumulating at one pole of the cell, were found and a round, slightly peripheric nucleus was observed (**Figure 52**). A second cell type was always found in the RPD lining the dorsal border of the NH. These latter, round cells stained a light gray with PAS-ABOG trichrome staining (**Figure 51**), and a dark

blue using the hematoxylin technique. They were classified as ACTH cells and characterized by their granules, which show a more electron-dense core that is separated from the surrounding membrane by electron-lucent hila. The elongated nucleus sometimes showed re-entrance and contained a peripheric nucleolus. The mitochondria were usually found dispersed in small groups (**Figure 54**). ACTH and PRL cells were found strongly opposed to the penetrations of the anterior NH in the PPD (**Figure 52**) (Jackson et al., 2005).

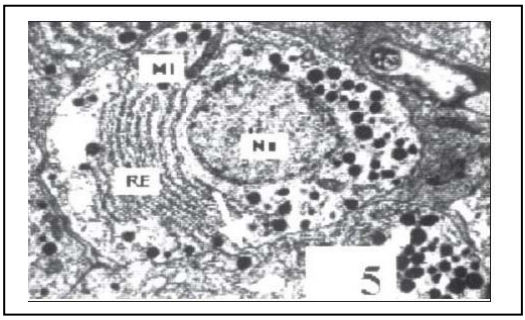

Figure 53. Detail of the prolactin (PRL) cell containing many secretory granules (arrows). Nucleus (Nu), endoplasmic reticulum (RE), mitochondria (Mi).

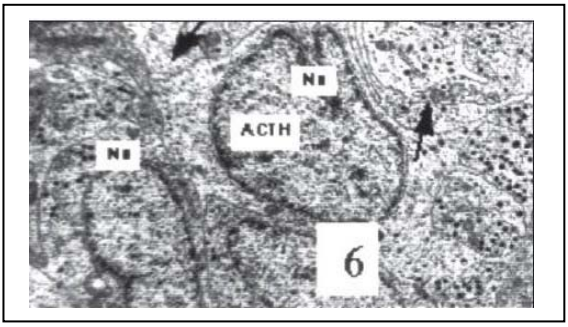

Figure 54. Detail of the ACTH cell containing a few secretory granules (arrows). Nucleus of ACTH cell (Nu).

In adult specimens, the major part of the AH is comprised of the PPD and PI. These two regions are closely related to the cells of one region that is occasionally found in the other. An acidophilic cell strongly stained by orange G and a basophilic cell stained dark purple by PAS and AB stains can be distinguished in the PPD (**Figure 55**). The first cell type is found in the dorsal part of the gland, where the NH sends axons into the AH, and distributed among the basophilic cells (Jackson et al., 2005).

These cells are classified as somatotrophs. Somatrotophs are round cells with a turgid appearance containing a peripheric elongated nucleus. Under the electron microscope, these cells are characterized by the presence of electron-dense granules filling the entire cytoplasm, which sometimes contains debris; the irregular nucleus is usually found along the periphery of the cell. A well-developed Golgi is also usually observed (**Figure 56**) (Jackson et al., 2005).

One layer of acidophilic cells similar to the somatotrophs was found bordering the branches of the NH. Gonadotrophs comprise most of the PPD; they are scattered in its central and ventral parts and along the gland's posterior edge. Antiserum against carp GtH-I and GtH-II b chain reacted in the same way with all GtH cells (**Figure 57** and **Figure 58**). GtH cells are large round cells stained by PAS-ABOG trichrome staining (**Figure 55**) (Jackson et al., 2005).

The GtH cells are easily recognized under the electron microscope

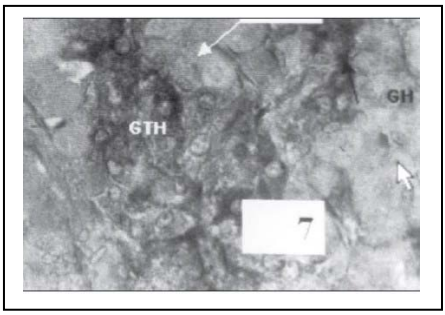

Figure 55. Proximal pars distalis (PPD) of the blue gourami showing two different cell types. Growth hormone (GH) cells, gonadotropin (GtH) cells, nucleus of GtH cell (white arrow), nucleus of GH cell (black arrow). PAS-ABOG trichrome staining.

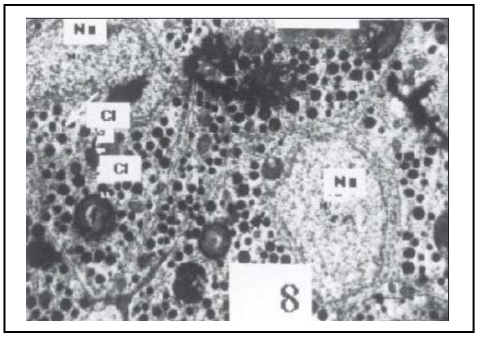

Figure 56. GH cells containing many secretory granules (arrows). Nucleus (Nu), cytoplasmic inclusions (Ci).

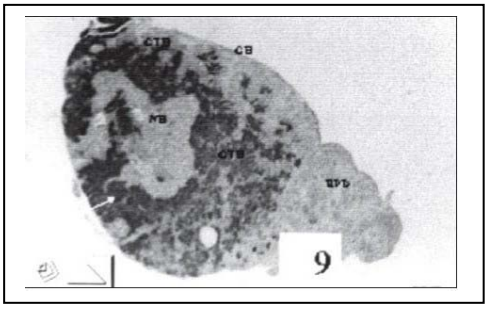

Figure 57. Reaction to anti-salmon GtH-I. Growth hormone cells (GH), rostral pars distalis (RPD), neurohypophysis (NH).

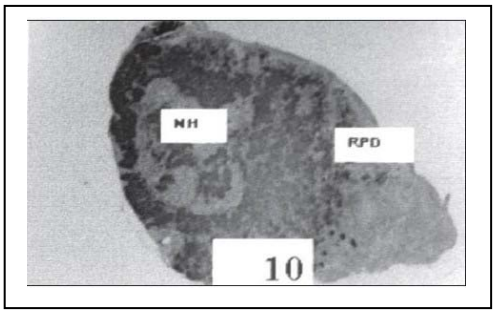

Figure 58. Reaction to anti-coho salmon GtH-II. Rostral pars distalis (RPD), neurohypophysis (NH).

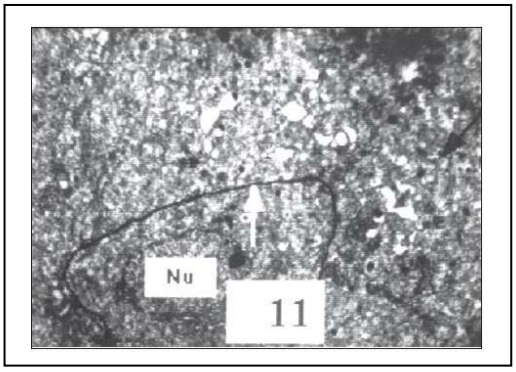

Figure 59. MSH (Pb hematoxylin positive)-producing cell showing nucleus (Nu) and very few secretory granules (arrow).

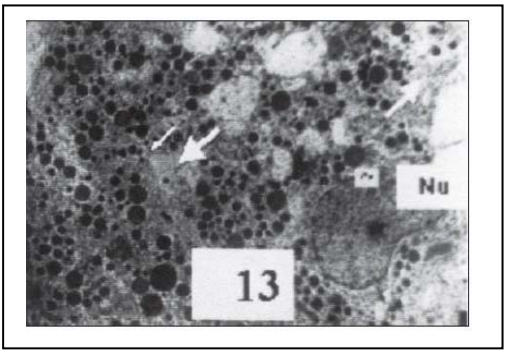

Figure 60. GtH cell of non-reproductive fish showing big globules (white arrow), secretory granules (black arrow) and nucleus (Nu).

because they are the only cell type in which globules are also present in the cytoplasm, in addition to the secretory granules (**Figure 60**). A third cell type was found in the PPD that was chromophobic, located in the dorsal part of the gland (**Figure 61**, **Figure 62**). The PI contains two different cell types. The predominant cell type stains with lead hematoxylin when PAS-ABOG trichrome is used, and remains chromophobic. This cell type probably corresponds to the MSH-producing cell previously described in other teleosts (**Figure 59**). The other cell type is positive for PAS and most likely corresponds to the somatolactin-secreting cell. The PAS cells are often elongated and have a central round or oval nucleus. Under the electron microscope, they show a little ER and a small Golgi apparatus. The secretory granules are membrane-bound and exhibit a slight variation in electron density. A round nucleus is usually found along the cell's periphery (**Figure 59**, **Figure 60**). The MSH-producing cell type shows a centrally located nucleus having a small nucleolus. A small number of granules are found in the cytoplasm, which is filled with vesicles containing electron-dense material. Little ER is found surrounding the nucleus (**Figure 59**). As in other teleosts, the NH can be classified as the anterior neurohypophysis (ANH) that is functionally related to the RPD and the PPD; the posterior neurohypophysis (PNH) is related to the PI. The ANH is found along the dorsal edge of the gland sending indentations between the somatotrophs in the PPD and the PRL and ACTH cells in the RPD. The PNH consists of the main trunk that pe-

netrates the AH in the middle of the gland, which closely relates to the PI sending many branches to this AH region. In some places, the PNH is surrounded by one layer of large acidophilic cells. Large blood vessels are found in both the main trunk and the lateral ramifications of the NH (**Figure 49**, **Figure 50**).

4.2.2. Changes in Gonadotropic Cells

Non-reproductive female fish: In a general view, the GtH cell region was well stained by PAS and AB. However, a more detailed observation showed that the cells found in the central part of the gland are lighter purple in color, with pink shading from the PAS staining. The cells found along the periphery were stained blue, being less positive for PAS. Some chromophobic cells were also found in the PPD, mainly in the dorsal part of the gland. Stained GtH cells were seen under the electron microscope to contain large globules and granules. The globules varied from having a homogeneous appearance to having an aspect of irregular masses containing electron-dense and electron-lucent regions. Vacuoles were also found occasionally inside the globule. The globules and granules were dispersed homogeneously in the cytoplasm, together with a well-developed Golgi apparatus and abundant mitochondria (**Figure 61**, **Figure 62**).

Females after pairing (reproductive fish): In the pituitary of females that have started the maturation process, a general decrease in staining of the entire gonadotrophic cell region was detected. Many

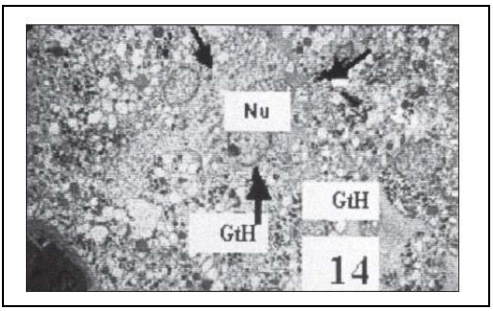

Figure 61. Cell types (arrows) found among the predominant gonadotropin (GtH) cells. Note the difference in size of granules in the PPD. Nucleus (Nu).

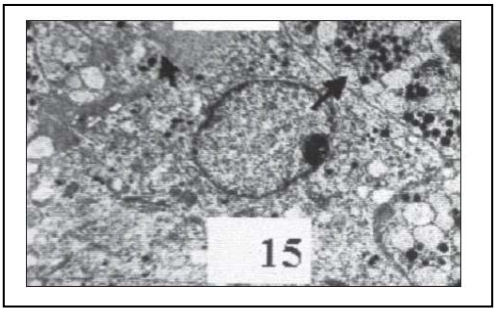

Figure 62. Detail of the cell type in **Figure 62**. Note the presence of small secretory granules (arrows) and the absence of the large globules.

non-stained cells were found in the PPD dispersed among intensely stained cells. An increase in the number of chromophobic cells was detected, mainly along the periphery (**Figure 63**). This contrasting staining pattern was found in both females during the maturation process and females that had spawned up to 24 h before being sampled. Many completely empty cells were found in a female sampled at the moment of spawning (after ovulation, but before expelling the eggs), dispersed among intensely stained cells in a highly contrasting staining pattern (**Figure 63**). Some GtH cells of reproductive fish

showed nuclei that were hypertrophic when compared to the nucleus of the GtH cells of non-reproductive females (**Figure 64**). In the stained GtH cells of reproductive females, the cytoplasmic content was concentrated at one pole of the cell (**Figure 63**). This phenomenon was confirmed by electron microscopy. In females sampled during final oocyte maturation or after spawning, a concentration of secretory material was found around the AH capillaries (**Figure 64**).

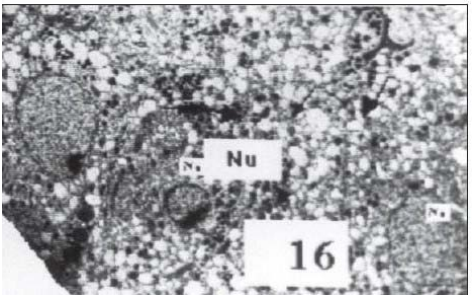

Figure 63. Gondotropin cells of reproductive fish found before spawning, showing the concentration of secretory granules at one pole of the cell (black arrow). Note the presence of many empty vesicles in the cytoplasm (white arrow). Nucleus (Nu).

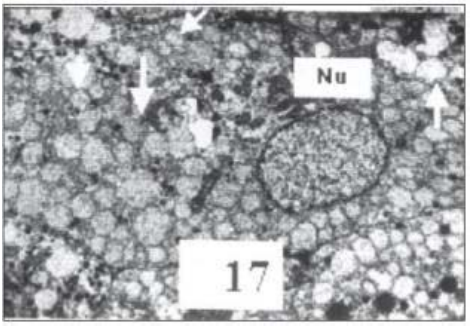

Figure 64. Gonadotropin cell of reproductive fish found after spawning, showing a decrease in the secretory granules (black arrow) and an increase in empty vesicles (white arrows).

A decrease in the number of secretory granules was detected under the electron microscope in some GtH cells of females sampled during final oocyte maturation (**Figure 65**). Large globules were still found, but without debris. GtH cells of females found after spawning were characterized by the presence of large vacuoles formed by a confluence of ER cisternae.

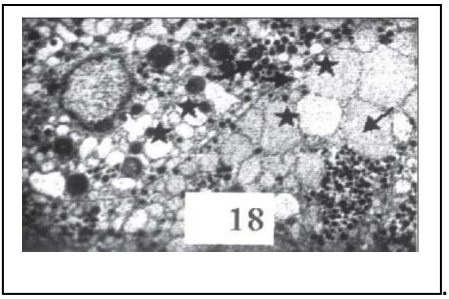

Figure 65. Gonadotropin (GtH) cells of reproductive fish after spawning. On the left, a GtH cell containing many globules (arrow) together with secretory granules (black arrow) and empty vesicles (H). On the right, a GtH cell showing the large electron-lucent regions that are the result of the coalescence of the empty vesicles (H). Secretory granules are concentrated at one pole of the cell (black arrow).

In fish examined after larvae were found in the nest (at least 48 h after spawning), the gonadotropic cells showed a staining pattern similar to that found in non-reproductive fish. In the central part of the gland, most of the gonadotrophic cells were intensely stained. Along the periphery of the dorsal and ventral borders of the gland, weakly stained and unstained cells were still found interspersed with well-stained cells. Nevertheless, the PNH was completely devoid of neurosecretions.

4.3. Pheromone of Blue Gourami Males Affects Oogenesis in Females

Chemical communication in fish species has aroused intense interest in recent years (Stacey and Sorensen, 2006), and such studies have shown that pheromones play an important role in different aspects of reproduction in teleosts (Becker et al., 1992). Those studies examined the connection between pheromones and the reproductive cycle; specifically, during maturation and ovulation (Degani and Schreibman, 1993) and during vitellogenesis. A number of studies concerning chemical communication in *Trichogaster trichopterus* (Anabantidae, Pallas 1770) have indicated that this species may serve as a model for the whole systematic group (Degani, 2001).

Oogenesis in female blue gourami is influenced by male pheromones (**Figure 66**). In the ovary of females in low vitellogenesis, the pheromones raise the percentage of oocytes in vitellogenesis (**Figure 66(a)**) and in females in advanced stages of vitellogenesis, the pheromones affect the change from vitellogenesis to maturation (**Figure 66(b)**) (Degani and Schreibman, 1993).

Gonadotropin cells in the pituitary of blue gourami females were stained for immunocytochemistry. A high immune-response effect was found in water holding a nest-building male. A low immune response was found in water holding blue gourami males in a group, under non-reproductive conditions (**Figure 67**).

The pheromones in fish are glucosteroids that dissolve in water and

transmit signals between pairs (Becker et al., 1992; Stacey and Sorensen, 2006). The steroids and glucosteroids detected in both male and female gonads of blue gourami by gas chromatography/mass spectrometry (GCMS), at a sensitivity of 0.01 ng, and extracted by organic solvent and water, are shown in **Table 4** and **Table 5**, and their electron impact mass spectra in **Figure 68** and **Figure 69** (Becker et al., 1992).

The organic fraction in the ovaries contained a very high concentration of lipids, making the identification of steroids difficult. Most of

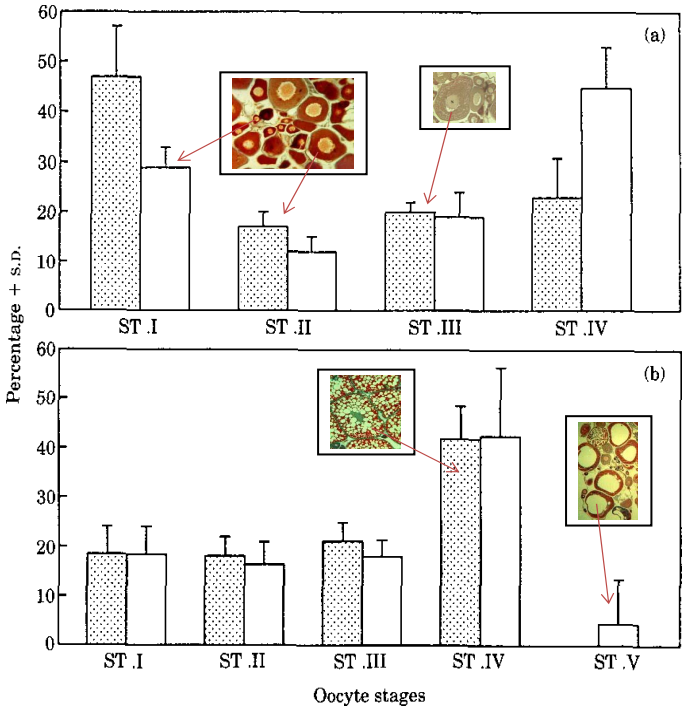

Figure 66. Percentage of oocytes at various stages of oogenesis in the ovary of females held in water containing pheromones from the nest-building male (b) and in tap water (control) (a). Ovary in low vitellogenesis (ST1-ST4). Ovary in advanced vitellogenesis (ST1-ST5).

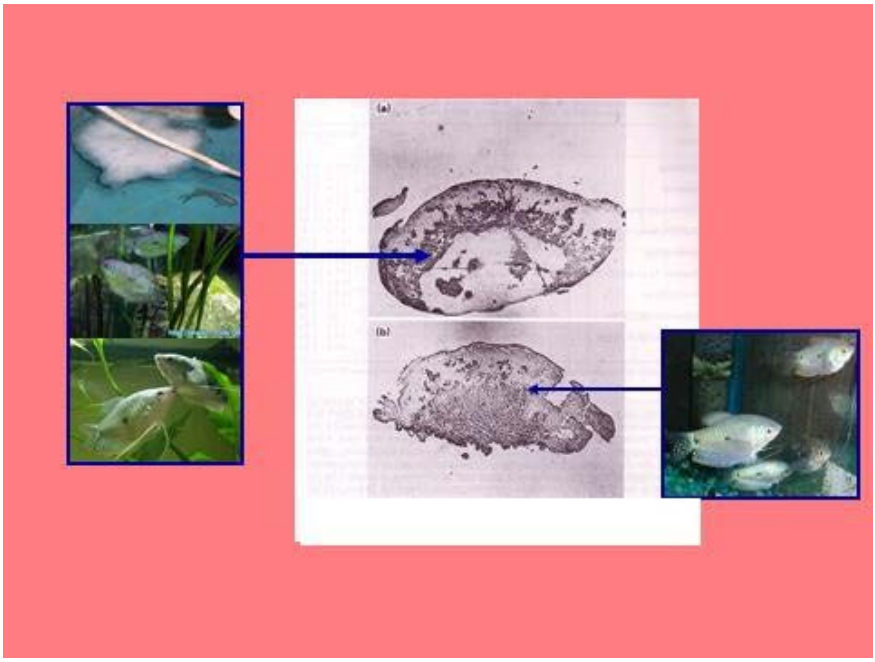

Figure 67. Gonadotropin cells in the pituitary of blue gourami females, stained for immunocytochemistry. (A) High immune-response effect in water holding nest-building male. (B) Low immune response in water holding blue gourami males in a group, non-reproductive conditions.

Table 4. Steroids detected by GCMS from the testis and ovary of blue gourami.

	In group				Reproductive		
	Male o.f*	Male w.f.†	Female o.f.	Female w.f.	Female w.f.	Male w.f.	Male o.f.
Steroids					(after injection)		
Estadiol-17β	+	+	+	+	+	+	+
Testosterone	+	+	O	+	O	+	+
J7α-Hydroxyprogesterone	+	+	O	+	+	+	+
Cholesterol	+	+	+	+	+	+	+
Stigmasterol	+	+	O	+	+	+	O
4-β-Methylcolesro	+	+	+	+	+	+	+

Sitosterol	+	+	0	+	+	+	+
Estrone	0	+	0	0	0	+	0
17α,20β-Dihydroxy-4-pregnen-3-one	0	0	+	+	+	0	0

*Organic fraction; †water fraction. GC-MS sensitivity = 0.01.

Table 5. Glucosteroids detected by GCMS in water holding blue gourami fish.

	Females (F)	Males (M)	F&M
Estradiol-17β	+	+	+
Estrone	0	+	0
17α-Hydroxyprogesterone	+	0	+
Cholesterol	+	+	+
4-β-Methylcholesterol	+	+	+
Stigmasterol	+	0	+
Sitosterol	+	+	+

the steroids from the gonads were detectable in the water fraction. The steroids E_2, T, 17ct-hydroprogesterone (17-P), cholesterol (C), 4-fl-methylcholesterol (4fl-MC), stigmasterol (S), estrone (ES) and 17,20-P were detected in both the organic and water fractions of the gonads, although 17,20-P was detected only in the female gonad (Becker et al., 1992).

Glucosteroids detected in the holding water are shown in **Table 5**. The difference between the results in **Table 4** and **Table 5** appears to be due to the concentration of glucosteroids, which is much lower in the aquarium water than in the gonads. A number of steroid glucuronides detected in the holding water of both males and females in this study were not mentioned in studies of other species, e.g., E_2,

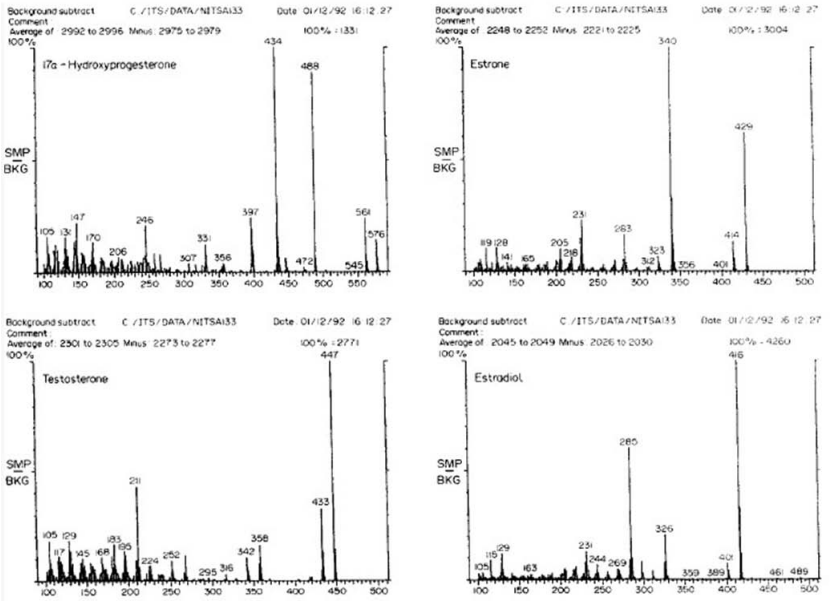

Figure 68. Mass spectra of 17α-hydroxyprogesterone, estrone, testosterone, estradiol as theoroxime-trimethylsilyl derivatives (Becker et al., 1992).

17-P and 4fl-MC (Becker et al., 1992).

In blue gourami, as in other fish, pheromones are endogenous signals between the reproductive tract and brain, and exogenous signals that synchronize oogenesis and spawning interactions between males and females.

4.4. Brain Involvement in Reproduction in Labyrinthici Fish Using Female Blue Gourami as a Model

4.4.1. Environmental, Internal and Sexual Behavioral Factors Affecting the Female Brain

The brain of Anabantoidei fish contains neurons that secrete hormones

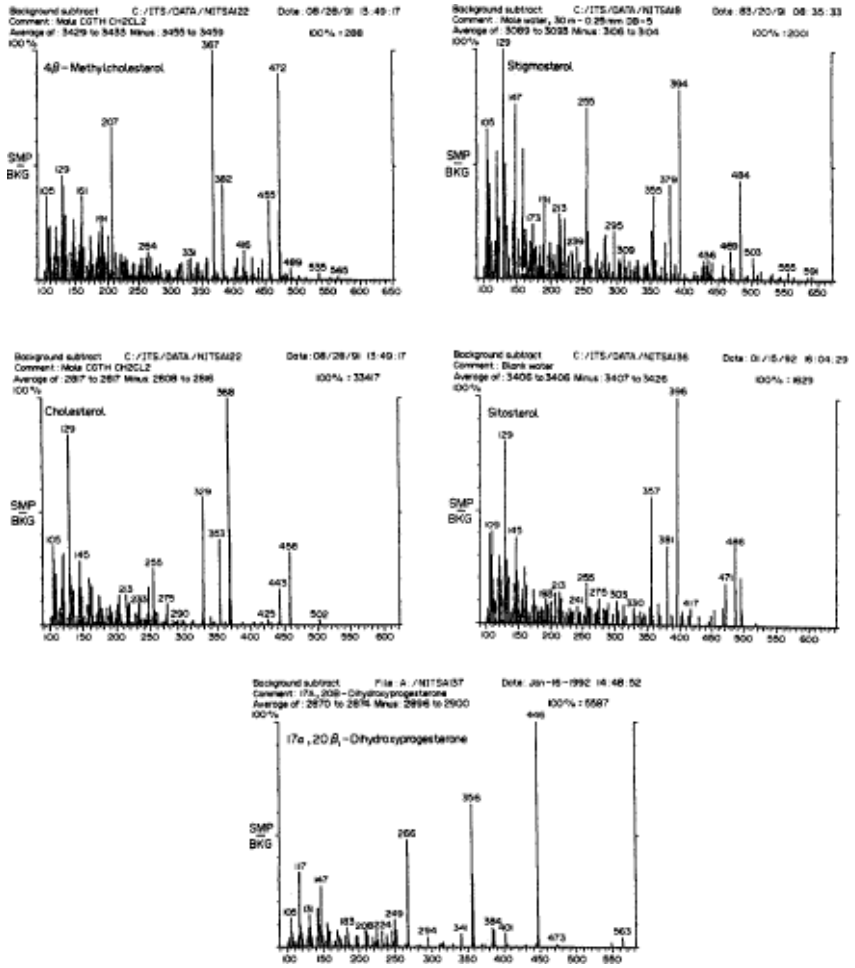

Figure 69. Mass spectra of 4β-methylcholesterol, cholesterol, stigmasterol, sitosterol and 17α20β-dihydroxy-progesterone as theoroxime-trimethylsilyl derivatives (Becker et al., 1992).

involved in growth and reproduction control and the interactions between them. This very complex system is summarized in the sketch in **Figure 47**. The environment, pheromones, sexual behavior and hormones are involved in oogenesis and the interactions be-

tween the two axes of blue gourami, BPG and BPLB, as supported by many studies (Becker et al., 1992; Degani, 1989, 1990, 1993a, 1993b, 1994, 2014a, 2014b, 2014c, 2015a, 2015b, 2016, 2018; Degani and Boker, 1992a, 1992b; Degani and Gallagher, 1996; Degani and Schreibman, 1993; Degani and Yom Din, 2011; Degani and Ziv, 2016; Degani et al., 1994, 1995, 1997, 1998, 2003, 2010, 2011, 2017a, 2017b; Ezagouri et al., 2008; Jackson et al., 1994, 1999, 2005; Levy and Degani, 2011, 2012, 2013; Levy et al., 2009, 2010, 2011; Mananos et al., 1997).

Environmental conditions such as water temperature (David and Degani, 2011), sexual behavior (Degani, 1993a) and pheromones (Becker et al., 1992; Degani and Schreibman, 1993) affect the brain within the neuroendocrine system in Labyrinthici fish, as described in detail for other teleosts (Zohar et al., 2010). The brain is the main organ that controls reproduction along the HPG axis (Yaron and Levavi-Sivan, 2011). Oogenesis and spermatogenesis in fish, as in other vertebrates, is a complex mechanism; many different processes are involved in the brain and it is difficult to differentiate between them. However, the male behavioral effect on oogenesis, the change from vitellogenesis to maturation, differs in blue gourami compared to other fish.

The transfer of oocytes from pre-vitellogenesis to vitellogenesis to maturation is controlled by the BPG axis. The brain transcriptome in female blue gourami changes dramatically during puberty (Degani et

al., 2019a). In the brain of blue gourami, 34,368 transcripts were identified, 23,710 of which were similar to other species. In the brain of female blue gourami, different genes were upregulated in juveniles (pre-vitellogenesis) compared to adults (vitellogenesis) (**Figure 70**, **Table 6**).

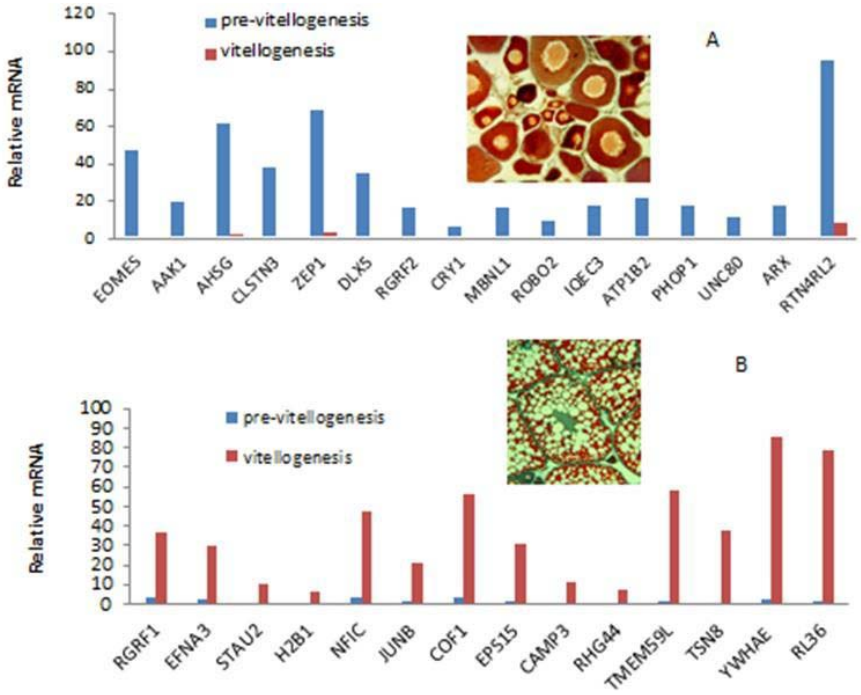

Figure 70. mRNA levels (based on RNA-Seq) of transcripts associated with known genes (**Table 6**) representing the differences in edgeR analysis ($P < 0.001$) between pre-vitellogenesis (A) and vitellogenesis (B) in female blue gourami brain (Degani et al., 2019a).

Table 6. Genes expressed differentially in pre-vitellogenesis/vitellogenesis (see **Figure 70**) and their putative functions (Degani, 2020a; Degani et al., 2019a).

Gene ID	**Gene name**	**GenBank function**
Upregulated in pre-vitellogenesis		
CERS6 CERS5	Ceramide synthase 6 Ceramide synthase 5	DNA binding. Dihydroceramide synthase. Catalyzes the acylation of sphingosine to form dihydroceramide.
AAK1	AP2-associated kinase 1	Regulates clathrin-mediated endocytosis by phosphorylating the AP2M1/mu2 subunit of the adaptor protein complex 2 (AP-2), which ensures high-affinity binding of AP-2 to cargo membrane proteins during the initial stages of endocytosis.
AHSG	(FETUA) alpha 2-HS glycoprotein	Probably involved in differentiation.
CLSTN3	Calsyntenin 3	May modulate calcium-mediated postsynaptic signals. Complex formation with APBA2 and APP, stabilizes APP metabolism and enhances APBA2-mediated suppression of beta-APP40 secretion due to the retardation of intracellular APP maturation.
ZEP1	Zeaxanthin epoxidase	Converts zeaxanthin to antheraxanthin and subsequently violaxanthin.
DLX5	Distal-less homeobox 5	Transcriptional factor involved in bone development. Acts as an immediate early BMP-responsive transcriptional activator essential for osteoblast differentiation.
RGRF2	Ras guanine nucleotide exchange factor 2	Functions as a calcium-regulated nucleotide exchange factor activating both Ras and rac1 through the exchange of bound GDP for GTP. May function in synaptic plasticity.
CRY1	Cryptochrome-1	Transcriptional repressor that forms a core component of the circadian clock.
MBNL1	Muscleblind like splicing regulator 1	Negative regulation of axon extension involved in axon guidance. Metal ion binding.
ROBO2	Roundabout guidance receptor 2	1. Anterior/posterior axon guidance. 2. Central nervous system projection neuron axonogenesis.

IQEC3	IQ motif and Sec7 domain 3	Acts as a guanine nucleotide exchange factor (GEF) for ARF1.
ATP1B2	ATPase Na^+/K^+ transporting subunit beta 2	This is the non-catalytic component of the active enzyme, which catalyzes the hydrolysis of ATP coupled with the exchange of Na^+ and K^+ ions across the plasma membrane. The exact function of the beta-2 subunit is not known.
PHOP1	Probable phosphatase phospho1	Involved in bone mineralization.
UNC80	Unc-80 homolog, NALCN activator	Component of the NALCN sodium channel complex required for channel regulation. UNC80 is essential for NALCN sensitivity to extracellular calcium.
ARX	Aristaless related homeobox	Appears to be indispensable for central nervous system development. May play a role in the neuronal differentiation of the ganglionic eminence and ventral thalamus. May also be involved in axonal guidance in the floor plate.
Rtn4rl2	Reticulon-4 receptor-like 2	Cell surface receptor. Plays a functionally redundant role in postnatal brain development and in regulating axon regeneration in the adult central nervous system. Contributes to normal axon migration across the brain midline and normal formation of the corpus callosum. Protects motoneurons against apoptosis.
Upregulated in vitellogenesis		
RGRF1	Ras protein Specific Guanine Nucleotide Releasing Factor 1	Promotes the exchange of Ras-bound GDP by GTP.
EFNA3	Ephrin A3	Binds promiscuous Eph receptors residing on adjacent cells, leading to contact-dependent bidirectional signaling into neighboring cells.
STAU2	Staufen double-stranded RNA binding protein 2	RNA binding.
H2B1	Histone H2B-like	DNA binding, protein heterodimerization activity.
NFIC	Nuclear factor I C	Recognizes and binds the palindromic sequence 5'-TTGGCNNNNNGCCAA-3' present in viral and cellular promoters and in the origin of replication of adenovirus type 2. These proteins are individually capable of activating transcription and replication.
JUNB	JunB proto-oncogene, AP-1	1. RNA polymerase II core promoter

	transcription factor subunit	proximal region sequence-specific DNA binding. 2. RNA polymerase II transcription factor activity, sequence-specific DNA binding. 3. Transcription coactivator activity, transcription factor binding.
COF1	Cofilin	Binds to F-actin and exhibits pH-sensitive F-actin depolymerizing activity. Regulates actin cytoskeleton dynamics. Important for normal progress through mitosis and normal cytokinesis.
EPS15	Epidermal growth factor receptor pathway substrate 15	Involved in cell growth regulation. May be involved in the regulation of mitogenic signals and control of cell proliferation. Involved in the internalization of ligand-inducible receptors of the receptor tyrosine kinase (RTK) type, in particular EGFR.
CAMP3	Calmodulin-regulated spectrin-associated protein 3	Microtubule minus-end binding protein that acts as a regulator of non-centrosomal microtubule dynamics and organization. Specifically required for the biogenesis and maintenance of zonula adherens by anchoring the minus-end of microtubules to zonula adherens and by recruiting the kinesin KIFC3 to those junctional sites.
RHG44	Rho GTPase-activating protein 44-like	GTPase-activating protein that stimulates the GTPase activity of Rho-type GTPases, thereby controlling Rho-type GTPase cycling between their active GTP-bound and inactive GDP-bound states.
TMEM59L	Transmembrane protein 59 like	Modulates the O-glycosylation and complex N-glycosylation steps occurring during the Golgi maturation of APP. Inhibits APP transport to the cell surface and further shedding.
TSN8	Tetraspanin-8	Integrin binding.
YWHAE (1433E)	Tyrosine 3-monooxygenase/tryptophan 5-monooxygenase activation protein epsilon	1. Monooxygenase activity. 2. Protein domain-specific binding.
RL36	Ribosomal protein 36 60S large ribosomal subunit	Component of the large ribosomal subunit.

Those genes' expression differ in juvenile females in pre-vitellogenesis vs. mature females in vitellogenesis, probably reflecting a connection

between puberty and gonadal maturation. However, the association is very complex. More specifically, it seems that that a relatively large number of neurons in the brain affect Kiss, which controls GnRHs (GnRH1 and 3) and the HPG axis, as described in other teleost fish (Zohar et al., 2010). It is hypothesized that in blue gourami, as in other Labyrinthici fish, the environment, pheromones and sexual behavior of males affect Kiss. Much of our data support this hypothesis, but more direct studies are required to confirm it.

Degani and colleagues (2017) described the mRNA levels of Kiss2 and Kiss receptors (GPR54 or Kiss2R, Kiss1R) in the brain of blue gourami (Degani, 2001). These hormones have also been described in other teleost fish, e.g., zebrafish (*Danio rerio*) (Lee et al., 2009; Servili et al., 2011), lamprey (*Petromyzon marinus*) (Lee et al., 2009), medaka (*Oryzias latipes*) (Kitahashi et al., 2009), goldfish (*Carassius auratus*) (Huang et al., 2009) and sea striped bass (*Morone saxatilis*) (Espigares et al., 2017).

A sketch is presented in **Figure 71** of suggested hormone secretion from the brain and pituitary of blue gourami females based on gene expression determined in various studies.

4.4.2. Hormones Involved in Reproduction and Growth in the Brain of Blue Gourami

It is generally accepted that in fish, the neuropeptide release of GnRH

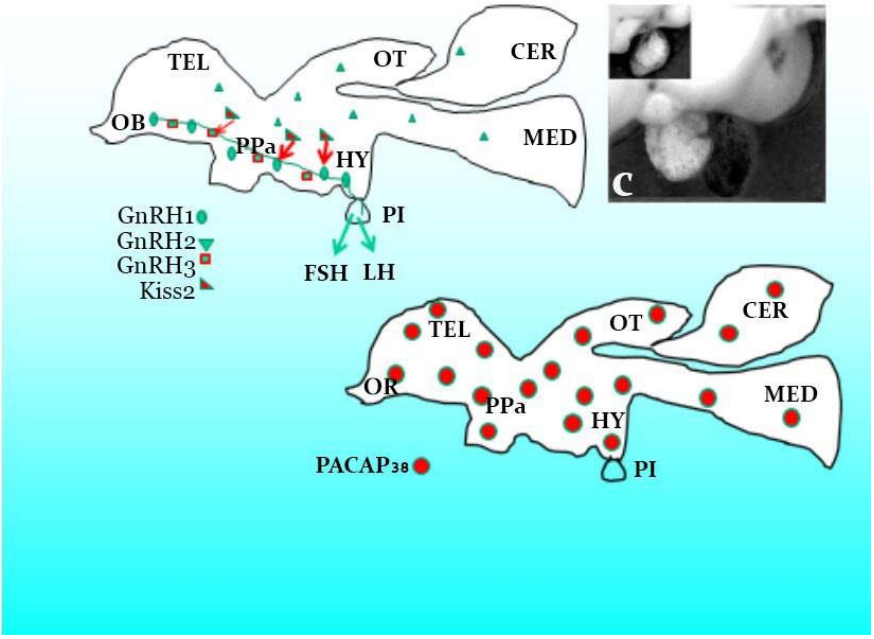

Figure 71. Sketch of suggested hormone secretion from the brain and pituitary of blue gourami females based on gene expression determined in various studies (Degani, 2014a, 2016, 2020a; Degani et al., 2017a, 2017b, 2019a; Levy and Degani, 2011, 2012, 2013; Levy et al., 2009, 2010). OB, olfactory bulb; OT, optic tectum; CER, carpus cerebelii; PPa, nucleus preopticus parvicellularis posterioris; PI, pituitary gland; HY, hypothalamus; Kiss2, kisspeptin 2; GnRH1, 2 and 3, gonadotropin-releasing hormone 1, 2 and 3; PACAP38, pituitary adenylate cyclase-activating polypeptide; FSH, follicle-stimulating hormone; LH, luteinizing hormone.

and dopamine is controlled by Kiss (Zohar et al., 2010). In the female blue gourami model Anabantoidei fish, three GnRHs (GnRH1, 2 and 3) have been studied in detail (Degani, 2016; Levy and Degani, 2012). Based on the results (Levy and Degani, 2012) (**Figure 72** and **Figure 73**) of the cloning and expression of these three GnRHs during growth

and puberty, and of the expression of Kiss2 and its receptors, it is suggested that Kiss2 affects GnRH1, which controls and regulates vitellogenesis in blue gourami (Degani, 2018; Degani et al., 2017a).

Although it is difficult to differentiate between the functions of GnRH1 and 3 in females (GnRH2 does not directly affect oogenesis), GnRH1 seems to have a greater effect during puberty on FSH and GnRH3 secretion, as well as on LH, which controls oocyte maturation and ovulation (**Figure 73**). It seems that GnRH3 and PACAP, which dramatically alter gene expression during oocyte maturation in blue gourami, control this process (**Figure 73**). Both oocyte maturation and ovulation are affected by male sexual behavior and male pheromones (see review by Degani, 1993a, 2001).

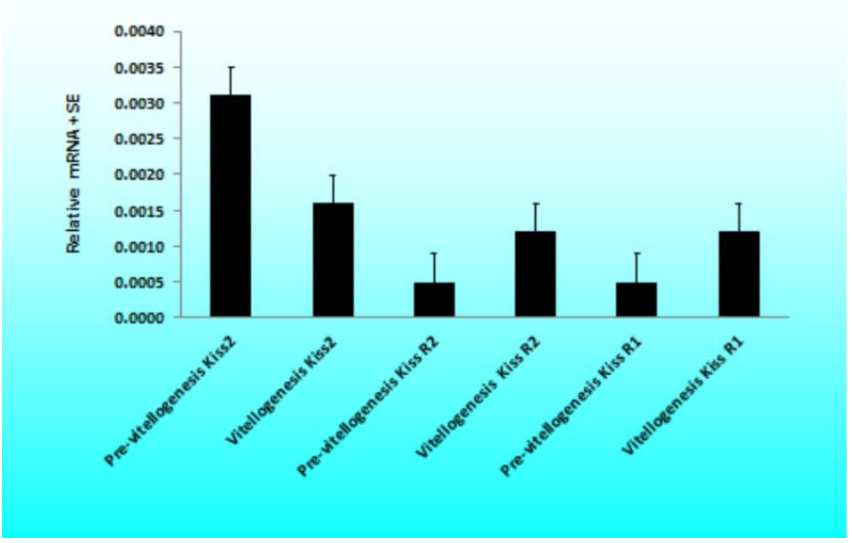

Figure 72. Comparison of gene transcription of *kiss*2, *kissR*1 and *kissR*2 in the brain of blue gourami females during oogenesis (Degani et al., 2017a).

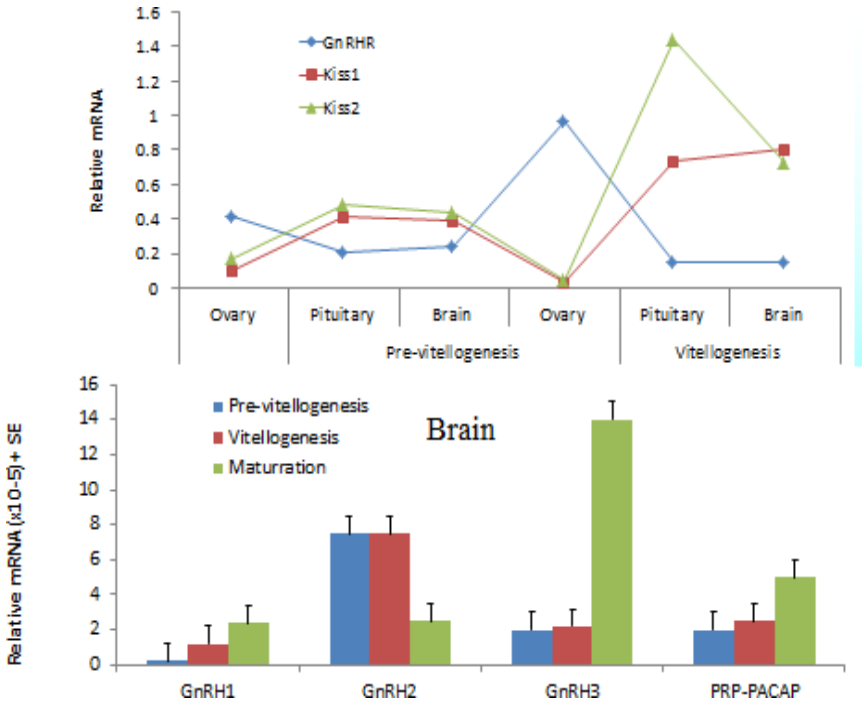

Figure 73. The transcription of kisspeptin (Kiss) 1 and 2, gonadotropin-releasing hormone (GnRH1, 2, 3) and pituitary adenylate cyclase-activating polypeptide (PACAP) in various tissues of blue gourami females along the BPG axis (Degani, 2020a; Degani et al., 2017a, 2019a; Levy and Degani, 2011, 2012, 2013).

The effects of both GnRH1 and GnRH3 are very similar in blue gourami, as are their sequences (Levy and Degani, 2012) (**Figure 73**). Apparently, during puberty, growth occurs in parallel to vitellogenesis (but independent of male pheromones or behavior) (Degani, 1993a; Degani and Schreibman, 1993). Kiss2, which controls GnRH1 and affects FSH and E_2 (Degani, 2018) secretion, controls vitellogenesis (Degani et al., 2017a) (**Figure 73**) and 17,20P secretion during maturation.

4.4.3. Pituitary Hormones Control Reproduction in Female Blue Gourami

The brain controls the pituitary gland hormones in blue gourami as in other teleost fish and is the main organ involved in effects on the BHPG axis (Yaron and Levavi-Sivan, 2011; Zohar et al., 2010). However, the BPLB axis is also important, and the interactions between the two axes are very complex.

Detailed studies have been carried out on hormones in the pituitary of blue gourami using histological methods based on light and electron microscopy (Jackson et al., 2005), as well as on molecular methods (Degani, 2014a, 2015a, 2015b, 2016; Goldberg et al., 2004; Jackson et al., 1999), which might help in understanding the control of oogenesis in this specific group. FSH and LH mRNA levels were found to be very high during advanced vitellogenesis and maturation, and both were involved in the two different stages (Jackson et al., 1999) (**Figure 73** and **Figure 74**). Both GtHs, which are affected by steroids (Degani and Boker, 1992a, 1992b), control oogenesis (**Figure 74**). Blue gourami is a group of multi-spawning fish. Sometimes, one group of oocytes arrives at maturation and another group is found at vitellogenesis (**Figure 41**). This is the proposed explanation for the high transcription of both FSH and LH at advanced vitellogenesis and maturation (**Figure 74**) (Degani, 2016; Jackson et al., 1999).

The cytochrome P450 aromatase gene (CYP19) seems to be involved directly and indirectly in the oogenesis of blue gourami

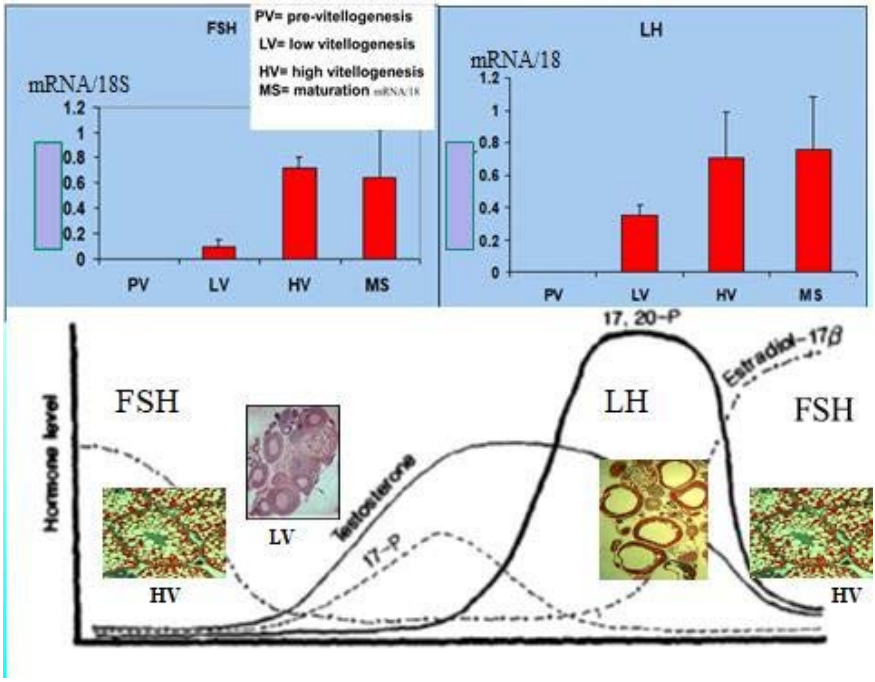

Figure 74. Suggested qualitative model showing the relationship between GtH levels and steroids during the gonadal cycle: low vitellogenesis (LV), high vitellogenesis (HV) and maturation (M). The steroids are: 17β-estradiol (E_2), testosterone (T), 17α,20β-dihydroxy-4-pregnen-3-one (17,20-P) (Degani, 2016, 2020a; Degani and Boker, 1992a, 1992b; Jackson et al., 1999).

(Ezagouri et al., 2008). The synthesis of estrogens from androgens is catalyzed by the heme-binding enzyme CYP19 in vertebrates. In the blue gourami brain, CYP19 was found (bgCYP19b) with very low mRNA expression during vitellogenesis but dramatically increased expression during maturation; gonadal CYP19 (bgCYP19a) was relatively high and mRNA expression was measured during various stages of oogenesis. The significantly lower aromatase gene mRNA levels in females during vitellogenesis compared to females during

maturation (Ezagouri et al., 2008) (**Figure 75**) suggest that this hormone is involved in the sexual behavior of female blue gourami and not in the control of oogenesis (Ezagouri et al., 2008).

Both GH and IGF1, as well as PRL, are involved in oogenesis (Degani et al., 2010, 2017b; Goldberg et al., 2004). The levels of GH and PRL mRNA were relatively constant during growth and oogenesis, and no significant differences were found (**Figure 76**). These hormones affect many biological processes, including reproduction.

GH and IGF1 are central hormones involved in somatic growth (somatotropic axis) (Degani, 2014c), as well as in reproductive

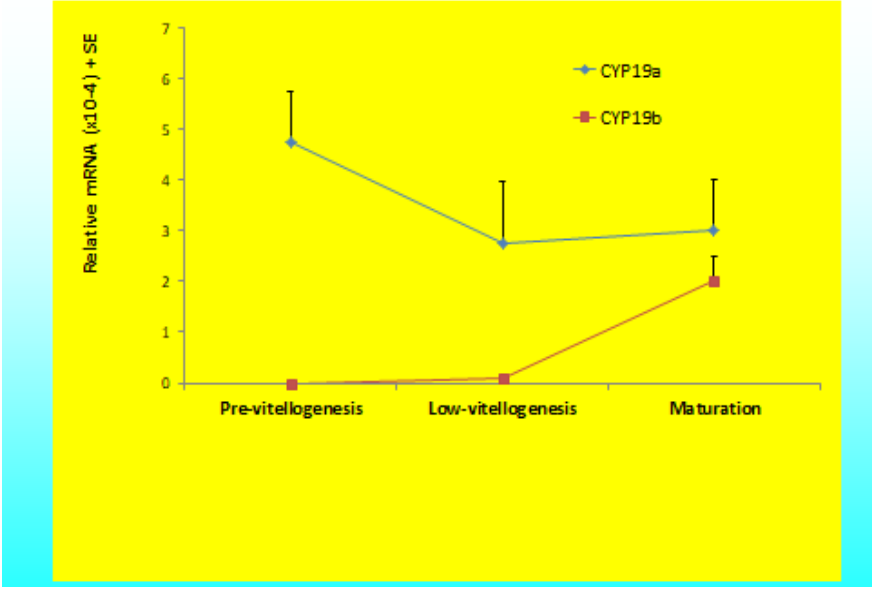

Figure 75. Transcription of ovary aromatase (CYP19a) and brain aromatase (CYP19b) in female blue gourami oocytes in stages of vitellogenesis and maturation (Ezagouri et al., 2008).

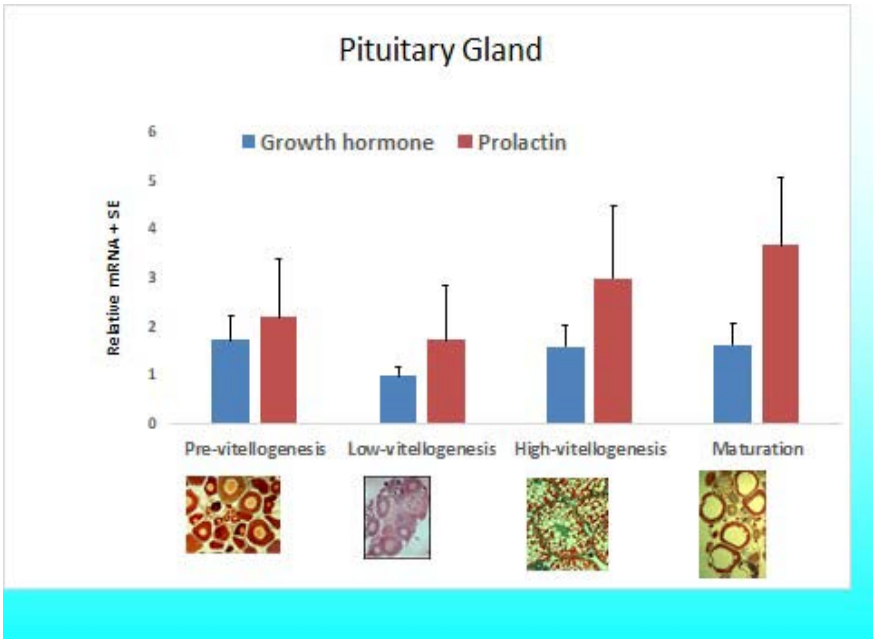

Figure 76. Variations in growth hormone (GH) and prolactin (PRL) mRNA levels during the gonadal cycle: pre-vitellogenesis, low vitellogenesis, high vitellogenesis and maturation. Each histogram presents the average of five independent measurements (mean ± SE) (Degani et al., 2010; Goldberg et al., 2004).

functions, and they are under multifactorial regulation by PACAP and PRP (Levy and Degani, 2011). These peptides coordinate as part of the complex regulatory mechanisms of reproduction at the brain-pituitary level; therefore, understanding the complex hormonal interactions regulating this axis is significant, particularly in fish, as reflected by the simple model system of female blue gourami (Levy and Degani, 2011, 2012; Levy et al., 2011). All of the various neuron secretory hormones in the brain with the gonadotropic and somatotropic axes control oogenesis in Anabantoidei fish: Kiss, GnRH1,

GnRH2, PACAP and PRP (Degani et al., 2017b, 2019a; Levy and Degani, 2011, 2012).

In summary, **Figure 77** shows the proposed complex interactions between hormones in the BPG and BPLB axes in the female blue gourami model.

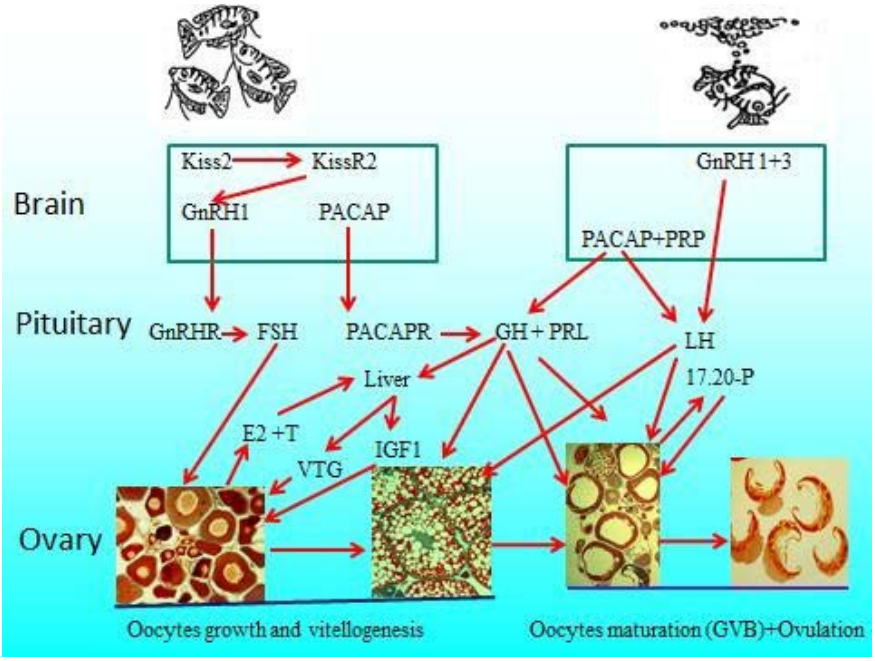

Figure 77. Interactions between the BPG and BPLB axes of blue gourami female in the control of oogenesis (Becker et al., 1992; Degani, 1989, 1990, 1993a, 1993b, 1994, 2014a, 2014b, 2014c, 2015a, 2015b, 2016, 2018, 2020a; Degani and Boker, 1992a, 1992b; Degani and Gallagher, 1996; Degani and Schreibman, 1993; Degani and Yom Din, 2011; Degani and Ziv, 2016; Degani et al., 1994, 1995, 1997, 1998, 2003, 2010, 2011, 2017a; Ezagouri et al., 2008; Jackson et al., 1994, 1999, 2005; Levy and Degani, 2011, 2012, 2013; Levy et al., 2009, 2010, 2011; Mananos et al., 1997).

Chapter 5

Biotic and Abiotic Factors Affecting the Reproduction of Blue Gourami

5.1. Effects of Temperature, Light, and Container Size on Blue Gourami Breeding

Research was conducted on the appropriate conditions for reproduction of blue gourami (Degani, 1989). Environmental variables affecting the construction of the bubble nest, the number of larvae that hatch from the eggs, and the optimal temperature were measured under laboratory conditions (Degani, 1989). The relationship between fish weight of males and females and the size of the bubble nest is presented in **Figures 78-80** (Degani, 1989).

No correlation was found between body weight of either sex and nest size. However, a relationship was found between fish body weight and number of larvae (**Figure 81**) (Degani, 1989).

The male blue gourami builds bubble nests at temperatures between 23°C and 29°C. Below 23°C, the males do not exhibit sexual behavior, nor do they build nests (**Figure 82**) (Degani, 1989).

Darkness had no adverse effect on bubble nest-building. The number of containers in which nests were built is shown in **Figure 83**. In the light, the females mostly laid their eggs by the second day

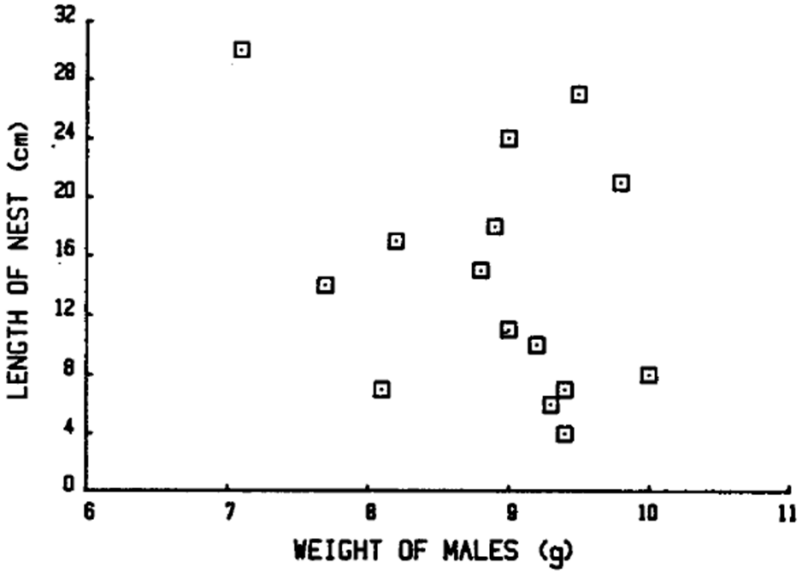

Figure 78. Relationship between weight of males and length of bubble nest.

Figure 79. Relationship between weight of females and length of bubble nest.

Figure 80. Relationship between weight of females and width of bubble nest.

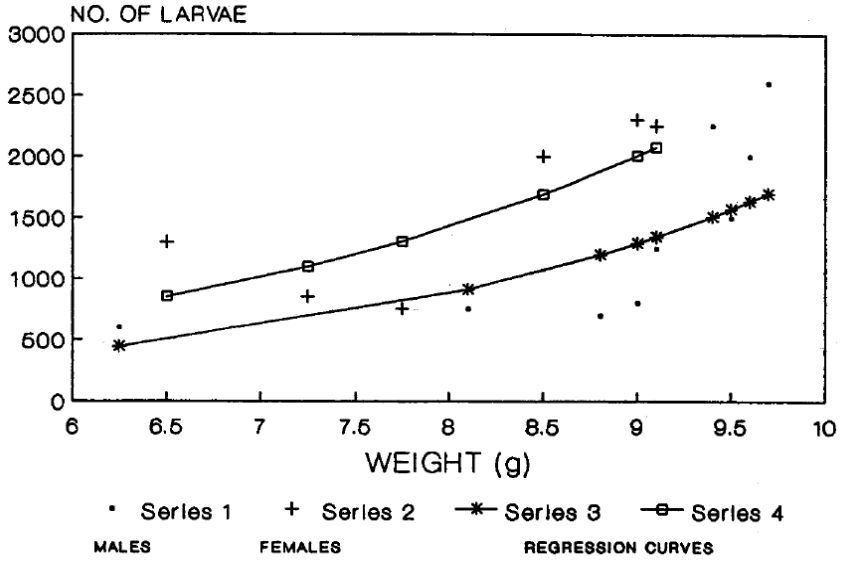

Figure 81. Relationship between body weight of males and females and number of larvae.

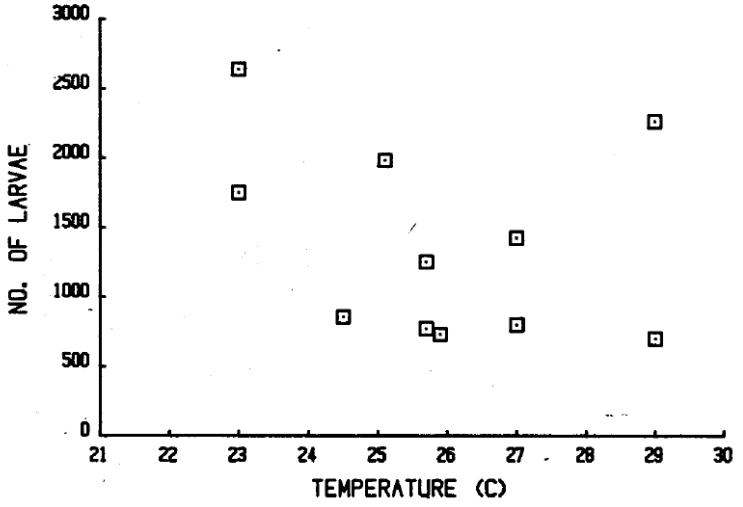

Figure 82. Relationship between temperature and number of larvae.

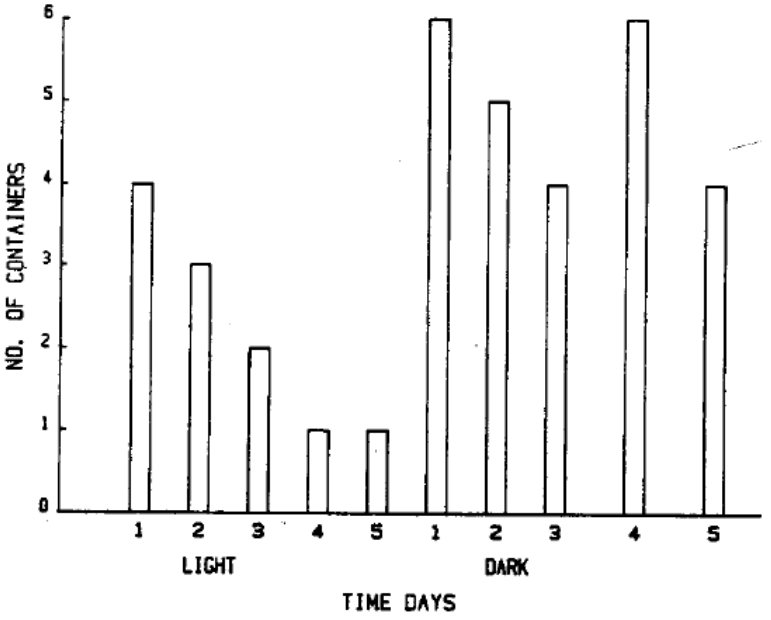

Figure 83. Number of containers in the light and in the dark in which nests were built.

after being placed for breeding, and then the number of nests built decreased. In the dark, they began laying eggs more slowly and the subsequent decrease was correspondingly slower. More nests, in total, were built in the dark than in the light. There was also a correlation between nest size and number of larvae, with more larvae found in the larger nests (**Figure 84** and **Figure 85**).

5.2. Male Blue Gourami Nest-Building Behavior Is Affected by Other Males and Females

Degani and Ziv (2016) examined the effect of blue gourami males and females on the nest-building behavior of the males under experimental conditions (Degani and Ziv, 2016). No significant differences

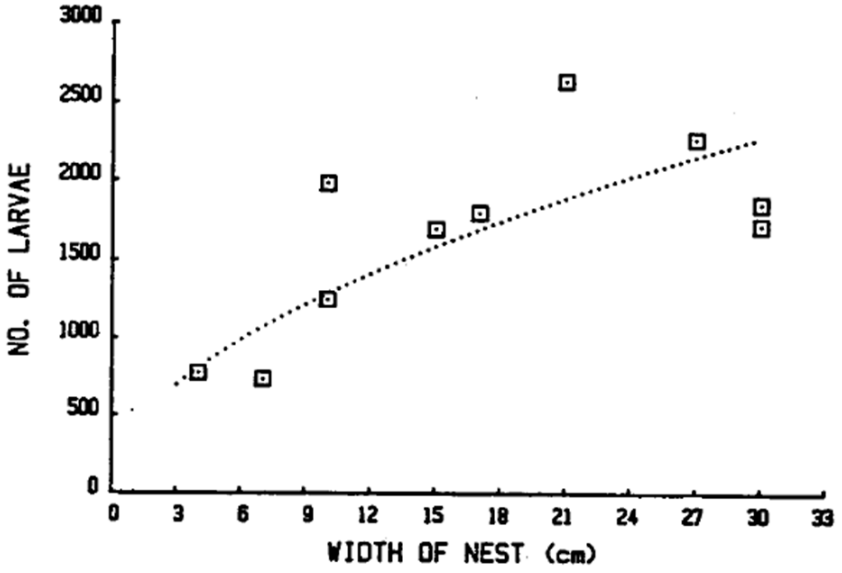

Figure 84. Relationship between width of nest and number of larvae. The highest number of larvae in any one batch was 2700.

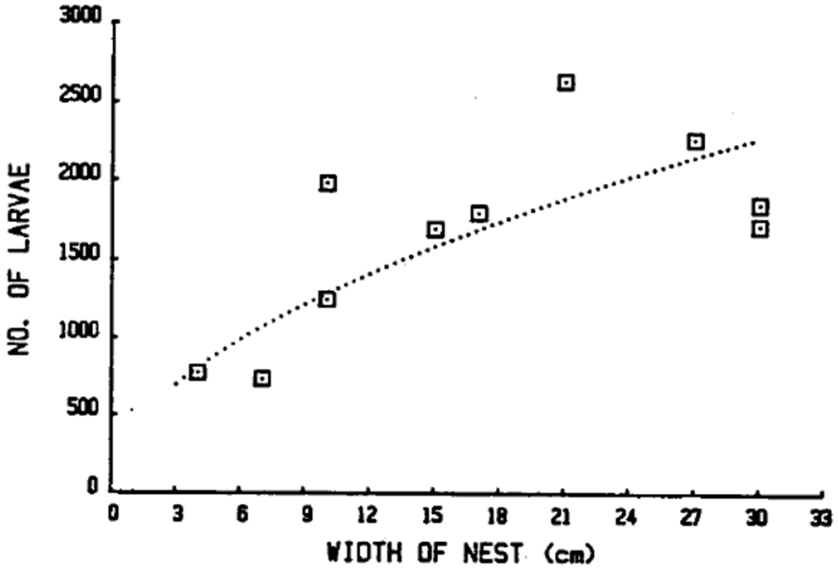

Figure 85. Relationship between length of nest and number of larvae.

were found between the experimental and control conditions in weight or length of fish in the three experiments (**Table 7**).

In the experimental group, two mature males were maintained in an aquarium (50 × 50 × 30 cm), and the occurrence of nest-building was monitored. There were no significant differences among the percentage of nest-building males in the experimental group (two males in one aquarium, 50% of males in the aquarium built nests) and the control group (one male in the aquarium, 62% of males in the aquarium built nests) (**Figure 86**) (Degani and Ziv, 2016).

On the other hand, nest-building was significantly reduced to 25% when three males were held in one aquarium (experimental group) compared to 50% in the control. Significant differences existed

Table 7. Comparison between the measurements of fish in experimental and control groups (Degani and Ziv, 2016).

Experiment Number	Number of Replications	Mean Weight (g) ± SD	Mean Length (cm) ± SD
Experiment 1	8	8.0 ± 2.6	7.85 ± 0.4
Control 1	8	7.5 ± 2.5	7.8 ± 0.4
P (Test)		P = 0.9 > 0.05	P = 0.7 > 0.05
Experiment 2	8	10.3 ± 3.5	7.9 ± 0.4
Control 2	8	10.0 ± 2.6	7.8 ± 0.5
P (Test)		P = 0.8 > 0.05	0.8 > 0.05
Experiment 3	8	10.2 ± 2.4	8.4 ± 0.5
Control 3	8	10.6 ± 4.1	8.4 ± 0.6
P (Test)		P = 0.5 > 0.05	P = 0.5 > 0.05

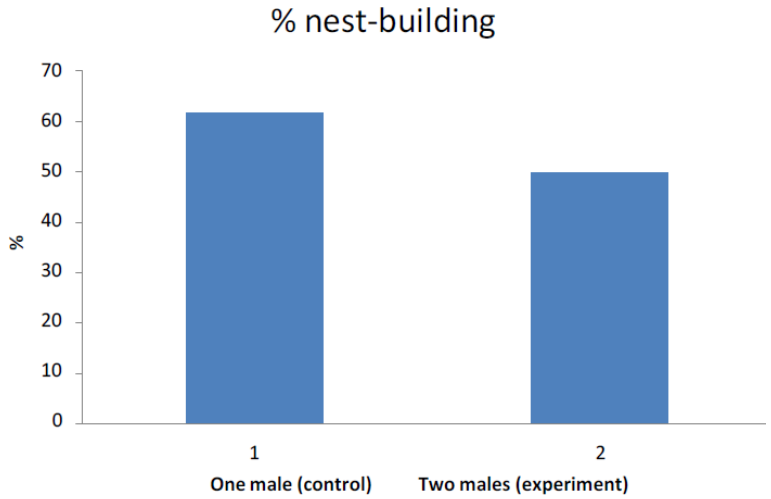

Figure 86. Comparison of % nest-building in experimental (two males per aquarium; n = 8 aquariums) and control group (one male per aquarium; n = 8 aquariums). No significant differences were found (X^2-test, $P > 0.05$) (Degani and Ziv, 2016).

between the control group (one male per aquarium) and the experimental group (three males per aquarium) (**Figure 87**). Similar re-

sults were found in the next experiment, where three males were maintained in the aquarium but two were held in a cage (**Figure 88**). The percentage of nest-building was significantly less (25%) compared to the control group (75%) in the aquariums with nest-building activity (**Figure 88**).

A comparison between percentage of nest-building in the experimental group (three females held in the aquarium with one male; n = 8 aquariums) and the control group (one male and one female held in the aquarium; n = 8 aquariums) is shown in (**Figure 89**).

It was suggested that when two males were held in the cage in the same aquarium, they were only affected by the pheromones of one

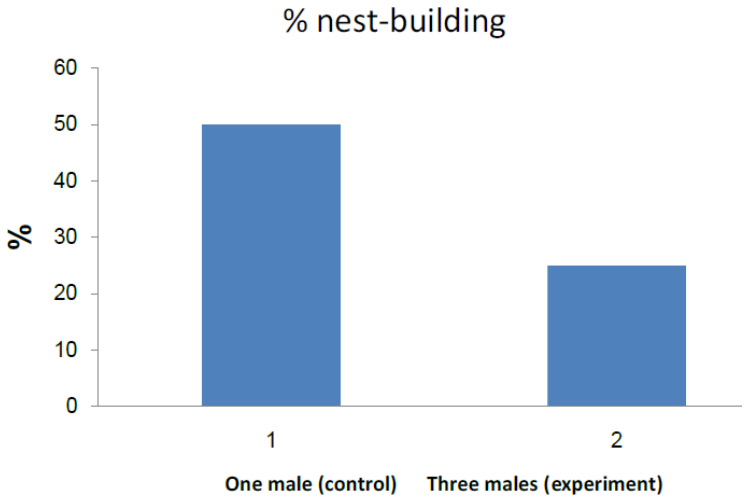

Figure 87. Comparison between % nest-building in the experimental group (three males per aquarium; n = 8 aquariums) and the control group (one male in the aquarium; n = 8 aquariums). Significant differences were found (X^2-test, $P < 0.05$) between the experimental and control group (Degani and Ziv, 2016).

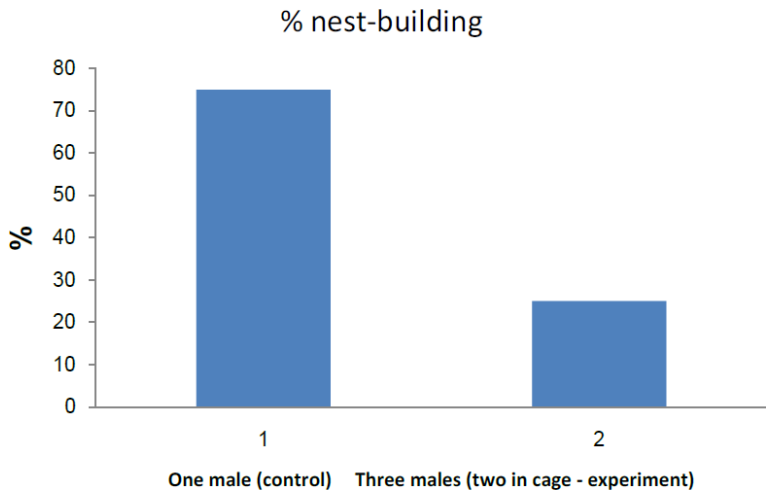

Figure 88. Comparison between % nest-building in the experimental group (three males held in the aquarium, two of them in a cage; n = 8 aquariums) and the control group (one male held in the aquarium; n = 8 aquariums). Significant differences were found (X^2-test) between the experimental and control groups (Degani and Ziv, 2016).

male reducing the number of nests built. The aggressive male behavior that enhances their ability to defend their territories was studied in detail. The study supported the hypothesis that territoriality also prevents the effect of pheromones of other males on sexual behavior and nest-building. During reproduction, only the dominant male, which has a territory, builds nests. The establishment of a territory results in the rejection of the other males, such that only the pheromones of the dominant male affect the female's gametogenesis and GtH cells in the pituitary (Becker et al., 1992). In summary, this and previous studies suggest that both aggressive behavior and pheromones affect interactions among males, and only the males that have territories are resistant to both factors and can build nests.

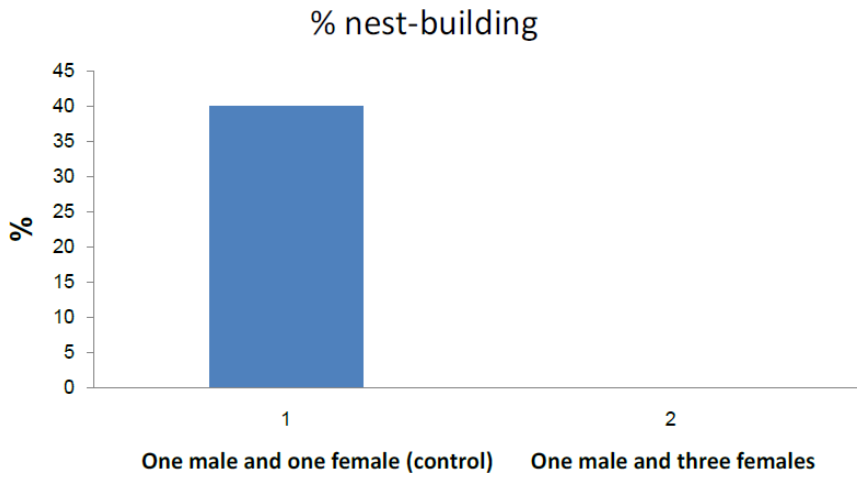

Figure 89. Comparison between % nest-building in the experimental group (three females held in the aquarium with one male; n = 8 aquariums) and the control group (one male and one female held in the aquarium; n = 8 aquariums) (Degani and Ziv, 2016).

5.3. Water Quality (Percentage of Underground Water) Affects Sexual Behavior and Gene Expression of Hormones Related to Reproduction in Blue Gourami Males

Degani and Levy (2013) studied the effect of underground water on reproduction and growth-related hormones in blue gourami males under non-reproductive and reproductive conditions. There was an increase in the percentage of males building nests under the highest percentage of underground water compared to fish maintained in a lower percentage of underground water in the first 2 days.

5.3.1. Effect of Underground Water on Male Sexual Behavior

Males maintained in groups (10 per aquarium) in different concen-

trations of underground water (0%, 50%, 100%) with high salinity and conductivity levels (**Table 8**) did not demonstrate any sexual behavior (they did not build nests) (Degani and Levy, 2013). In contrast, males that were kept separate (one per aquarium) built nests in all three concentrations of underground water. However, there was high and significant variation in the percentage of males that built nests in 100% underground water compared to fish maintained at low underground water concentrations in the first 2 days ($P < 0.05$, one-tailed Student's t-test) (**Figure 90**) (Degani and Levy, 2013). No morphological differences were observed among the testes of males maintained in the three different underground water conditions at any stages of spermatogenesis (spermatogonia, spermatocyte, spermatids and spermatozoa) (**Figure 91**). The gonadosomatic index (GSI, %) of males building nests was higher than that of non-reproductively active males in water containing the lowest percentage of underground

Table 8. Quality of water with different percentages of underground water (Degani and Levy, 2013).

% of underground water	0%		50%		100%	
	mean	SD	mean	SD	mean	SD
Dissolved Oxygen (mg/L)	6.91	0.34	7.25	0.36	6.56	0.28
Conductivity (uS)	346.27	27.48	954.89	29.42	1908	43.47
Temperatures (˚C)	27.05	0.94	27.14	0.84	27.3	0.94
Salinity (ppm)	0.2	0.02	0.56	0.05	1.11	0.06
Ammonia (ppm)	0.6	0	0.6	0	0.6	0
NO_2 (ppm)	0.74	0.15	0.74	0.16	0.75	0.15

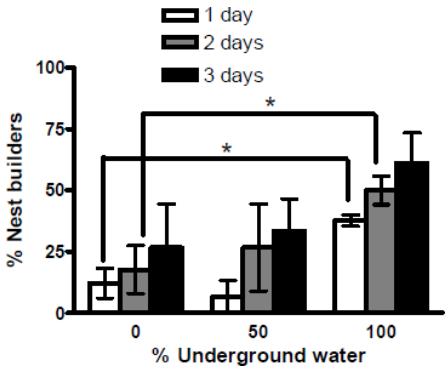

Figure 90. The percentage of males building nests in water with different percentages of underground water (0%, 50% and 100%) having high NaCl concentration (0.2 ± 0.02 ppm, 056 ± 0.05 ppm, and 1.11 ± 0.06 ppm, respectively). Asterisk denotes a significant difference between 0% underground water and the other percentages of underground water on each day ($P < 0.05$, one-tailed Student's t-test) (Degani and Levy, 2013).

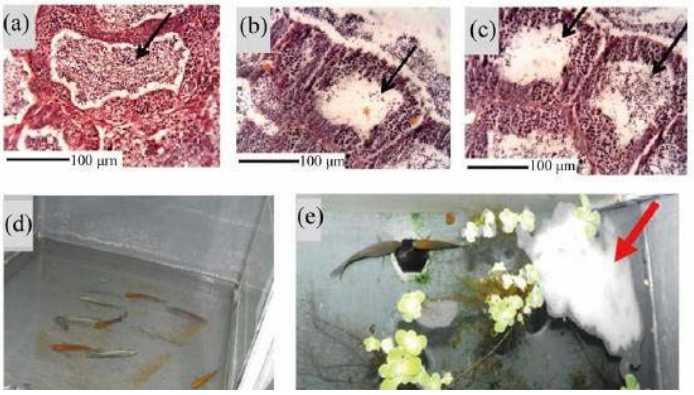

Figure 91. Histological analysis of testis sections from non-reproductively active males (a) and reproductively active males (b, c) (note the high concentration of spermatozoa in the middle of the lobule in panel a), fish under non-reproductive conditions maintained in a group (d), and fish under reproductive conditions building nests (e). Spermatogenesis stages in the gonads of mature non-reproductively active blue gourami males. The histological sections show the cellular spermatogenesis stages in the gonad of mature non-reproductively active blue gourami males (a). Cellular spermatogenesis stages are present on the periphery of the lobule. Sections were stained with hematoxylin and eosin (Degani and Levy, 2013).

water ($P < 0.05$, one-tailed Student's t-test) (**Figure 92**) (Degani and Levy, 2013).

5.3.2. Effect of Underground Water on Relative mRNA Levels of Brain and Pituitary Hormones of Blue Gourami Males Maintained in Groups (Non-Reproductive Conditions)

The mRNA levels of brain hormones (GnRH1 and GnRH3) and pituitary hormones (βLH, βFSH, GH and PRL) in water with various percentages of underground water in males under non-reproductive conditions are presented in **Figure 93**. GnRH1, βLH and βFSH mRNA levels were significantly higher at 50% and 100% underground water compared to 0%; PRL mRNA levels were significantly higher only in 100% underground water compared to 0%. On the other hand, no

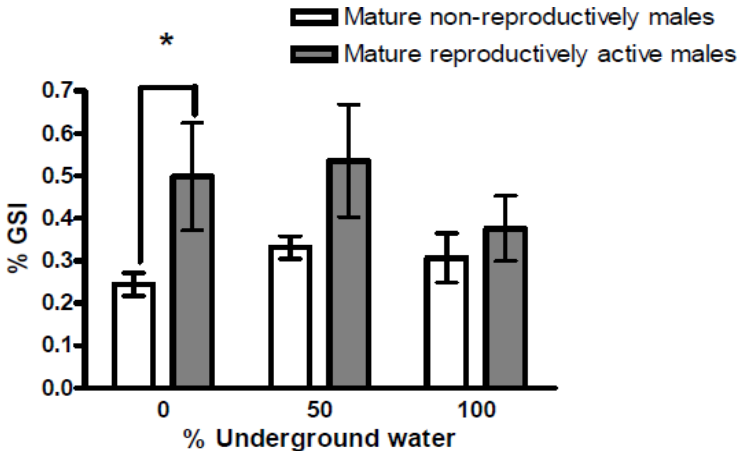

Figure 92. Gonadosomatic index (GSI, %) of fish in water with various percentages of underground water (mean ± SEM; n = 5 - 10). Significant differences were found compared to 0% underground water ($P < 0.05$, Student's t-test).

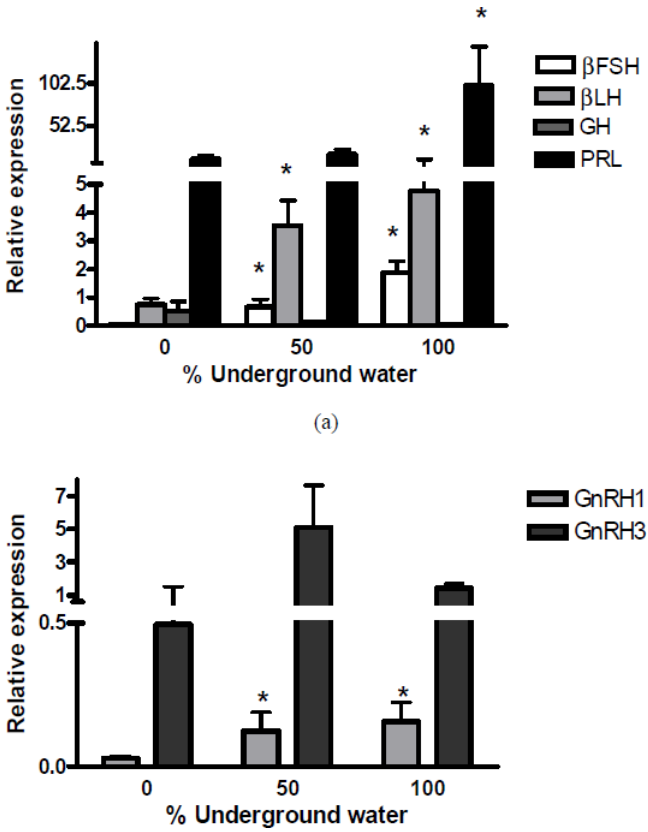

Figure 93. Effect of different concentrations of underground water on mRNA levels of brain and pituitary hormones in males under non-reproductive conditions. (a) *β*LH, *β*FSH GH and PRL. (b) GnRH1 and GnRH3. Blue gourami males maintained in groups were selected randomly and acclimated to the water for 4 days. The experiment was then carried out for 4 days, 10 fish per container (n = 30). Total RNA from brains and pituitaries was reverse- transcribed for real-time qPCR. Each histogram presents the average of 7 - 10 independent measurements (mean ± SEM). Asterisk denotes a significant difference between mRNA levels in 0% underground water compared to other underground water conditions ($P < 0.05$, t-test) (Degani and Levy, 2013).

significant differences were found in GnRH3 or GH mRNA levels in the different underground water conditions (**Figure 93**) (Degani and

Levy, 2013).

5.3.3. Effect of Underground Water on Relative mRNA Levels of Brain and Pituitary Hormones of Blue Gourami Males Maintained Alone (Reproductive Conditions)

The mRNA levels of brain hormones (GnRH1 and GnRH3) and pituitary hormones (βLH, βFSH, GH and PRL) of males under reproductive conditions in various concentrations of underground water are presented in **Figure 94** (Degani and Levy, 2013). GnRH1 mRNA levels were significantly higher in 50% and 100% underground water compared to 0%; PRL mRNA levels were significantly higher in 100% underground water compared to 0%; and GnRH3 mRNA levels were significantly higher in 50% underground water compared to 0%. On the other hand, no significant differences were found for βLH, βFSH or GH mRNA levels in the different percentages of underground water.

In summary, the water quality (percentage of underground water, and therefore levels of salinity and electrical conductivity) affects hormone control of reproduction and supports observations of the hormones that are most involved in the sexual behavior of blue gourami males.

5.4. Effect of Temperature on Gene Expression of Hormones Controlling Growth and Reproduction in the Male Blue Gourami

Temperature has various effects on biological and physiological

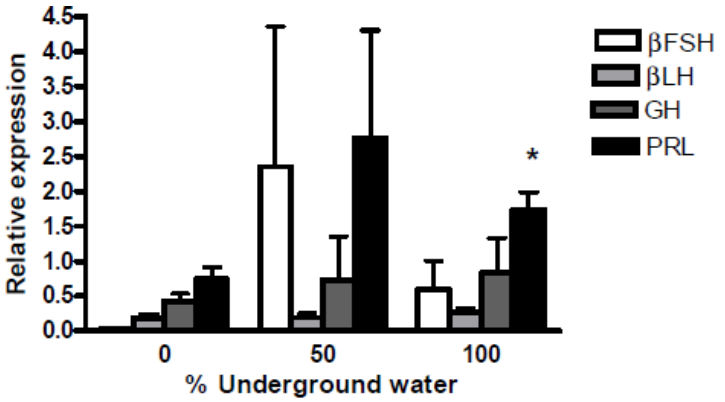

(a)

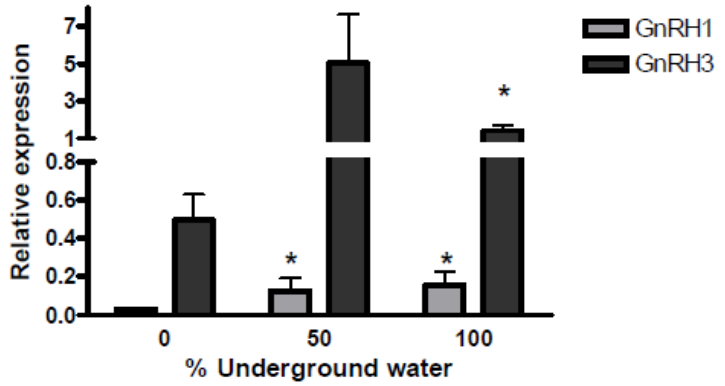

(b)

Figure 94. Effect of different underground water conditions on mRNA levels of brain and pituitary hormones in males under reproductive conditions. (a) *β*LH, *β*FSH, GH and PRL. (b) GnRH1 and GnRH3. Blue gourami males maintained with females under reproductive conditions. After a 4-day acclimation period in a group, the fish were separated for 3 days (so that each aquarium contained only one male and a mature female was added to each aquarium after the first day). Total RNA from brains was reverse-transcribed for real-time qPCR. Each histogram presents the average of 5 - 7 independent measurements (mean ± SEM). Asterisk denotes a significant difference between mRNA levels in males in 0% underground water compared to the other underground water conditions ($P < 0.05$, Student's t-test) (Degani and Levy, 2013).

aspects in all living systems, but particularly in fish which are poikilothermic organisms. In fish, temperature affects hormone synthesis, gametogenesis, and reproductive fitness (David and Degani, 2011; Yaron and Levavi-Sivan, 2011).

5.4.1. Effect of Temperature on the Relative mRNA Levels of GnRH3, PACAP, PRP, and IGF1 in Brains of Blue Gourami Males Maintained in Groups (Non-Reproductive Conditions)

The relative mRNA levels of GnRH3 and PACAP in brains excised from males maintained in groups at 27˚C were significantly higher (ANOVA and t-test, $P < 0.05$) than in males kept in groups at 23˚C and 31˚C (t-test, $P < 0.05$). However, there were no significant differences in PRP mRNA levels at the three temperatures (**Figure 95**) (ANOVA and t-test, $P > 0.05$). The mRNA level of IGF1 was significantly higher in the brains of males maintained at 27˚C compared to the other temperatures (t-test, $P < 0.05$).

5.4.2. Variations in *β*FSH, *β*LH, GH, and PRL mRNA Levels in Males Maintained in Groups (under Non-Reproductive Conditions) at Different Temperatures

The relative mRNA levels of *β*FSH, *β*LH, GH, and PRL in the pituitaries of blue gourami males maintained in groups at different temperatures: 23˚C, 27˚C, and 31˚C, are presented in **Figure 96**. No significant difference was found between the *β*FSH mRNA levels of males maintained at 23˚C and 27˚C (ANOVA and t-test, $P > 0.05$), but the level

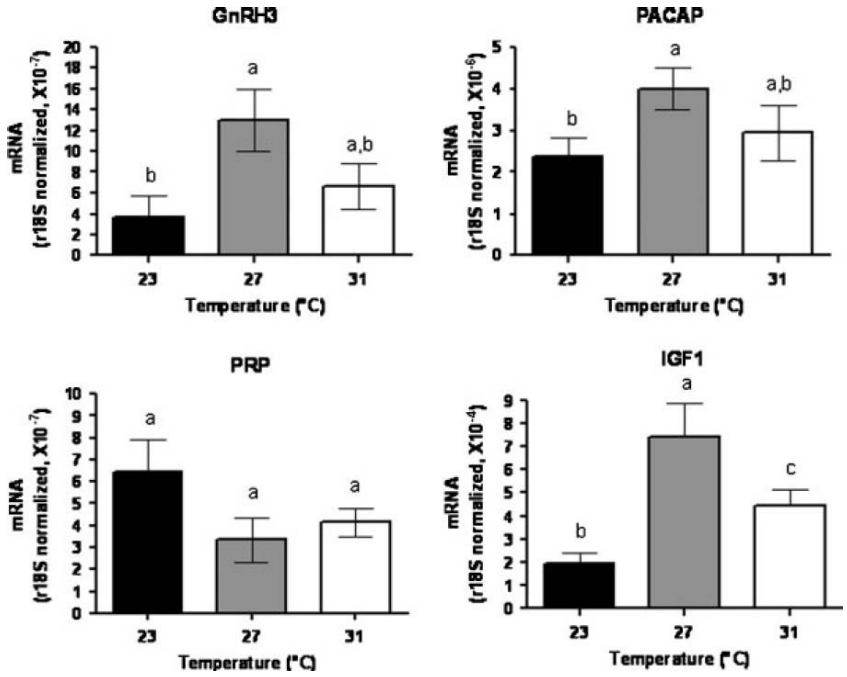

Figure 95. Relative mRNA levels of GnRH3, PACAP, PRP, and IGF1 in brains of blue gourami males maintained in groups. Mature male fish were maintained for 9 days at 23˚C, 27˚C, or 31˚C, after an acclimation period of 5 days. Total RNA was reverse-transcribed, and the resulting cDNA was amplified by real-time PCR. The relative amount of mRNA reflects the relative amount of transcription. Each bar of the histogram presents the average of at least five independent measurements (mean ± SEM; n = 5 - 9). Different letters denote a significant difference among the mRNA levels ($P < 0.05$, one-tailed Student's t-test).

was significantly lower in fish maintained at 31˚C as compared with those kept at 23˚C (t-test, $P < 0.05$). The relative mRNA levels of βLH and PRL in pituitaries excised from males maintained in groups at 27˚C were significantly higher (ANOVA and t-test; $P < 0.05$) than in pituitaries of males kept at 23˚C and 31˚C (**Figure 96**). The mean mRNA level of GH in males maintained at 27˚C tended to be higher

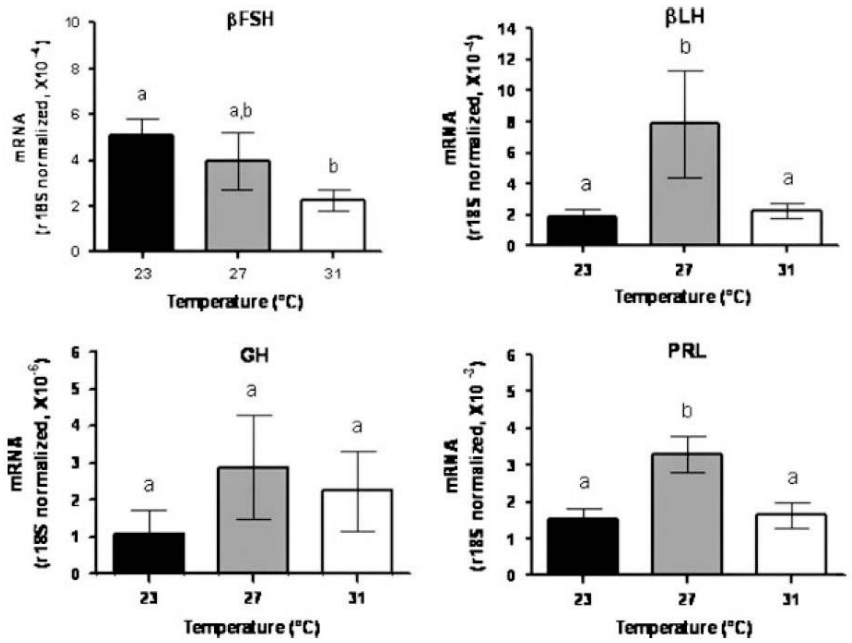

Figure 96. Relative mRNA levels of *β*FSH, *β*LH, GH, and PRL in pituitaries of blue gourami males maintained at different temperatures: 23˚C, 27˚C, or 31˚C. Total RNA from pituitaries was reverse-transcribed, and the cDNA was amplified by real-time qPCR. The relative amount of hormone mRNA reflects the relative amount of transcription of the specific gene. Each bar of the histogram presents the average of at least five independent measurements (mean ± SEM; n = 5 - 9). Different letters above each bar denote a significant difference among the mRNA levels ($P < 0.05$, one-tailed student's t-test).

than those in fish kept at the other temperatures, but the differences were not statistically significant (ANOVA and t-test; $P > 0.05$), i.e., GH transcription was not significantly affected by temperature.

5.4.3. Effect of Temperature on the Relative mRNA Levels of GnRH3, PACAP, PRP, and IGF1 in Brains of Blue Gourami Males Maintained Alone (Reproductive Conditions)

At 27˚C, the transcription levels of GnRH3 in males that built nests

was significantly higher than that in males maintained alone that did not build nests (ANOVA and t-test, $P < 0.05$) (David and Degani, 2011). No significant differences were observed in the GnRH3 mRNA levels among males that did and did not build nests at 23˚C and 31˚C (**Figure 97**; ANOVA and t-test, $P > 0.05$). The mRNA level of PACAP was significantly higher in males that showed sexual behavior (nest-building) and that were maintained at 27˚C than in fish at this temperature that did not build nests (**Figure 97**; ANOVA and t-test, $P < 0.05$) (David and Degani, 2011). Similar results were obtained for IGF1 transcription in the brain. However, no significant differences were found for pituitary PRP transcription in nest-building males kept at the three temperatures (ANOVA and t-test, $P > 0.05$). In addition, no significant differences related to temperature were detected in the mRNA level of the hormones tested (GnRH3, PACAP, PRP and IGF1) in the brains of males that did not build nests (**Figure 97**; ANOVA and t-test, $P > 0.05$) (David and Degani, 2011).

5.4.4. Variations in *β*FSH, *β*LH, GH, and PRL mRNA Levels in Males Maintained Alone (Reproductive Conditions) at Different Temperatures

Relative mRNA levels of *β*FSH, *β*LH, GH, and PRL in pituitaries of blue gourami male nest builders and non-nest builders, held separately, are shown in **Figure 98** (David and Degani, 2011). The mRNA levels of *β*FSH and *β*LH were significantly higher in males demonstrating sexual behavior (nest-building), as compared to those that did not,

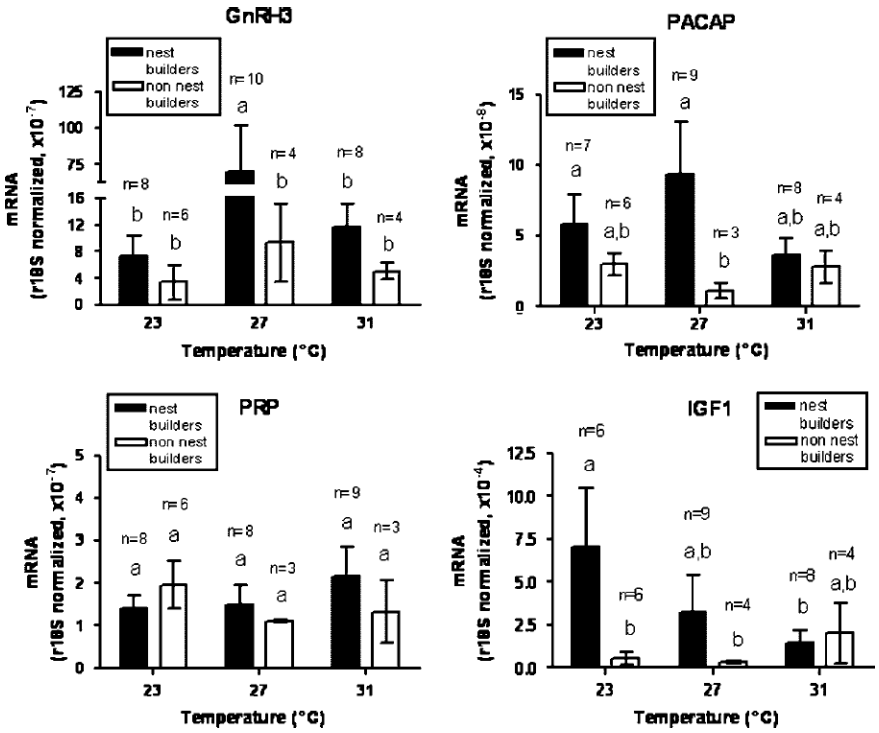

Figure 97. Relative mRNA levels of GnRH3, PACAP, PRP, and IGF1 in brains from mature nest builders and mature non-nest builders among blue gourami males that were maintained alone. Mature male gouramis were isolated and maintained for 1 - 6 days at various temperatures: 23˚C, 27˚C, or 31˚C, after an acclimation period of 3 days. Total RNA from their brains was reverse-transcribed, and the cDNA was amplified by real-time qPCR. The relative amount of hormone mRNA reflects the relative amount of transcription of the specific gene precursor. Each bar of the histogram presents the average of at least five independent measurements (mean ± SEM; n = 5 - 9). Different letters denote a significant difference among the mRNA levels (P < 0.05, one-tailed student's t-test) (David and Degani, 2011).

when maintained at 27˚C and 31˚C (ANOVA and t-test, P < 0.05). Similar results were obtained for PRL. Higher transcription levels of PRL were found in males that built nests than in males that did not, at all three temperatures (**Figure 98**). This is in contrast to the mRNA

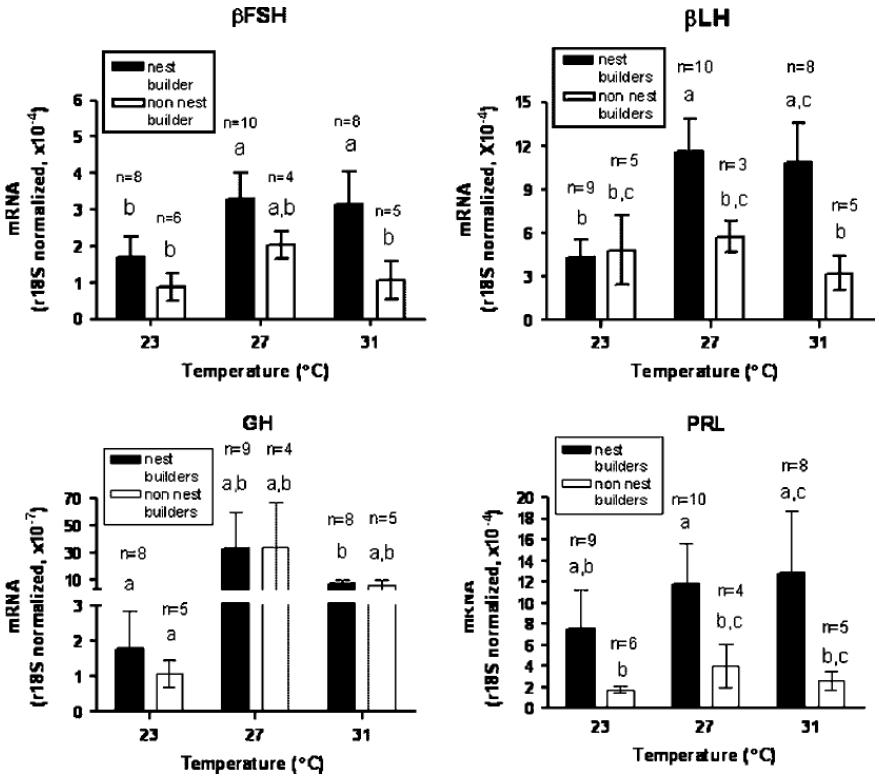

Figure 98. Relative mRNA levels of *β*FSH, *β*LH, GH, and PRL in pituitaries of mature nest-building and non-nest-building blue gourami males held alone. Mature male gouramis were isolated and maintained for 1 - 6 days at various temperatures: 23˚C, 27˚C or 31˚C, after an acclimation period of 3 days. Total RNA from the pituitaries was reverse-transcribed, and the cDNA was amplified by real-time qPCR. The relative amount of mRNA reflects the relative amount of transcription of the specific gene. Each bar of the histogram presents the average of at least three independent measurements (mean ± SEM; n = 3 - 10). Different letters denote significant difference among mRNA levels ($P < 0.05$, one-tailed Student's t-test) (David and Degani, 2011).

levels of GH, where no significant differences were found between nest builders and non-nest builders (**Figure 98**; ANOVA and t-test, $P > 0.05$). In addition, no significant differences were detected among the

mRNA levels of βFSH, βLH, and PRL in non-nest-building males that were maintained separately at the various temperatures (ANOVA and t-test, $P > 0.05$). GH transcription varied with temperature, being higher at 27˚C and 31˚C than at 23˚C (**Figure 98**; ANOVA and t-test, $P < 0.05$) (David and Degani, 2011).

5.5. Effect of Environmental Temperature on Growth- and Reproduction-Related Hormones' Gene Expression in the Female Blue Gourami

5.5.1. Effect of Temperature on the Female Gonadal Cycle under Non-Reproductive and Reproductive Conditions at 23˚C, 27˚C and 31˚C

No significant differences were observed among the GSI values of non-reproductive females (FNRC) (n = 10) or reproductive females held with reproductive males (FRM) and females held with non-reproductive males (FNRM) at 23˚C, 27˚C or 31˚C ($P > 0.05$, t-test) (data not shown). A higher percentage of oocytes in the advanced vitellogenic stage was found in FNRC kept at 27˚C than in those kept at 23˚C or 31˚C ($P < 0.05$, t-test) (**Figure 99(A)**). In contrast, in the FRM and FNRM groups, a lower percentage of females at the final oocyte maturation stage was observed at 23˚C than at 27˚C ($P < 0.05$, t-test) (**Figure 99(B)**). When comparing the effect of temperature on final oocyte maturation in females under the two reproductive conditions at 23˚C and 31˚C, a higher percentage of females at final oocyte maturation was detected in FRM compared to FNRM (**Table 9**).

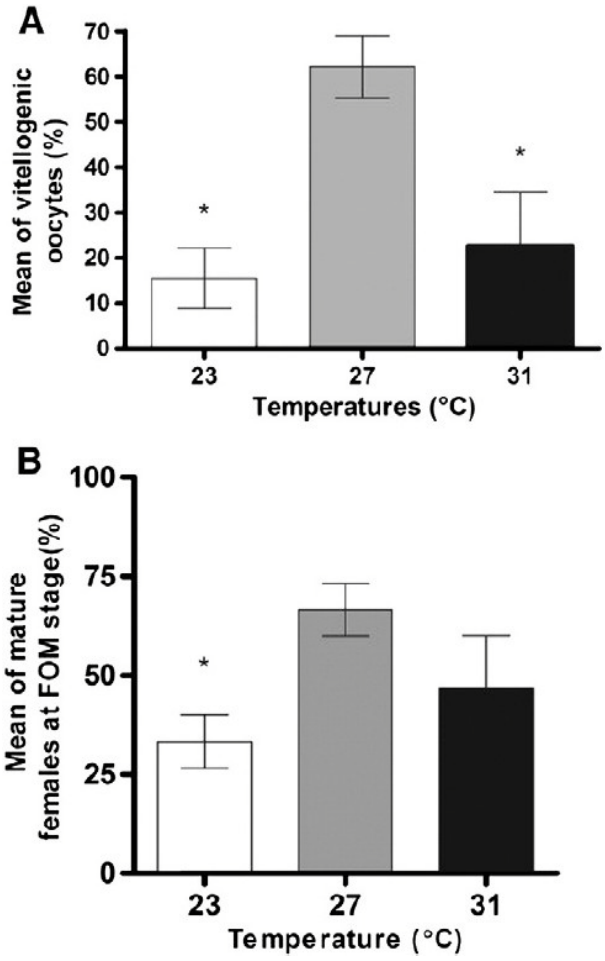

Figure 99. (A) Percentage of oocytes at the advanced vitellogenic stage in the ovaries of adult females held without males (FNRC). The FNRC fish were selected randomly and kept for 9 days at 23˚C, 27˚C or 31˚C, following an acclimation period of 5 days (mean ± SEM; n = 6 - 10). (B) Percentage of females held with reproductive males (FRM) and females held with non-reproductive males (FNRM) in final oocyte maturation (FOM) or ovulation. Females at the vitellogenic stage were separated after an acclimation period of 4 days and kept at 23˚C, 27˚C or 31˚C in the presence of a mature male for 1 day (mean ± SEM; n = 15) and % fish in final oocyte maturation was determined. Different letters denote significant difference between temperatures ($P < 0.01$, t-test).

Table 9. Percentage of females at the final oocyte maturation (FOM) stage held with reproductively active males (nest-builders) (FRM) or with non-reproductively active males (non-nest-builders) (FNRM). Results are the means of three different experiments ($P < 0.05$, t-test).

Temperature	23˚C		27˚C		31˚C	
Reproductive conditions	FNRM	FRM	FNRM	FRM	FNRM	FRM
% of females at FOM	0	33.33	26.66	33.33	6.66	31.66
SEM	0	6.66	13.33	18.05	6.66	13.47
P value (t-test)	P < 0.05		P > 0.05		P < 0.05	

5.5.2. Effect of Temperature on mRNA Levels of Brain and Pituitary Hormones in Females under Non-Reproductive Conditions

In females under non-reproductive conditions kept at 27˚C, significantly higher brain mRNA levels of GnRH3 and pituitary *β*LH and GH were found (2.74-, 14.7- and 1.96-fold, respectively), compared to fish maintained at 31˚C ($P = 0.004$, 0.038 and 0.0005, respectively, t-test) (**Figure 100**). GH mRNA levels were also 1.89-fold lower in these fish when maintained at 23˚C compared to 27˚C ($P < 0.03$, t-test). No significant differences in the mRNA levels of brain IGF1, PACAP, PRP-PACAP, *β*FSH or PRL were observed in these females at 23˚C or 31˚C compared to 27˚C (**Figure 100**).

5.5.3. Effect of Temperature on mRNA Levels of Brain and Pituitary Hormones in Females under Reproductive Conditions (FRM and FNRM)

In the FNRM group, brain mRNA levels of long and short transcripts of PACAP (PACAP and PRP-PACAP), *β*LH, *β*FSH and GH were higher

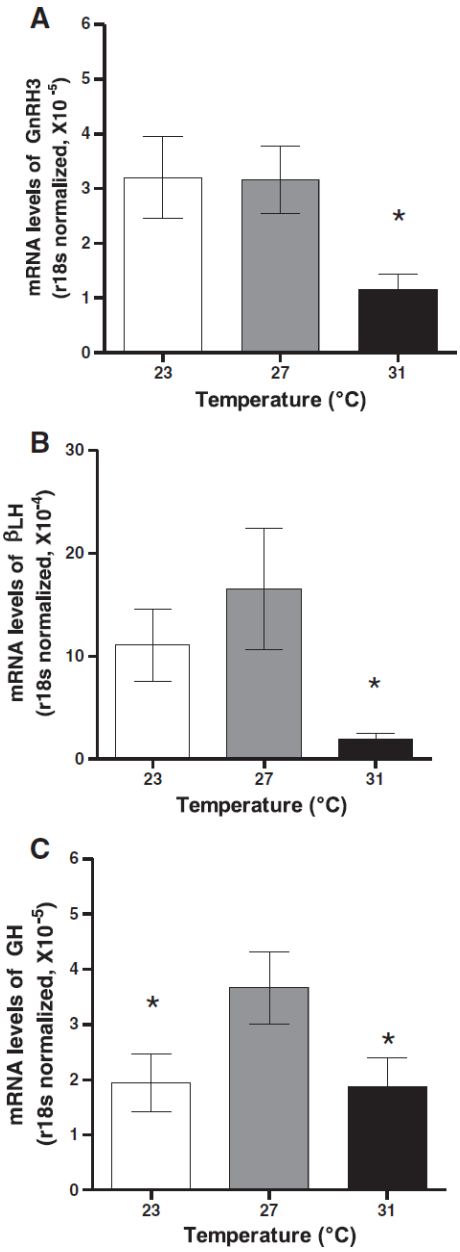

Figure 100. Effect of temperature on mRNA levels of brain and pituitary hormones in females under non-reproductive conditions. (A) GnRH3, (B)

*β*LH, (C) GH. Blue gourami females maintained in groups were selected randomly and kept for 9 days at 23˚C, 27˚C or 31˚C following an acclimation period of 5 days. Total RNA from the brain was reverse-transcribed and subjected to real-time qPCR. The relative amount of hormones reflects the relative amount of the specific gene precursor's transcription. Each histogram presents the average of at least five independent measurements (mean ± SEM; n = 5 - 9). Different letters denote a significant difference among the mRNA levels in females kept at 23˚C or 31˚C compared to the control group at 27˚C ($P < 0.05$, t-test).

when kept at 27˚C vs. 23˚C (1.76-, 1.67-, 1.76-, 1.7- and 2.82-fold, respectively; $P = 0.01 - 0.03$, t-test). mRNA levels of these hormones were also lower in females kept at 31˚C compared to 27˚C, although non-significantly so for GH and PRP-PACAP, respectively ($P = 0.02 - 0.03$, t-test) (**Figure 101**).

In the FRM group, mRNA levels of PACAP, PRP-PACAP, GnRH3, IGF1, *β*LH, *β*FSH and GH were higher in fish kept at 27˚C vs. 23˚C respectively ($P = 0.003 - 0.04$, t-test) (**Figure 102**). mRNA levels of PACAP and GH were also lower at 31˚C compared to 27˚C (1.82- and 2.46-fold, respectively, $P = 0.01 - 0.02$, t-test) (**Figure 102(B)**, **Figure 102(G)**). No significant changes in PRL mRNA levels were detected in any of the females under reproductive conditions (data not shown).

5.5.4. Conclusions

It can be concluded that reproduction in blue gourami fish, which are ectothermic organisms, is closely regulated by external factors such as temperature, possibly mediated by the brain-pituitary axis. These effects can be partially coordinated by social conditions, such as the presence of a male and the male's capacity to build a bubble nest.

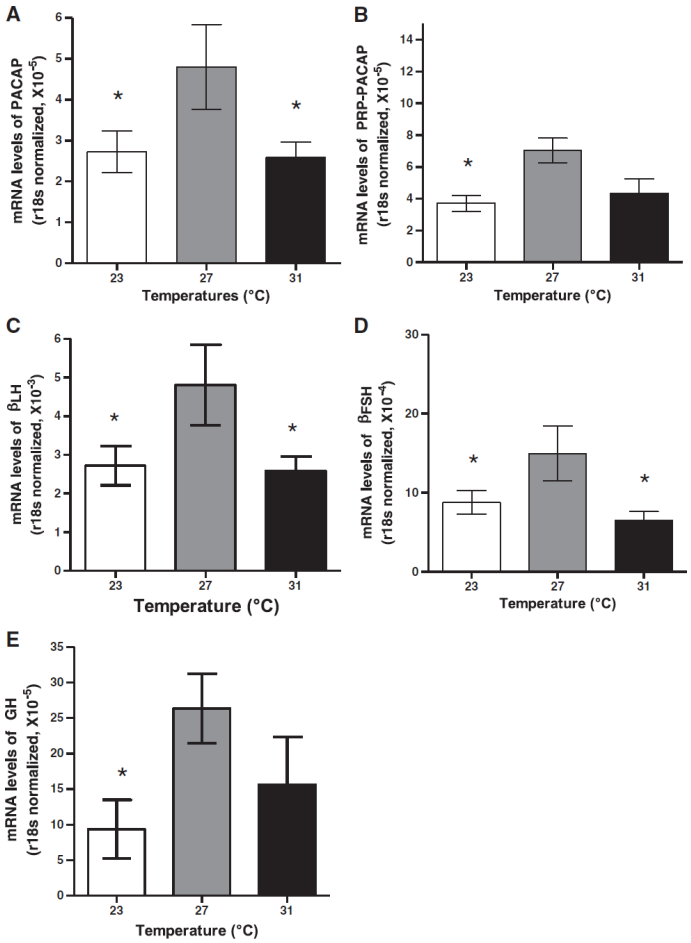

Figure 101. Effect of temperature on mRNA levels of brain and pituitary hormones in females maintained with non-reproductively active males (non-nest-builders) (FNRM). (A) PACAP, (B) PRP-PACAP, (C) *β*LH, (D) *β*FSH, (E) GH. Blue gourami females maintained in groups were selected randomly and kept for 9 days at 23˚C, 27˚C or 31˚C following an acclimation period of 5 days. Total RNA from the brain was reverse-transcribed and subjected to real-time qPCR. The relative amount of hormones reflects the relative amount of the specific gene precursor's transcription. Each histogram presents the average of at least five independent measurements (mean ± SEM; n = 5 - 10). Different letters denote a significant difference among the mRNA levels in females kept at 23˚C or 31˚C compared to the control group at 27˚C ($P < 0.05$, t-test).

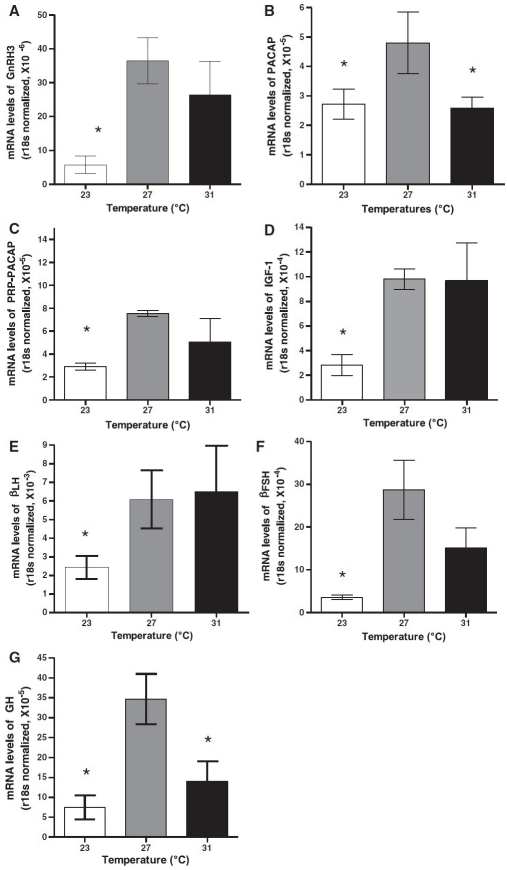

Figure 102. Effect of temperature on mRNA levels of brain and pituitary hormones in females maintained with reproductively active males (nest-builders) (FRM). (A) GnRH3, (B) PACAP, (C) PRP-PACAP, (D) IGF1, (E) *β*LH, (F) *β*FSH, (G) GH. Females were selected randomly and kept for 9 days at 23˚C, 27˚C or 31˚C following an acclimation period of 5 days (mean ± SEM; n = 6 - 10). At the vitellogenic stage, they were separated and after an acclimation period of 4 days, kept at 23˚C, 27˚C or 31˚C in the presence of a mature male for 1 day. Total RNA from pituitaries was reverse-transcribed and subjected to real-time qPCR. The relative amount of hormone mRNA reflects the relative amount of transcription of the specific gene. Each histogram presents the average of at least five independent measurements (mean ± SEM; n = 5 - 9). Different letters denote a significant difference among the mRNA levels in females kept at 23˚C or 31˚C compared to the control group at 27˚C ($P < 0.05$, t-test).

Conflicts of Interest

The authors declare no conflict of interest.

References

Becker, D., Galili, N., Degani, G., 1992. GCMS-identified steroids and steroids glucoronides in gonads and holding water of *Trichogaster trichopterus* (Anabantidae, Pallas 1770). Comp. Biochem. Physiol. B 103, 15-19.

Castro, A., Becerra, M., Manso, M.J., Tello, J., Sherwood, N.M., Anadon, R., 2009. Distribution of growth hormone-releasing hormone-like peptide: immunoreactivity in the central nervous system of the adult zebrafish (*Danio rerio*). J. Comp. Neurol. 513, 685-701.

Chauhan, T., Rajiv, K., 2010. Molecular markers and their applications in fisheries and aquaculture. Adv. Biosci. Biotechnol. 1, 281-291.

Cheal, M., Davis, R.E., 1974. Sexual behavior: social and ecological influences in the anabantoid fish, *Trichogaster trichopterus*. Behav. Biol. 10, 435-445.

Davey, J.W., Hohenlohe, P.A., Etter, P.D., Boone, J.Q., Catchen, J.M., Blaxter, M.L., 2011. Genome-wide genetic marker discovery and genotyping using next generation sequencing. Nat. Rev. Genet. 12, 499-510.

David, D., Degani, G., 2011. Temperature affects Brain and pituitary gene expression related to reproduction and growth in the male blue gouramis, *Trichogaster trichopterus* J. Exp. Zool. 313A 1-11.

Degani, G., 1989. The effect of temperature, light, fish size and container size on breeding of *Trichogaster trichopterus.* Isr. J. Aquacult. 41, 67-73.

Degani, G., 1990. The effects of human chorionic gonadotropin on steroid changes in *Trichogaster trichopterus* (B & S 1801). Comp. Biochem. Physiol. A 96, 525-528.

Degani, G., 1993a. The effect of sexual behavior on oocyte development and steroid changes in *Trichogaster trichopterus*. Copeia 4, 1091-1096.

Degani, G., 1993b. Reproduction control in multi-spawning asynchronic *Trichogaster trichopterus* (Pallas) as a model for Anabantidae family. Trend. Comp. Biochem. Physiol. 1, 1269-1275.

Degani, G., 1994. Effect of gonadotropin and steroids on vitellogenesis during ovarian development in *Trichogaster trichopterus*. J. Aquacult. Trop. 9, 15-23.

Degani, G., 2001. Blue Gourami (*Trichogaster trichopterus*) Model for Labyrinth Fish. Laser Pages Publishing, Jerusalem, Israel.

Degani, G., 2013. Mitochondrial DNA sequence analysis in Anabantoidei fish. Adv. Biol. Chem. 3, 347-355.

Degani, G., 2014a. Involvement of GnRH and gonadotropin genes in oocyte development of blue gourami females (*Trichogaster trichopterus*). Adv. Biol. Chem. 4, 197-202.

Degani, G., 2014b. Expression of SOX3 and SOX9 genes in gonads of blue gourami. Adv. Biol. Chem. 4, 322-330.

Degani, G., 2014c. Expression of the growth hormone and insulin-like growth factor 1 genes in the male and female blue gourami (*Trichogaster*

trichopterus) at different temperatures. J. Asian Sci. Res. 4, 413-427.

Degani, G., 2015a. Somatolactin transcription during oogenesis in female blue gourami (*Trichogaster trichopterus*). Adv. Biol. Chem. 5, 279-285.

Degani, G., 2015b. 11-ketotesterone (Kt-11), estradiol (E2) level and cytochrome P450 (Bgcyp19a) transcription in the testis of male blue gourami (*Trichogaster trichopterus*). Int. J. Sci. Res. 4, 641-643.

Degani, G., 2016. Oogenesis control in multi-spawning blue gourami (*Trichogaster trichopterus*) as a model for the Anabantidae family. Int. J. Sci. Res. 5, 179-184.

Degani, G., 2017. Steroids controlled by various hormones influence oogenesis and spermatogenesis of the model fish, *Trichogaster Trichopterus* (Anabantidae, Pallas). In: Advances in Sex Steroids. Chapter 1: Sex Steroids. Avid Science Publications, pp. 1-31.

Degani, G., 2018. Oocytes development in the fry of blue gourami, *Trichogaster trichopterus*. Int. J. Zool. Invest. 4, 11-20.

Degani, G., 2020a. Brain control reproduction by the endocrine system of female blue gourami (*Trichogaster trichopterus*). Biology 9, 1-16.

Degani, G., 2020b. A qualitative model of the interaction of sexual behavior and hormone gene transcription in male blue gourami during reproduction. J. Biophys. Chem. 11, 43-50.

Degani, G., Alon, A., Hajouj, A., Meerson, A., 2019a. Vitellogenesis in blue gourami is accompanied by brain transcriptome changes. Fishes 4, 54.

https://doi.org/10.3390/fishes4040054

Degani, G., Alon, A., Stoler, A., Bercocvich, D., 2017a. Evidence of a reproduction-related function for brine Kisspeptin 2 and its receptors in Anabantidae fish (*Trichogaster trichopterus*). Int. J. Zool. Invest. 2, 106-122.

Degani, G., Boker, R., 1992a. Sensitivity to maturation-inducing steroids and gonadotropin in the oocytes of blue gourami *Trichogaster trichopterus* (Anabantidae, Pallas, 1770). Gen. Comp. Endinocrinol. 85, 430-439.

Degani, G., Boker, R., 1992b. Vitellogenesis level and the induction of maturation in the ovary of the blue gourami *Trichogaster trichopterus* (Anabantidae, Pallas 1770). J. Exp. Zool. 263, 330-337.

Degani, G., Boker, R., Jackson, K., 1998. Gonadotropin, growth hormone cells and oocyte development in female gourami after injection of gonadotropin-releasing analogue. J. Aquacult. Trop. 13, 159-170.

Degani, G., David, D., Levy, G., 2011. The effect of temperature on oogenesis and brain gene expression of hormones involved in reproduction and growth in the female blue gourami (*Trichogaster trichopterus*). Indian J. Sci. Technol. 4, 109-1010.

Degani, G., Gal, E., Vaya, J., 1994. *In vitro* biosynthesis of steroids in ovary of asynchronic *Trichogaster trichopterus* (Pallas, 1770). Comp. Biochem. Physiol. 109, 715-723.

Degani, G., Gallagher, M.L. 1996. Steroid and carp pituitary extract influences on follicle frequency in vitellogenesis and maturation of *Trichogaster trichopterus*. Aquacult. Trop. 11, 39-48.

Degani, G., Hurvitz, A., Eliraz, Y., Meerson, A., 2019b. Sex-related gonadal gene expression differences in the Russian sturgeon (*Acipenser gueldenstaedtii*) grown in stable aquaculture conditions. Anim. Reprod, Sci. 200, 75-85.

Degani, G., Jackson, K., Goldberg, D., Sarfati, R., Avtalion, R., 2003. βFSH, βLH and growth hormone gene expression in blue gourami (*Trichogaster trichopterus*, Pallas 1770) during spermatogenesis and male sexual behavior. Zool. Sci. 20, 737-743.

Degani, G., Jackson, K., Marmelstein, G., 1995. The effect of LHRH analogue on sex steroid profiles in female *Trichogaster trichopterus* (Anabantidae, Pallas). J. Aquacult. Trop. 10, 297-307.

Degani, G., Jackson, K., Yom-Din, S., Goldberg, D., 2006. cDNA cloning and mRNA expression of growth hormone in Belontiidae (Anabantoidei suborder) fish. Isr. J. Aquacult. 58, 124-136.

Degani, G., Levy, G., 2013. Underground water affects sexual behavior and gene expression of hormones related to reproduction in blue gourami males. Adv. Biol. Chem. 3. https://doi.org/10.4236/abc.2013.31016

Degani, G., Mananos, E.L., Jackson, K., Abraham, M., Zohar, Y., 1997. Changes in plasma and pituitary in female blue gourami during the end of vitellogenesis and final oocyte maturation. J. Exp. Zool. 279, 377-385.

Degani, G., Schreibman, M.P., 1993. Pheromone of male blue gourami and its effect on vitellogenesis, steroidogenesis and cells in pituitary of the female. J. Fish Biol. 43, 475-485.

Degani, G., Veit, M., 1990. Electrophoretic variations of isozyme systems in the muscle and liver of Anabantidae fish. Isr. J. Aquacult. 42, 67-76.

Degani, G., Yom Din, S., 2011. Hormones transcription in the testis of blue gourami (*Trichogaster trichopterus*, Pallas 1770) during sexual behavior. Bull. Univ. Agric. Sci. Vet. Med. Cluj-Napoca Anim. Sci. Biotechnol. 68, 43-50.

Degani, G., Yom-Din, S., Goldberg, D., Jackson, K., 2010. cDNA cloning of blue gourami (*Trichogaster trichopterus*) prolactin and its expression during the gonadal cycles of males and females. J. Endocrinol. Invest. 33, 7-12.

Degani, G., Yom-Din, S., Hurvitz, A., 2017b. Transcription of insulin-like growth factor receptor in Russian sturgeon (*Acipenser gueldenstaedtii*) ovary during oogenesis. Univ. J. Agric. Res. 5, 119-124.

Degani, G., Ziv, M.B., 2016. Male blue gourami (*Trichogaster trichopterus*) nest-building behavior is affected.by other males and females. Open J. Anim. Sci. 6, 195-201.

Espigares, F., Rocha, A., Gómez, A., Carrillo, M., Zanuy, S., 2017. Photoperiod modulates the reproductive axis of European sea bass through regulation of kiss1 and gnrh2 neuronal expression. Gen. Comp. Endocrinol. 240, 35-45.

Ezagouri, E., Yom-Din, M.S., Goldberg, D., Jackson, K., Levavi-Sivan, B., Degani, G., 2008. Expression of the two CYP19 (P450 aromatase) genes in the male and female blue gourami (*Trichogaster trichopterus*) during the reproduction cycle. Gen. Comp. Endocrinol. 159, 208-213.

Forselius, S., 1975. Studies of anabantid fishes. Parts I, II, III. Zoologiska Bidrag Fran Uppsala 32, 593-597.

Froese, R., Pauly, D., 2019. *Trichopodus trichopterus* (Pallas, 1770). FishBase Trichogaster labiosus distribution U.S. Fish and Wildlife Service, http://www.fishbase.org/summary/Trichopodus-trichopterus

Goldberg, D., Jackson, K., Yom-Din, S., Degani, G., 2004. Growth hormone of *Trichogaster trichopterus*: cDNA cloning, sequencing and analysis of mRNA expression during oogenesis. J. Aquacult. Trop. 19, 215-229.

Huang, T., Huang, X., Lu, D.W., Zhu, P., Shi, Y., Cheng, C.H., Liu, X., Lin, H., 2009. Structural and functional multiplicity of the kisspeptin/GPR54 system in goldfish (*Carassius auratus*). J. Endocrinol. 201, 407-441.

Hubert, N., Meyer, C.P., Bruggemann, H.J., Guerin, F., Komeno, R.J.L., Espiau, B., Causse, R., Williams, J.T., Planes, S., 2012. Cryptic diversity in Indo-Pacific coral reef fishes revealed by DNA-barcoding provides new support to the centre of overlap hypothesis. PLoS ONE 7, e28987. https://doi.org/10.1371/journal.pone.0028987

Jackson, K., Abraham, M., Degani, G., 1994. Oocyte maturation triggered by the presence of male in the Blue Gourami, *Trichogaster trichopterus*. J. Morphol. 220, 1-9.

Jackson, K., Abraham, M., Degani, G., 2005. Cellular events in *Trichogaster trichopterus* adenohypophysis during final oocyte maturation. Indian J. Fisheries 52, 1-13.

Jackson, K., Goldberg, G., Ofir, R., Abraham, M., Degani, G., 1999. Blue goura-

mi (*Trichogaster trichopterus*) gonadotropic subunits (I & II) cDNA sequences and expression during oogenesis J. Mol. Endocrinol. 23, 177-187.

Kitahashi, T., Ogawa, S., Parhar, I.S., 2009. Cloning and expression of kiss2 in the zebrafish and medaka. Endocrinology 150, 821-831.

Kumar, S., Stecher, G., Li, M., Knyaz, C., Tamura, K., 2018. MEGA X: Molecular Evolutionary Genetics Analysis across computing platforms. Mol. Biol. Evol. 35, 1547-1549.

Lancien, F., Mimassi, N., Conlon, J.M., Le Mevel, J.C., 2011. Central pituitary adenylate cyclase-activating polypeptide (PACAP) and vasoactive intestinal peptide (VIP) decrease the baroreflex sensitivity in trout. Gen. Comp. Endocrinol. 171, 245-251.

Lee, Y.R., Tsunekawa, K., Moon, M.J., Um, H.N., Hwang, J.-I., Osugi, T., Otaki, N., Sunakawa, Y., Kim, K., Vaudry, H., Kwon, H.B., Seong, J.Y., Tsutsui, K., 2009. Molecular evolution of multiple forms of kisspeptins and GPR54 receptors in vertebrates. Endocrinology 150, 2837-2846.

Levy, G., David, D., Degani, G., 2011. Effect of environmental temperature on growth- and reproduction-related hormones gene expression in the female blue gourami (*Trichogaster trichopterus*). Comp. Biochem. Physiol. A 160, 381-389.

Levy, G., Degani, G., 2011. Evidence for a reproduction-related function of pituitary adenylate cyclase-activating polypeptide-related peptide (PRP) in an Anabantidae fish. J. Mol. Endocrinol. 46, 101-110.

Levy, G., Degani, G., 2012. Involvement of GnRH, PACAP and PRP in the reproduction of blue gourami females (*Trichogaster trichopterus*). J. Mol. Neurosci. 48, 9730-9738.

Levy, G., Degani, G., 2013. The role of brain peptides in the reproduction of blue gourami males (*Trichogaster trichopterus*). J. Exp. Zool. A Ecol. Genet. Physiol. 319, 461-470.

Levy, G., Goldberg, D., Jackson, K., Degani, G., 2010. Association between pituitary adenylate cyclase activating polypeptide and reproduction in the blue gourami. Gen. Comp. Endocrinol. 166, 83-93.

Levy, G., Gothilf, Y., Degani, G., 2009. Brain gonadotropin releasing hormone3 expression variation during oogenesis and sexual behavior and its effect on pituitary hormonal expression in the blue gourami. Comp. Biochem. Physiol. A Mol. Integr. Physiol. 154, 241-248.

Mananos, E., Zohar, Y., Degani, G., 1997. The relationship between gonadotropin and sexual behavior of male *Trichogaster trichopterus* (Pallas). Indian J. Fisheries 44, 239-246.

Maqsood, H.M., Ahmad, S.M., 2017. Advances in molecular markers and their applications in aquaculture and fisheries. Genet. Aquat. Organ. 1, 27-41.

Miller, J.R., 1964. Studies on the social behavior of the blue gourami, *Trichogaster trichopterus* (Pisces, Belontiidae). Copeia 3, 469-496.

Miller, R.J., Robison, H.W., 1974. Reproductive behavior and phylogeny in the genus *Trichogaster* (Pisces, Anabantoidei). Z. Tierpsychol. 34, 484-499.

Oakley, A.E., Clifton, D.K., Steiner, R.A., 2009. Kisspeptin signaling in the brain. Endocrinol. Rev. 30, 713-743.

Okumus, F., Ciftci, Y., 2003. Fish population genetics and molecular markers: II-Molecular markers and their applications in fisheries and aquaculture. Turk. J. Fisheries Aquat. Sci. 3, 51-79.

Pongthana, N., 2001. Aquaculture genetics research in Thailand. In: Gupta, M.V. and Acosta, B.O. (Eds.), Fish Genetics Research in Member Countries and Institutions of the International Network on Genetics in Aquaculture. The World Fish Center, Penang, Malysia, pp. 77-89.

Ratnasingham, S., Hebert, P.D.N., 2007. BOLD: The Barcode of Life Data system. Mol. Ecol. Notes 7, 355-364.

Ruber, L., Britz, R., Zardoya, R., 2006. Molecular phylogenetics and evolutionary diversification of labyrinth fishes (Perciformes: Anabantoidei). Syst. Biol. 55, 374-397.

Servili, A., Le Page, Y., Leprince, J., Caraty, A., Escobar, S., Parhar, I.S., Seong, J.Y., Vaudry, H., Kah, O., 2011. Organization of two independent kisspeptin systems derived from evolutionary-ancient kiss genes in the brain of zebrafish. Endocrinology 152, 1527-1540.

Shahjahan, M., Motohashi, E., Doi, H., Ando, H., 2010. Elevation of Kiss2 and its receptor gene expression in the brain and pituitary of grass puffer during the spawning season. Gen. Comp. Endocrinol. 169, 48-57.

Small, B.C., Nonneman, D., 2001. Sequence and expression of a cDNA encoding both pituitary adenylate cyclase activating polypeptide and growth

hormone-releasing hormone-like peptide in channel catfish (*Ictalurus punctatus*). Gen. Comp. Endocrinol. 122, 354-363.

Sower, S.A., Freamat, M., Kavanaugh, S.I., 2009. The origins of the vertebrate hypothalamic-pituitary-gonadal (HPG) and hypothalamic-pituitary-thyroid (HPT) endocrine systems: new insights from lampreys. Gen. Comp. Endocrinol. 161, 20-29.

Stacey, N.E., Sorensen, P.W., 2006. Reproductive pheromones. Characterization of sex pheromone response in sailfin mollies. In: Sloman, K.A., Wilson, R.W. and Balshine, S. (Eds.), Behavior and Physiology of Fish. Elsevier, Amsterdam, pp. 359-412.

Syaifudin, M., Jubaedah, D., Yonarta, D., Hastuti, Z., 2019. DNA barcoding of snakeskin gourami *Trichogaster pectoralis* and blue gourami *Trichogaster trichopterus* based on cytocrome c oxidase subunit I (COI) gene. Earth. Enviro. Sci. 384, 012031.

Van der Laan, R., Eschmeyer, W.N., Fricke, R., 2014. Family-group names of Recent fish. Zootaxa 3882, 1-230.

Vaughan, J.M., Rivier, J., Spiess, J., Peng, C., Chang, J.P., Peter, R.E., Vale, W., 1992. Isolation and characterization of hypothalamic growth-hormone releasing factor from common carp *Cyprinus carpio*. Neuroendocrinology 56, 539-549.

Vierke, J., 1988. Bettas, Gouramis and Other Anabantoids: Labyrinth Fishes of the World. T.F.H. Publications, Neptune City, NJ.

Yaron, Z., Levavi-Sivan, B., 2011. Endocrine regulation of fish reproduction.

In: Farrell A.P. (Ed.), Encyclopedia of Fish Physiology: From Genome to Environment. Academic Press, San Diego, CA, pp. 1500-1508.

Yom Din, S., Hurvitz, A., Goldberg, D., Jackson, K., Levavi-Sivan, B., Degani, G., 2008. Cloning of Russian sturgeon (*Acipenser gueldenstaedtii*) growth hormone and insulin-like growth factor 1 and their expression in male and female fish during the first period of growth. J. Endocrinol. Invest. 31, 201-210.

Zohar, Y., Munoz-Cueta, J.A., Elizur, A., Kah, O., 2010. Neuroendocrinology of reproduction in teleost fish. Gen. Comp. Endocrinol. 165, 438-455.


$25.00
ISBN 978-1-64997-226-2
52500>
9 781649 972262